Plant Physiology Preview. Published on February 3, 2015, as DOI:10.1104/pp.114.254367

Running Title: Regulation of monoterpene synthesis in kiwifruit

Corresponding Author:

Niels J. Nieuwenhuizen

The New Zealand Institute for Plant & Food Research Limited (PFR), Private Bag 92169, Auckland, New Zealand

Tel +64-9-9257248

E-mail: niels.nieuwenhuizen@plantandfood.co.nz

Natural variation in monoterpene synthesis in kiwifruit: transcriptional regulation of terpene synthases by NAC and EIN3-like transcription factors

Niels J. Nieuwenhuizen[1,2], Xiuyin Chen[1], Mindy Y. Wang[1], Adam J. Matich[3], Ramon Lopez Perez[1,4], Andrew C. Allan[1,2], Sol A. Green[1] and Ross G. Atkinson[1]

[1] The New Zealand Institute for Plant & Food Research Limited (PFR), Private Bag 92169, Auckland, New Zealand

[2] School of Biological Sciences, University of Auckland, Private Bag 92019, Auckland 1142, New Zealand

[3] PFR, Private Bag 11600, Palmerston North, New Zealand

[4] Current address: German Cancer Research Center, Clinical Cooperation Unit Molecular Radiooncology, Im Neuenheimer Feld 280, 69120 Heidelberg, Germany

Footnotes

This work was funded by the Foundation for Research, Science and Technology of New Zealand (CO6X0403 and C11X1007) and the Ministry of Science and Innovation.

Corresponding Author:

Niels J. Nieuwenhuizen E-mail: niels.nieuwenhuizen@plantandfood.co.nz

ABSTRACT

Two kiwifruit (*Actinidia*) species with contrasting terpene profiles were compared to understand the regulation of fruit monoterpene production. High rates of terpinolene production in ripe *A. arguta* fruit were correlated with increasing gene and protein expression of a terpene synthase *AaTPS1* and correlated with an increase in transcript levels of the MEP pathway enzyme 1-deoxy-D-xylulose-5-phosphate synthase (*DXS)*. In *A. chinensis*, *AcTPS1* was identified as part of an array of eight tandemly duplicated genes and *AcTPS1* expression and terpene production was observed only at low levels in developing fruit. Transient over-expression of *DXS* in tobacco leaves elevated monoterpene synthesis by AaTPS1 >100-fold, indicating that DXS is likely to be the key step in regulating MEP substrate flux in kiwifruit. Comparative promoter analysis identified potential NAC and EIN3-like transcription factor (TF) binding sites in the *AaTPS1* promoter, and cloned members of both TF classes were able to activate the *AaTPS1* promoter in transient assays. Electrophoretic mobility shift assays showed that AaNAC2, 3 and 4 bind a 28 bp fragment of the proximal NAC binding site in the *AaTPS1* promoter but not the *AcTPS1* promoter, where the NAC binding site was mutated. Activation could be restored by re-introducing multiple repeats of the 12 bp NAC core-binding motif. The absence of NAC transcriptional activation in ripe *A. chinensis* fruit can account for the low accumulation of *AcTPS1* transcript, protein and monoterpene volatiles in this species. These results indicate the importance of NAC transcription factors in controlling monoterpene production and other traits in ripening fruits.

INTRODUCTION

Fruit and flower volatiles are important signals to attract mutualists and repel antagonists involved in pollination, fruit predation and seed dispersal. They have additional roles in protecting these tissues against pathogens and insects and may be involved in indirect trophic interactions such as attracting herbivore predators (Rodriguez et al., 2013). Flavor volatiles are also important targets in modern plant breeding programs where specific combinations are selected to enhance the taste, aroma and health properties of the fruit. Terpenoids form an important part of the aroma profile of many fruits. During fruit ripening, concentrations of many terpenoid compounds (including C10 monoterpene and C15 sesquiterpene volatiles) increase in conjunction with changes in texture, taste and color. Fruit volatile terpenoids have been well characterized in *Citrus* spp. (Moufida and Marzouk, 2003), mango (*Mangifera indica*) (MacLeod and Pieris, 1984), apple (*Malus* x *domestica*) (Nieuwenhuizen et al., 2013), tomato (*Solanum lycopericum*) (Buttery et al., 1988) and grape (*Vitis vinifera*) (Battilana et al., 2009; Duchêne et al., 2009). In kiwifruit (*Actinidia* spp.), volatile terpenoid concentrations also vary greatly, with some species such as *A. arguta* showing very high concentrations of monoterpenes, while others such as *A. chinensis* and *A. deliciosa* show very low concentrations (Crowhurst et al., 2008).

In nature, the diverse array of terpene compounds essentially derives from the simple C5 prenyldiphosphate precursor isopentenyl diphosphate (IDP) and its allylic isomer dimethylallyl diphosphate (DMADP). In plants, IDP is synthesized via two compartmentally segregated substrate pathways, namely the mevalonate (MEV) pathway located in the cytosol and the plastidial 2-C-methyl-D-erythritol 4-phosphate pathway (MEP) (Rodriguez-Concepcion and Boronat, 2002). In both compartments, IDP and DMADP are condensed by the action of short chain prenyltransferases to generate the direct precursors for terpene synthase (TPS) enzymes including the plastid-derived C10 mono-TPS substrate geranyl diphosphate (GDP) and the cytosol-derived C15 sesqui-TPS substrate farnesyl diphosphate (FDP). TPS enzymes are unique in their capacity to direct the formation of a myriad of products through subtle variations in their conserved catalytic fold (Yoshikuni et al., 2006; O'Maille et al., 2008; Chen et al., 2011) and in their propensity to generate multiple products from a single prenyldiphosphate substrate. Contrasting terpene profiles can also be caused by differences in the composition of TPS genes due to changes in copy number, variation of gene and protein expression, and variation in catalytic efficiency as seen in Sitka spruce and the production of the monoterpene (+)-3-carene associated with white pine weevil resistance (Hall et al., 2011). In maize, the ability of roots or leaves to attract natural enemies upon

herbivory was dependent on expression of an (*E*)-β-caryophyllene synthase allele which was lost in many maize lines during breeding (Kollner et al., 2008). For the scented species *Clarkia breweri*, floral linalool release likely evolved from its extant non-scented species *C. concinna* through changes in expression of an *S*-linalool synthase (Dudareva et al., 1996).

The 1-deoxy-D-xylulose-5-phosphate synthase (DXS) gene has been shown to encode an important rate-limiting step in the biosynthesis of MEP-derived isoprenoids such as chlorophylls, tocopherols, carotenoids, abscisic acid, and gibberellins in *Arabidopsis* (Matthews and Wurtzel, 2000; Estévez et al., 2001) and other biological systems (Rodriguez-Concepcion and Boronat, 2002; Cordoba et al., 2009). In tomato fruit, regulation of the MEP pathway by DXS has been extensively studied in relation to carotenoid biosynthesis (Lois et al., 2000; Enfissi et al., 2005). The DXS gene also appears to have an important role in regulating monoterpene biosynthesis in fruit, as quantitative trait loci (QTL) for variation in concentrations of linalool, geraniol, nerol, citronellol and α-terpineol co-locate with candidate DXS genes in grape (Battilana et al., 2009; Duchêne et al., 2009). DXS is not the only gene regulating substrate flux through the MEP pathway, as later steps in the MEP pathway mediated by deoxyxylulose 5-phosphate reductoisomerase (DXR) and HMBPP reductase (HDR) have also been shown to be rate limiting in the leaves of Arabidopsis and peppermint (*Mentha* x *piperita L.*) (Mahmoud and Croteau, 2001; Botella-Pavía et al., 2004). Over-expression of DXR increased biosynthesis of chlorophylls, carotenoids and transgene-derived taxadiene in Arabidopsis as well as essential oil concentrations in peppermint (Mahmoud and Croteau, 2001). Over-expression of a tomato HDR gene in Arabidopsis gave similar results (Botella-Pavía et al., 2004). In tobacco, over-expression of a snapdragon GDP synthase (GDPS.SSU) increased monoterpene emissions but at the expense of other isoprenoids such as carotenoids, chlorophyll and gibberellins (Orlova et al., 2009).

In fruit crops such as tomato, apple and banana (*Musa acuminata*), a rapid increase of ethylene production accompanied by a ‘climacteric’ burst in respiration (Alexander and Grierson, 2002) initiates rapid fruit ripening. During climacteric fruit ripening, autocatalytic (type II) ethylene production initiates a transcriptional cascade that controls many ripening traits, including softening and flavor volatile production (Solano et al., 1998). The EIL (EIN3-like) class of transcription factors (TFs) are the most downstream signaling components of the ethylene-signaling pathway and have been shown to modulate a multitude of downstream transcriptional cascades and hormone response pathways (Chang et al., 2013). Ethylene-induced stabilization of EIN3 protein is mediated by removal of EIN3-binding F-box proteins (EBFs) through the proteasome. In the absence of ethylene, EBFs are up-

regulated and mediate EIN3 degradation (Solano et al., 1998). EIL TFs act on the promoters of early ethylene responsive genes such as *ERF1* (*ETHYLENE-RESPONSE-FACTOR1*), which encodes a GCC-box-binding protein, by binding to the primary ethylene response element (PERE) in the promoters of these genes (Yamasaki et al., 2005). EILs in kiwifruit were able to activate the *AdACO1 (ACC OXIDASE1*) gene promoter, thus implicating them in a role during autocatalytic ethylene production (Yin et al., 2010). Antisense *LeERF1* tomatoes had longer fruit postharvest life (Li et al., 2007), and *LeERF2* regulates ethylene production in tomato and tobacco by interaction with the promoters of *LeACO3* and *NtACS3* (Zhang et al., 2009). In banana, ERFs have also been shown to bind to the promoters of *MaACO1* (*ACC OXIDASE1*) and *MaACS1* (*ACC SYNTHASE1*) genes involved in ethylene biosynthesis (Xiao et al., 2013).

Transcriptional control of specific flavor and aroma genes is currently poorly understood with respect to development/senescence and ethylene production. In *Petunia hybrida* flowers, benzenoid scent production has been shown to be transcriptionally controlled through the ODO1 R2R3 MYB TF targeting the 5-enol-pyruvylshikimate-3-phosphate synthase promoter (Verdonk et al., 2005). Transgenic roses that over-expressed the PAP1 R2R3 MYB TF produced 6.5-fold higher concentrations of terpenoids than control flowers, which was partly explained by up-regulation of a *GERMACRENE D SYNTHASE* gene, although no direct evidence of promoter interaction was presented (Zvi et al., 2012). In cotton, the action of a WRKY TF regulates the sesquiterpene synthase gene (+)-δ-*CADINENE SYNTHASE-A* involved in gossypol production (Xu et al., 2004), while in Arabidopsis inflorescences the bHLH MYC2 directly binds and activates the promoter of the sesquiterpene synthase gene TPS21 inducing sesquiterpene release (Hong et al., 2012). In tomato, pleiotropic mutants such as *rin, nor* and *Cnr* affect a wide range of ripening-related characters including ethylene production and downstream volatile compound synthesis. The *rin* mutation has been shown to be encoded by a MADS box TF (Vrebalov et al., 2002) and *Cnr* by a SQUAMOSA promoter-binding protein (Manning et al., 2006). An uncharacterized NAC-domain TF mutation leads to the *nor* mutant phenotype (Martel et al., 2011) whilst SlNAC4 could interact with NOR and RIN proteins to affect fruit ripening and carotenoid accumulation (Zhu et al., 2014). Other tomato TFs shown to influence volatile production in fruit include the homeobox protein LeHB-1 (Lin et al., 2008), which induces *LeACO1* and ethylene production, and the MADS box protein TAGL1 (Itkin et al., 2009; Vrebalov et al., 2009) through direct activation of *LeACS2*. In Arabidopsis, *AtNAP*, a NAC family transcription factor gene, regulates silique senescence by affecting ethylene biosynthesis, perception, and

154 signaling (Kou et al., 2012). Studies in banana have shown that expression levels of several
155 NAC TFs are induced during fruit ripening and that some of these can physically interact
156 with EIL TFs (Shan et al., 2012). No information is available on the transcriptional regulation
157 of monoterpenes in any plant species.
158 In this study we examine the terpenes and corresponding terpene synthases during fruit
159 development and ripening in two kiwifruit species, *A. chinensis* and *A. arguta*, which vary
160 greatly in their terpene volatile content. Our results reveal how natural variation in TF
161 binding sites can influence a key ripening trait in fruit.
162

MATERIALS AND METHODS

Plant material and headspace volatile analysis

Fruit were ripened at room temperature without exogenous ethylene application before headspace sampling, with the exception of *A. chinensis* 'Hort16A'. Headspace volatiles from ripe fruit were obtained from a 1-1.5 g sample of pulped tissue from 5-10 whole fruit (including skin) and collected for 20 min by a purge and trap method onto Chromosorb™105 tubes (Matich et al., 2003). Thermal desorption and gas chromatography–mass spectrometry (GC-MS) peak identification were as described in Wang et al. (2011). Volatiles were semi-quantitatively analyzed by comparison with the average response factor of a standard containing methyl butanoate, ethyl butanoate, hexanol and methyl benzoate using flame ionization detection (Wang et al., 2011).

A. arguta (Sieb. et Zucc.) Planch. ex Miq. 'Hortgem Tahi' is derived directly from a cross between two wild (non-cultivated) parents. Fruit volatiles were trapped for 3 h using sliced fruit at 75 days after pollination (DAP), and for 15 min using pulped fruit at 120 DAP (harvest, stage a0) and during ripening (stages a1-a5). Soluble solids content (Table S1) and ethylene production were monitored using standard protocols (Atkinson et al., 2011). Fruit firmness was monitored non-destructively as described in Wang et al. (2011). Fruit were distributed into ripening stages based on firmness - a0: harvest (firmness 8 N), a1: unripe (3.0-2.0 N); a2: near ripe (1.95-1.50), a3: eating ripe (1.45-1.00 N), a4: near over-ripe (0.95-0.70 N) and a5: over-ripe (<0.5 N).

A. chinensis Planch. 'Hort16A' is derived from a cross between a wild (non-cultivated) male parent and a female parent that is one cross from wild material. Fruit volatiles were trapped monthly during development from 30 to 120 (DAP) for 3 h using sliced fruit and during ripening (stages based on days post ethylene treatment: 0 d (c0), 1 d (c1), 2 d (c2), 4 d (c3) and 6 d (c4) for 15 min using pulped fruit. After harvest (175 DAP), fruit were held at room temperature then coordinately ripened with ethylene (100 µL L^{-1}, 20 h). Soluble solids (Table S1) content and ethylene production were monitored as described above. Fruit firmness was measured using a 7.9-mm diameter probe attached to a GUSS Fruit Texture Analyser (GUSS Manufacturing Ltd, South Africa) with probe speed, trigger force and measurement distance set to 10 mm/s, 50 g and 8 mm, respectively. Fruit were sampled at five ripening stages, c0-c4, as described above. In parallel, material from both cultivars was stored at -80°C for RNA and protein isolation.

Gene identification and sequence alignments

AaTPS1 was identified in an *A. arguta* 'Hortgem Tahi' ripe fruit EST library and *AcTPS1* in an *A. chinensis* 'Hort16A' young fruit (14-30 DAP) EST library (Crowhurst et al., 2008) using known TPS sequences in GenBank as query sequences, and cloned using the primers and vectors described in Table S2A. Kiwifruit MEP pathway genes were identified in available EST assemblies (Crowhurst et al., 2008) using *A. thaliana* MEP pathway genes (Phillips et al., 2008), AT5G16440 (IDI) and AF182827 (ssGDPS) as query sequences. Full length *AcDXS*, *AaDXR* and *AaIDI* genes were cloned from ripe *A. arguta* and *A. chinensis* fruit cDNA (stages a3/c2 respectively) as described in Table S2A. *AdHDR* was obtained directly from an *A. deliciosa* EST library. Putative NAC-like TFs were identified from predicted gene models based on an in-house, low coverage, *A. chinensis* genome assembly and from the kiwifruit genome assembly for the cultivar 'Hongyang' (Huang et al., 2013). Deep sequencing data of an *A. arguta* fruit library (stage a3) were then read mapped to identify TFs highly expressed in ripe fruit and to map the likely transcriptional start site. *Aa/AcNAC1-4* were cloned from ripe cDNA (a3/c2 stage) using the primers and vectors described in Table S2B. *Aa/AcEIL1-4* were also cloned from ripe fruit cDNA (a3/c2 stage) using the primers and vectors described in Table S2B, based on available *EIL* sequences from *A. deliciosa* (Yin et al., 2010). Chloroplast signal peptide predictions were carried out using ChloroP (Emanuelsson et al., 1999) and sequences were aligned using Geneious® (www.geneious.com).

Gene expression analysis

Total RNA was extracted according to Nieuwenhuizen et al. (2007) from a mixture of three or more representative fruit and treated with 10 U of DNaseI (Roche Applied Science, Mannheim, Germany) before cDNA synthesis. First-strand cDNA was synthesized using the Transcriptor First Strand cDNA Synthesis Kit (Roche) according to the manufacturer's instructions and diluted 50-fold before use. Relative quantification real-time gene expression analyses were performed on a LightCycler® 480 platform using the LightCycler 480 SYBR Green master mix in quadruplicate technical replicates, and results were analyzed using the LightCycler 480 software (Roche) with PCR efficiency corrections for all primer pairs. Program: 5 min at 95°C; 40 cycles of 10 s at 95°C, 10 s at 60°C, and 20 s at 72°C; followed by melting curve analysis: 95°C 5 s, 65°C 60 s then ramping at 0.18°C/s to 95°C. Gene specific primers used in PCR are given in Table S2C. The data were analyzed using the Target/Reference ratio calculated with the LightCycler® 480 software 1.5 as described in

Montefiori et al. (2011), enabling a comparison of the level of expression of two different genes to a stably expressed reference gene (EF1α).

Expression of putative terpene synthases in vitro *and western analysis*

For functional studies, N-terminal truncated *AcTPS1* and *AaTPS1* ORFs were amplified to remove the chloroplast-targeting peptide while retaining the RRX_8W motif crucial for cyclic mono-TPS activity and TOPO (Invitrogen)-cloned into a bacterial expression vector. Primers and vectors used are given in Table S2D. Recombinant N-terminal His-tagged proteins were expressed by auto-induction in *Escherichia coli* BL21 Star (DE3) (Invitrogen, Carlsbad CA, USA) and purified by Ni^{2+} affinity and size exclusion chromatography as described previously (Nieuwenhuizen et al., 2013). AcTPS1 purified recombinant protein (500 µg) was used to raise a polyclonal antibody in rabbit (AgResearch, NZ).

For western analysis, kiwifruit tissue (100 mg) was ground to a fine powder in liquid N_2 and boiled with 0.4 ml 4x SDS loading buffer (Schägger and von Jagow, 1987) for 5 min. Protein extracts (10 µl) were separated by reducing SDS-PAGE and transferred to PVDF membrane (BioRad) as previously described (Nieuwenhuizen et al., 2007). Blots were incubated with 1:250 diluted rabbit anti-AcTPS1 primary polyclonal antibody and 1:1000 diluted secondary Qdot® 655 goat anti-rabbit IgG conjugate (Invitrogen) according to Mansfield (1995), and visualized on a Typhoon 9400 scanner (GE Healthcare, Buckinghamshire, England).

Enantioselective GC-MS and kinetic analysis

Purified recombinant AaTPS1 and AcTPS1 were incubated with 100 µM GDP (Keller and Thompson, 1993) at RT for 1 h. Reactions were overlaid with a 1:1 mixture of pentane:ether to extract volatile terpenes, according to Green et al. (2012). Volatile terpenes were solvent extracted from eating ripe *A. arguta* 'Hortgem Tahi' fruit (a3/a4) according to Matich et al. (2003). Enantioselective analysis of terpene products was performed as described in Nieuwenhuizen et al. (2013).

All kinetic analyses were performed in quadruplicate as described in Green et al. (2012) in buffer containing 50 mM Bis-Tris propane (pH 7.5). For GDP kinetics, 20 mM $MgCl_2$ was included. Cofactor determinations for Mg^{2+} and Mn^{2+} were performed in the presence of 50 µM $^3H_1$-GDP. Kinetic constants were calculated from Bq data by non-linear regression of the

Michaelis–Menten equation using the Origin 7.5 (Microcal Software Inc. Northampton, MA, USA) graphics package.

Transient expression of TPS, NAC, EIL *and MEP pathway genes in* Nicotiana benthamiana

Kiwifruit TPS genes and *AdHDR* were cloned directionally from the original EST plasmids (Crowhurst et al., 2008) using gene specific primers into pENTR/D-TOPO (Invitrogen). The additional MEP pathway genes (*AaDXR*, *AcDXS*, *AaIDI*), *NAC* and *EIL* genes were cloned from ripe fruit cDNA by Gateway BP cloning into pDONR221 (Invitrogen) using the primers described in Table S2A/B and then transferred by Gateway LR reactions as recommended by the manufacturer (Invitrogen) into the binary destination vector pHEX2. pHEX2 contains the CaMV 35S promoter and octopine synthase terminator (Hellens et al., 2005). *Agrobacterium* strain GV3101 infiltration of the above constructs including a pHEX2-GUS control and subsequent headspace volatile analysis was carried out as described previously (Green et al., 2012).

Cloning of AaTPS1 *and* AcTPS1 *promoters*

The *AaTPS1* promoter was cloned by inverse PCR (Triglia, 2000). *A. arguta* genomic DNA was isolated using a DNeasy Plant Mini Kit (Qiagen, Hilden, Germany) and digested with *Hin*dIII for 5 h. The reaction was column purified and the DNA ligated overnight at 4°C in 200 µl reaction buffer using 6 U of T4 DNA ligase (New England Biolabs, Ipswich, MA) according to the manufacturer's instructions. Promoter fragments were PCR amplified using iProof™ polymerase (Bio-Rad Laboratories, CA, USA) in 50 µl reactions using 5 µl of the ligation as template, 98°C denaturation, 65°C annealing and 1 min extension at 72°C for 35 cycles amplification using primers F1_717/R1_131 (Table S2E). A second, nested round of PCR was performed using 1 µl of the first PCR reaction as template with primers F2_757/ R2_101 for 20 cycles. Primers AaProF/R containing *Bam*HI/*Nco*I sites were then used to amplify a 911 base pair (bp) fragment (Aa *TPS*1_{pro}-911). A 3 kb promoter fragment of *AcTPS1* (Ac *TPS*1_{pro}-3000) was identified by a BLASTn search of an in-house *A. chinensis* genomic sequence database. Primers AcProF/R (also containing *Bam*HI/*Nco*I sites, Table S2E) were used to amplify the promoter from *A. chinensis* 'Hort16A' genomic DNA and confirmed by sequencing.

Promoter deletion constructs and mutants were generated by PCR using the primers in Table S2E. The 238 bp Aa *TPS*1_{pro}-238 promoter and mutant were generated by PCR using primers F-238 and F-238mut respectively in combination with AaProR. The 600 bp Ac

296 *TPS*1$_{pro}$-600 and 229 bp Ac *TPS*1$_{pro}$-229 were generated by PCR using primers F-600 and F-
297 229 respectively in combination with AcProR. The Ac *TPS*1$_{pro}$-208 constructs (I, II and III)
298 were generated by PCR using forward primers 208 (I)F, (II)F and (III)F in combination with
299 AcProR. All fragments (including 5'-UTR) were cloned by *Bam*HI/*Nco*I digestion into
300 pGreenII 0800-LUC upstream of the LUC reporter gene *Nco*I site/ATG start, then transferred
301 into *A. tumefaciens* strain GV3101 harboring pSOUP (Hellens et al., 2005).
302
303 *Promoter activation assays*
304 *A. tumefaciens* infiltrations of 3- to 4-week-old *N. benthamiana* leaves were carried out as
305 described previously (Green et al., 2012) with single promoter:TF combinations in 1:4 ratio,
306 with the starting concentration for each component having an A_{600} = 0.5. *Agrobacterium*
307 infiltrations with two TFs were carried out in 1:2:2 (promoter:TF1:TF2) ratio. Infiltrations
308 with more than two TFs (equimolar mix) were carried out at 1:4 (promoter:TF mix) ratio.
309 Promoter activation was assessed by comparison of firefly:renilla luciferase luminescence
310 ratios (LUC/REN) determined 3-4 d after infiltration according to Hellens et al. (2005).
311
312 *Electrophoretic mobility shift assays (EMSA)*
313 The DNA binding domains of *AaNAC1-4* were amplified by PCR (Table S2F) and Gateway
314 cloned into the *E. coli* expression vector pET300 according to manufacturer's instructions
315 (Invitrogen), then expressed and purified as described for the terpene synthase enzymes.
316 Complementary 28 bp oligonucleotides for EMSA were 3'-end biotin labeled (Macrogen,
317 Korea) and slowly annealed at RT after heat denaturation. For the binding assay, 1.5 µg of
318 recombinant NAC protein was mixed with 0.3 pmol of double-stranded DNA probe in
319 binding buffer [0.2 mM DTT, 0.02 mM EDTA, 5 mM HEPES-KOH, pH 7.6, 30 mM NaCl,
320 0.8 mg of salmon sperm DNA (sheared), 0.2 mg poly(dI-dC)] in a 20 µl reaction at room
321 temperature for 20 min. The bound complexes were resolved by electrophoresis on native 4%
322 polyacrylamide gels in 0.5% Tris-Borate EDTA (TBE) buffer containing 5% glycerol, pH 8.3,
323 at 200 V for 25 min at 4°C. The gels was electroblotted onto positively charged Hybond N+
324 membrane (GE Healthcare) (25V/15 min) and cross-linked using a UVC500 (Hoefer) at 120
325 mJ/cm^2. Blots were blocked in Tris buffered saline (TBS) containing 3% BSA for 1 h and
326 incubated with 1:1000 Streptavidin−Peroxidase Polymer (Sigma) for 1 h in TBS with 0.05%
327 Tween-20 (TBS-T). All washes (6x 5 min) were in TBS-T. Imaging was conducted with ECL
328 Select substrate (GE Healthcare) using a ChemiDoc MP imager (Bio-Rad).
329

Accession Numbers

GenBank accession numbers:

KF319035 (*AcTPS1*), KF319036 (*AaTPS1*), KF319037 (*AcDXS1*), KF319038 (*AaDXR1*), KF319039 (*AdHDR1*), KF319040 (*AaIDI1*), KF319041 (*AcEIL1*), KF319042 (*AcEIL2*), KF319043 (*AcEIL3*), KF319044 (*AcEIL4*), KF319045 (*AaEIL4*), KF319046 (*AaNAC1*), KF319047 (*AaNAC2*), KF319048 (*AaNAC3*), KF319049 (*AaNAC4*), KF319050 (*AcNAC1*), KF319051 (*AcNAC2*), KF319052 (*AcNAC3*), KF319053 (*AcNAC4*), KF319054 (*AcTPS1* promoter), KF319055 (*AaTPS1* promoter).

RESULTS

Volatile terpenes in ripe Actinidia *fruit*

An extensive collection of wild kiwifruit (*Actinidia* spp.) germplasm was examined for variation in terpene production using a combination of volatile headspace sampling and GC-MS analysis. The concentrations of terpenes produced in ripe fruit varied greatly among the different kiwifruit species (Fig 1; for individual compounds see Table S3). Fruit from some species such as *A. arguta* and *A. chrysantha* produced very high concentrations of terpenes, while fruit from others such as *A. chinensis* and *A. deliciosa* produced much lower amounts. From this survey we selected the small green-fleshed *A. arguta* cultivar 'Hortgem Tahi' and larger yellow-fleshed *A. chinensis* cultivar 'Hort16A' for detailed volatile analysis during fruit development and across different ripening stages (Fig 2A and 2B). *A. arguta* ('Hortgem Tahi') ripe fruit pulp released much higher concentrations of terpenes than *A. chinensis* ('Hort16A') (1000 ng gFW^{-1} h^{-1} v. 7 ng gFW^{-1} h^{-1}) at the respective eating ripe stages (a3/c2), and in both species the profile predominantly consisted of cyclic monoterpenes. In *A. arguta,* volatile terpene production increased rapidly during the fruit ripening phase and correlated with large increases in ethylene release and fruit softening (Fig 2E). The *A. arguta* headspace terpene profile was dominated by terpinolene (59% of terpene content at a3 eating ripe stage), myrcene (13%), α-pinene (11%) and limonene (10%). *A. chinensis* released relatively low concentrations of mainly 1,8-cineole (eucalyptol) at the over-ripe stage (Fig 2B/F).

Identification of AaTPS1 and AcTPS1 terpene synthase genes

A single TPS candidate, *AaTPS1*, represented by multiple ESTs, was identified from an *A. arguta* 'Hortgem Tahi' ripe fruit EST library (n = 10,400 ESTs). No candidate TPS genes were identified in *A. chinensis* 'Hort16A' ripe fruit libraries (n = 7,900 ESTs), however a

highly homologous gene, *AcTPS1* with 88.7% amino acid identity, was identified from an *A. chinensis* 'Hort16A' young fruit library (n = 10,200). *In silico* ORF prediction showed that the *AaTPS1* and *AcTPS1* genes encoded proteins of 603 and 604 amino acids respectively and that these proteins contained the expected divalent metal binding regions (i.e. DDXXD and NSE/DTE motifs) necessary for TPS activity (Cane and Kang, 2000; Rynkiewicz et al., 2001). *AaTPS1* and *AcTPS1* also possessed the RRX_8W motif common to cyclic monoterpene producing enzymes (Williams et al., 1998) and were both predicted to contain chloroplast-targeting peptides (Fig S1A).

AaTPS1 *and* AcTPS1 *likely originate from a common ancestral gene*

An analysis of the kiwifruit genome sequence of the cultivar 'Hongyang' (Huang et al., 2013) identified 35 terpene synthase gene models within the kiwifruit genome (Fig S1B). Phylogenetic clustering showed that *AaTPS1* and *AcTPS1* grouped with other mono-TPS genes in the *Tps-b* subfamily (Fig S1B) (Bohlmann et al., 1998), and that the eight gene models most closely related to *AaTPS1* and *AcTPS1* were part of a single scaffold of tandemly repeated genes (Fig S2A) covering about 155 kb. The existing gene models were refined manually by identifying and extracting individual exons homologous to *AcTPS1* exons 1-7. Phylogenetic analysis of the curated/translated proteins (Fig S2B) showed that *AaTPS1* and *AcTPS1* are likely to be orthologs originating from a common ancestral gene and that *A. chinensis* paralogs arose due to multiple tandem duplication events (Fig 3). These events were accompanied by significant loss of exons and promoters, non-sense mutations and insertions/deletions within the scaffold, resulting in only three gene models that could potentially encode functional TPS proteins (Achn286231, Achn286241 and Achn2862XX). Gene model Achn286231 represents the corresponding *AcTPS1* sequence within the 'Hongyang' genome, sharing 99% amino acid identity in the coding region sequence. Other TPS scaffold members shared between 69-96% amino acid identity (Fig S2C).

RNA and protein expression analysis

AaTPS1 expression increased sharply during fruit ripening with the highest levels of expression being found in over-ripe fruit (stages a4/a5, Fig 2C), while *AcTPS1* expression was modest (< 1/1000 of *AaTPS1*) in developing fruit (30 to 60 DAP) and not present in ripe fruit (Fig 2D). Western analysis using a polyclonal antibody that detects both kiwifruit TPS enzymes (Fig 2C and 2D lower panels) showed that the AcTPS1 protein could be detected weakly in young fruit (30 DAP). In contrast, AaTPS1 protein was present at much higher

concentrations, with accumulation first becoming apparent at the a2 stage, then increasing sharply and peaking in over-ripe fruit (a5 stage). The other two full length TPS genes identified within the 'Hongyang' TPS scaffold (Achn286241 and Achn2862XX) were not expressed at harvest or in ripe *A. chinensis* 'Hort16A' fruit. TPS expression using primers universal for *AaTPS1* and *AcTPS1* was strongly ripening induced in the three high level terpene producing species (*A. arguta*, *A. eriantha* and *A. macrosperma* x *melanandra*) but undetectable in the low species (*A. chinensis*, *A. deliciosa*, *A. macrosperma*) (Fig S3A).

Functional characterization of AaTPS1 and AcTPS1

Recombinant proteins were expressed in *E. coli* and purified using a combination of Ni^{2+} affinity and size exclusion chromatography. *In vitro* solvent extraction assays followed by enantioselective GC-MS showed that the recombinant AaTPS1 enzyme catalyzed the conversion of GDP to both cyclic and non-cyclic monoterpene products. Specifically, α-terpinolene was the predominant terpene produced, accounting for ~67% of the total monoterpenes, followed by ß-myrcene (10%), predominantly (*S*)-limonene (9%) and smaller amounts of α-pinene, linalool and α-terpineol (Fig 4). AcTPS1 produced the non-cyclic monoterpenes geraniol and β-myrcene as the major products rather than 1,8-cineole, which is the predominant terpene associated with *A. chinensis* fruit. The enantiomeric composition of terpenes produced by AaTPS1 *in vitro* and those produced in ripe *A. arguta* 'Hortgem Tahi' fruit (stage a3/a4) were very similar (Fig 4). To verify the likely *in planta* function of *AaTPS1* and *AcTPS1* further, both genes were transiently expressed in *N. benthamiana* leaves. Leaves transiently expressing *AaTPS1* produced a monoterpene profile very similar to that seen in ripe *A. arguta* fruit and also from the *in vitro* enzyme analysis (Fig S4A). Tobacco leaves expressing *AcTPS1* produced β-myrcene in low amounts as the only gene-specific product (Fig S4B). Geraniol, which was observed in the AcTPS1 *in vitro* analysis, was not identified after transient expression *in planta* likely due to glycosylation, which has been previously observed in *N. benthamiana* with a transiently expressed geraniol synthase (Dong et al., 2013).

Kinetic characterization of the recombinant AaTPS1 and AcTPS1 enzymes confirmed their requirement for a divalent metal ion co-factor (Table 1). AcTPS1 favored Mn^{2+} over Mg^{2+} (K_m = ~20 µM and 1.5 mM respectively) and also showed a two-fold increase in maximal velocity (V_{max}) with Mn^{2+} compared with Mg^{2+}. AaTPS1 binding constants for Mn^{2+} and Mg^{2+} were similar to AcTPS1, although a higher V_{max} was observed with Mg^{2+}. Despite a

~three-fold increase in AaTPS1 turnover compared with AcTPS1, catalytic efficiencies (k_{cat}/K_m) for both enzymes were similar. K^+ had no effect on AaTPS1 and AcTPS1 activities and neither enzyme used FDP as a substrate.

Substrate flux of terpene precursors though the MEP pathway

The principal route for monoterpene substrate synthesis is located in the plastids where the 2-*C*-methyl-D-erythritol-4-P (MEP) pathway (see Fig 5) produces IDP, which can be isomerized to DMADP through the action of IDP isomerase (IDI). To investigate the potential role of genes in the MEP pathway in controlling substrate flux in kiwifruit, gene candidates were identified in fruit EST collections for each of the MEP pathway enzymes. Patterns of gene expression were determined by qPCR in both *A. arguta* and *A. chinensis* in unripe (stages a0/c0), eating ripe (a3/c2) and over-ripe (a5/c4) fruit (Fig 5) and full-length candidate genes were cloned for *in planta* expression analysis. Results showed that DXS gene expression was strongly induced (>20-fold) during fruit ripening in both kiwifruit species. Although the remaining MEP pathway genes showed small differences in gene expression, there was no discernible correlation with ripening and volatile release and little consistency in expression patterns across the two kiwifruit species.

Expression of MEP pathway genes in a transient system

Transient over-expression of the DXS gene cloned from ripe *A. chinensis* fruit (*AcDXS1*) resulted in small but significant increases in endogenous terpene production from the infiltrated *N. benthamiana* leaves (Fig 6). Co-infiltrating *AcDXS1* with *AaTPS1* resulted in a large increase (>100-fold) in terpene production compared with infiltration of *AaTPS1* alone. Combining transient expression of *AaTPS1* and *AcDXR1* resulted in a significant (α=0.05) increase of about two-fold in terpene production, while the other two genes tested (*AcHDR1* and *AcIDI1*) had no stimulatory effect. Combining over-expression of all four MEP pathway genes with *AaTPS1* did not enhance the production compared with transient expression of DXS alone (possibly because of a transgene dilution effect). These results demonstrate that the DXS gene is a rate-limiting step in the production of terpenes *in planta* by endogenous *N. benthamiana* terpene synthases, and supports the hypothesis that that DXS is the rate-limiting enzyme in terpene synthesis in ripe *A. arguta* fruit where DXS and TPS genes are both transcriptionally up-regulated.

Upstream regulatory elements in the AaTPS1 *and* AcTPS1 *promoters*

The promoter regions of *AaTPS1* and *AcTPS1* including 35 bp of 5'-untranslated region (Fig S5A) were isolated to compare the upstream regulatory elements controlling transcription of both genes. A 911 bp *AaTPS1* promoter fragment (Aa *TPS*1_{pro}-911) was obtained by inverse PCR while a 3 kb promoter fragment of *AcTPS1* (Ac *TPS*1_{pro}-3000) was obtained by PCR based on *A. chinensis* genome assemblies. The two promoters shared 68% identity (Fig S5B). Comparison of the *AaTPS1* promoter region with the 'Hongyang' TPS scaffold members showed that only Achn286231 (the gene corresponding most closely to *AcTPS1*, 99% identity) and Achn286241 shared similar promoter identity (Fig S5B). Achn286241 contained a 1.2 kb insertion close to the predicted TATA box (Fig S5B) which would likely render the promoter inactive.

Potential NAC and EIL binding sites were identified manually within the first 911 bp of the *AaTPS1* and *AcTPS1* promoter fragments as well as multiple Ethylene Response Elements (EREs) based on previously identified consensus binding sites (Fig 7A, Fig S6). The Aa *TPS*1_{pro}-911 proximal region had five copies of the ERE, while the equivalent Ac *TPS*1_{pro} region only had two. Furthermore, Aa *TPS*1_{pro}-900 contained a potential proximal NAC binding site with a conserved ACGTA core motif, while this core was mutated in *AcTPS1* (Fig S6).

Identification of NAC and EIL transcription factors in ripe kiwifruit

NAC and EIL TFs expressed in ripe *A. chinensis* and *A. arguta* fruit were identified by screening a wide range of ripe kiwifruit EST libraries (Crowhurst et al., 2008) supplemented with next generation sequencing data. Five candidate EIL TFs (*AcEIL1-4/AaEIL4*) and eight NAC TFs (*Aa/AcNAC1-4*) were identified and cloned from ripe *A. arguta* and *A. chinensis* cDNA. Within each class there was high amino acid sequence identity (Fig S7 and Fig S8). The four NAC TFs were all strongly induced during ripening (3- to 74-fold) and highly expressed relative to the reference gene EF1α in both *A. chinensis* and *A. arguta* (Fig 8). Interestingly there were also significant differences in the expression profiles between the two species. *NAC1* showed the lowest induction in both species. *NAC4* was the most up-regulated in *A. arguta* (32-fold), while *NAC3* was most up-regulated in *A. chinensis* (74-fold). Overall, the five EIL TFs had lower expression levels than the NAC TF class, with *EIL2* showing the highest level of expression but all show a degree of transcriptional induction (2- to 6-fold) over the course of ripening. To test whether the *NAC1-4* transcriptional induction was a conserved phenomenon during kiwifruit fruit ripening, expression was tested on a

taxonomically wider panel of *Actinidia* species. In all cases, the NAC genes (1-4) were strongly induced in ripe fruit compared to fruit at harvest (Fig S3B-E), strongly supporting the idea that NAC genes form an integral part of the fruit ripening program within the *Actinidia* genus.

Functional testing of kiwifruit NAC and EIL transcription factors

Promoter activation was assessed by comparison of firefly:renilla luciferase luminescence ratios determined 3-4 d after *Agrobacterium* infiltration into *N. benthamiana* leaves. Aa *TPS*1_{pro}-911 was activated three- to six-fold by all individual *AaNAC* and *AcEIL*/*AaEIL* TFs tested (Fig 9A and 9C). Infiltration with an equimolar mixture of all four *AaNAC* TFs activated the Aa *TPS*1_{pro}-911 more strongly than any of the individual *AaNAC* TFs, but the difference was only significantly higher ($\alpha = 0.01$) than with *AaNAC3* and *4*. Infiltration of *AaNAC* TFs in paired combinations typically (five of the six combinations tested) led to higher and more consistent promoter activation than activation by individual TFs, suggesting that heterodimers might activate more favorably (Fig 9A). In contrast, Ac *TPS*1_{pro}-3000 and two promoter deletion constructs (Ac *TPS*1_{pro}-600 and -229) were all weakly activated (<2-fold) by the equimolar mixtures of *AcEIL*/*AaEIL* TFs, and no significant activation was observed for the mixture of NAC TFs (Fig 9B).

For the EIL TFs there was little difference in activation of Aa *TPS*1_{pro}-911 between individual TFs versus a mix of all five EIL TFs (Fig 9C). Combining all EIL and NAC TFs did not further activate Aa *TPS*1_{pro}-911 compared with NAC TFs alone, suggesting that there are no interactive or additive activation effects between these two classes of TFs.

A 238 bp minimal *AaTPS1* promoter clone (Aa *TPS*1_{pro}-238) was generated to compare activation directly with that of the equivalent region in *AcTPS1* (Ac *TPS*1_{pro}-229), which contains a substitution in the conserved NAC core-binding motif (ACGTA→ACATA). An Aa *TPS*1_{pro}-238 mutant ($_{pro}$-238Mut) was also generated that contained five nucleotide substitutions around the NAC core (Fig S9) compared with Aa *TPS*1_{pro}-238. Neither the $_{pro}$-238Mut nor the Ac *TPS*1_{pro}-229 promoter was activated by AaNAC TFs, while the $_{pro}$-238Mut still showed activation by *AcEIL*/*AaEIL* TFs (albeit slightly less than Aa *TPS*1_{pro}-238). These data strongly suggest that a proximal NAC binding region is present in the *AaTPS1* promoter and is important for NAC activation, which has been lost in the *AcTPS1* promoter.

To test the importance of the NAC binding region further, 12 bp (spanning the conserved core-binding motif) of the NAC binding site in the *AaTPS1* promoter was re-inserted into the

AcTPS1 promoter at position -208 to generate a minimal promoter that contained intact NAC binding sites (Fig S9). Inserting this repeat was able to rescue the activation of Ac *TPS*1_{pro}-208 by AaNAC TFs. Five tandem copies of the repeat restored NAC activation of the minimal 208 bp promoter, while one and three copies were insufficient (Fig 9E). Enhanced auto-activation of the apple MYB10 promoter containing multiple repeats of a MYB binding site has been previously observed (Espley et al., 2009).

In vitro *binding of AaNACs to the proximal* AaTPS1 *NAC binding site*

Electrophoretic mobility shift assays **(**EMSAs) were undertaken to directly test for binding of the four AaNAC TFs to the proximal NAC binding site in the *AaTPS1* promoter. The predicted NAC DNA binding domains of all four *AaNACs* were over-expressed in *E. coli* and purified by Ni^{2+} affinity and size exclusion chromatography (SEC) to > 95% purity. Based on SEC, all four proteins ran as dimers. The EMSAs demonstrated strong binding between a biotin labeled 28 bp double strand DNA fragment of the proximal *AaTPS1* NAC binding site (spanning the conserved core-binding motif) and AaNAC2 and weaker binding to AaNAC3, and AaNAC4 (Figure 10). No binding was observed using the binding domain of AaNAC1. The equivalent 28 bp fragment from the *AcTPS1* promoter with the mutated NAC core binding motif showed essentially no capacity to bind to the NAC TFs. Together with the transient expression analyses, these results demonstrate the requirement for the proximal NAC binding site and NAC TF binding for controlling monoterpene production in kiwifruit.

Discussion

Kiwifruit have only very recently been domesticated and different accessions and cultivars show wide natural variation in the types and quantity of terpenes they produce during ripening (Crowhurst et al., 2008; Fig 1 and Table S3). This variation provides an excellent resource for studying the mechanisms that control terpene production in fruit. Here we report on the mechanisms that lead to differential monoterpene production in the fruit of two species of kiwifruit, namely *A. arguta* 'Hortgem Tahi', which produces high concentrations of terpinolene during the final climacteric ripening stages (Fig 2) and *A. chinensis* 'Hort16A', which produces low concentrations of 1,8-cineole during the equivalent stages. In 'Hortgem Tahi', the *AaTPS1* gene can account for the qualitative variation in ripe fruit monoterpene production (Fig 4), while in 'Hort16A' fruit, *AcTPS1* gene is expressed at low levels and makes β-myrcene and geraniol, which are found in negligible amounts during fruit development and ripening. The production of 1,8-cineole in 'Hort16A' fruit indicates that a

second TPS is expressed during ripening in this cultivar, but the corresponding gene was not identified in ripe fruit EST libraries or genome sequences. Considering the inherent functional plasticity within TPS enzymes (Yoshikuni et al., 2006; Keeling et al., 2008; O'Maille et al., 2008), it is not surprising that AcTPS1 and AaTPS1, despite sharing ~90% amino acid homology (excluding chloroplast transit peptide), have very different product specificities.

MEP pathway analysis

Quantitative variation in monoterpene production can be controlled by substrate flux through the MEP pathway (Munoz-Bertomeu et al., 2006). The MEP pathway is subject to multiple levels of regulation, including transcriptional, post-transcriptional, product feedback inhibition and retrograde chloroplast to nuclear signaling (Cordoba et al., 2009; Banerjee et al., 2013). In *A. arguta*, expression of *DXS* increased dramatically during fruit ripening, while the transcript levels of other MEP pathway genes were induced to a much lesser extent (Fig 5). Over-expression of the *AcDXS* gene in *N. benthamiana* leaves resulted in significantly increased concentrations of *AaTPS1*-derived monoterpenes (>100-fold), while transient over-expression of *DXR* only resulted in a two-fold increase in monoterpene production. These results suggest that transcriptional control of the *DXS* gene is likely to be a key step in controlling terpene substrate flux in *A. arguta* fruit (Fig 6). These data contrast with results from Arabidopsis, where over-expression of DXS, DXR and HDR all led to only moderate (three- to 13-fold) increases in transgenic taxadiene production (Botella-Pavía et al., 2004; Carretero-Paulet et al., 2006), probably because modifying the MEP flux leads to deleterious phytohormone concentrations (ABA/gibberellins) and also alters amounts of chlorophyll and carotenoids in stably transformed transgenic plants.

In *A. chinensis*, expression of *DXS* also increased strongly during fruit ripening, and transient over-expression of *DXS* with *AcTPS1* resulted in a 10-fold increase in production of myrcene. This increase was not as large as observed with AaTPS1, suggesting that structural differences in the two enzymes may be influencing their respective capacities to use the increased amounts of substrate present. This may also reflect the three-times reduced turnover rate of AcTPS1 compared with AaTPS1. These results suggested that lack of MEP substrate flux was not a major contributor to the low terpene production observed in ripe 'Hort16A' fruit, but rather reduced terpene synthase activity.

Terpene synthase transcriptional regulation

Ethylene biosynthesis is tightly controlled during fruit development and two modes of regulation have been proposed (Barry et al., 2000). During vegetative growth and in immature fruit, system I ethylene is auto-inhibitory, while during climacteric ripening and senescence system II ethylene is auto-catalytic and can be induced by ethylene application. In kiwifruit, studies on ethylene biosynthesis (ACO) knockdown *A. chinensis* 'Hort16A' lines indicated that volatile production was tightly associated with system II/climacteric ethylene production (Atkinson et al., 2011). Here we show that several NAC and EIL TFs are induced during climacteric ripening and expressed at high levels in ripe *A. arguta* and *A. chinensis* fruit (Fig 7). EIL TFs have been shown to be regulated post-translationally because of stabilization of the protein in the presence of ethylene (Guo and Ecker, 2003; Potuschak et al., 2003; Yanagisawa et al., 2003). The *AaTPS1* promoter, which contains several predicted NAC and EIN3 binding sites (Figs 7, 9), was activated by all the kiwifruit NAC and EIL TFs tested. EMSA showed that a 28 bp of the *AaTPS1* promoter (spanning the conserved core-binding motif) but not the *AcTPS1* fragment (containing a mutated form of the core-binding motif) physically interacts with the AaNAC2-4 DNA binding domain. AaNAC1 doesn't bind to the fragment, so likely binds to a different site in the *AaTPS1* promoter. The EIL activation was similar for all the class members. Notably, for the NAC class, our data suggest that heterodimers might activate the *AaTPS1* promoter more favorably than homodimers, and more strongly than EIL activation. Plant NAC TFs have previously been shown to act as homo- and heterodimers (Hegedus et al., 2003; Jeong et al., 2009). This allows for increased combinatorial potential, as NACs are one of the largest families of plant-specific TFs, with estimated >100 members in various plant species (Ooka et al., 2003; Rushton et al., 2008). Recent work suggests that some NAC members may also physically interact with EIL TFs (Shan et al., 2012), although the biological relevance of this is still unclear.

For most NACs, the biochemical and functional specificity is associated with both the DNA binding domain (DBD) and the transcriptional regulation domain (TRD) (Jensen et al., 2010). Furthermore, NAC TFs act not only as activators, since they carry the NARD repression domain (Hao et al., 2010). It is conceivable that prior to fruit ripening, other flavor-related gene promoters and promoters involved in ethylene biosynthesis and softening are actively repressed. Such complexity has been observed in tomato, where the action of the AP2 class TF SlAP2a/AP2a (Chung et al., 2010; Karlova et al., 2011) negatively regulates fruit ripening, while the action of positive signals such as LeMADS-RIN (Vrebalov et al., 2002), CLEAR NON-RIPENING/Cnr (Manning et al., 2006), TAGL1 (Vrebalov et al., 2009),

LeHB-1 (Lin et al., 2008), and the NAC TFs SlNAC4 and NOR (Martel et al., 2011; Zhu et al., 2014) promote ripening.

By exploring natural variation in *TPS1* gene promoters, we show that high terpene production in *A. arguta* ripe fruit is mediated through NAC activation of the *AaTPS1* promoter, whilst low terpene production in *A. chinensis* 'Hort16A' ripe fruit is due to lack of *AcTPS1* expression/NAC activation. NAC TF levels are highly up-regulated in ripening in all kiwifruit species tested, while TPS up-regulation is restricted to species producing high levels of terpenes (Fig S3). These results clearly identify that NAC TFs are important in controlling monoterpene production in kiwifruit and are likely to be activating/repressing ripening traits in many fruits.

Supplementary Material

Table S1. Characteristics of *Actinidia arguta* 'Hortgem Tahi' and *A. chinensis* 'Hort16A' ripening fruit.

Table S2. Cloning and PCR primers.

Table S3. Ripe fruit headspace terpene compounds in fourteen kiwifruit species.

Figure S1. (A) Alignment of the deduced amino acid sequences of *AaTPS1* and *AcTPS1* and other *Tps-b* subfamily terpene synthases. (B) Unrooted Maximum Likelihood tree of *AcTPS1* and *AaTPS1* with other terpene synthases from kiwifruit, grape, apple, tomato and poplar.

Figure S2. (A) Mapping of *AcTPS1* exons 1-7 onto scaffolds in the kiwifruit genome. (B) Amino acid alignment of manually curated kiwifruit TPS1-like gene models. (C) Sequence identity table of aligned kiwifruit TPS1-like amino acid sequences.

Figure S3. Real-time qPCR analysis of *TPS1* (A) and *NAC1-4* (B-E) gene expression levels in harvest and ripe fruit for six *Actinidia* species.

Figure S4. GC-MS analysis of the monoterpenes produced by transient expression of *AaTPS1* and *AcTPS1 in planta.*

Figure S5. (A) Identifying the transcriptional start site in the 5'-UTR of *AaTPS1*. (B) Sequence alignment of *AaTPS1, AcTPS1* and *Achn286241* promoter regions.

Figure S6. Binding sites in the *AaTPS1* and *AcTPS1* promoter regions.

Figure S7. (A) ClustalW alignment of the *Actinidia chinensis* and *A. arguta NAC1-4* proteins. (B) Unrooted Maximum Likelihood tree of selected *Arabidopsis thaliana*, *A. arguta* and *A. chinensis* NACs.

Figure S8. (A) ClustalW alignment of the *Actinidia deliciosa*, *A. chinensis* and *A. arguta EIL1-4* proteins. (B) Unrooted Maximum Likelihood tree of *A. deliciosa*, *A. arguta* and *A. chinensis* EIN3-like transcription factors compared to *Arabidopsis thaliana*.

Figure S9. Sequence alignment of minimal Aa $TPS1_{pro}$ and Ac $TPS1_{pro}$ promoter fragments.

ACKNOWLEDGEMENTS

We would like to thank Monica Dragulescu and Wade Wadasinghe for maintaining the *N. benthamiana* plants, Mark Wohlers for help with statistics, Tim Holmes and Darren Snaith for help with imaging, Robert Schaffer, Kevin Davies and William Laing for critically reviewing the manuscript, Andrew Gleave and the cloning team for help with vector construction, and Lesley Beuning for preliminary gene mining.

References

Alexander L, Grierson D (2002) Ethylene biosynthesis and action in tomato: a model for climacteric fruit ripening. Journal of Experimental Botany **53:** 2039-2055

Atkinson RG, Gunaseelan K, Wang MY, Luo L, Wang T, Norling CL, Johnston SL, Maddumage R, Schroder R, Schaffer RJ (2011) Dissecting the role of climacteric ethylene in kiwifruit (*Actinidia chinensis*) ripening using a 1-aminocyclopropane-1-carboxylic acid oxidase knockdown line. Journal of Experimental Botany **62:** 3821-3835

Banerjee A, Wu Y, Banerjee R, Li Y, Yan HG, Sharkey TD (2013) Feedback inhibition of deoxy-D-xylulose-5-phosphate synthase regulates the methylerythritol 4-phosphate pathway. Journal of Biological Chemistry **288:** 16926-16936

Barry CS, Llop-Tous MI, Grierson D (2000) The regulation of 1-aminocyclopropane-1-carboxylic acid synthase gene expression during the transition from system-1 to system-2 ethylene synthesis in tomato. Plant Physiology **123:** 979-986

Battilana J, Costantini L, Emanuelli F, Sevini F, Segala C, Moser S, Velasco R, Versini G, Grando M (2009) The 1-deoxy-D-xylulose 5-phosphate synthase gene co-localizes with a major QTL affecting monoterpene content in grapevine. Theoretical and Applied Genetics **118:** 653-669

Bohlmann J, Meyer-Gauen G, Croteau R (1998) Plant terpenoid synthases: Molecular biology and phylogenetic analysis. Proceedings of the National Academy of Sciences USA **95:** 4126-4133

Botella-Pavía P, Besumbes Ó, Phillips MA, Carretero-Paulet L, Boronat A, Rodríguez-Concepción M (2004) Regulation of carotenoid biosynthesis in plants: evidence for a key role of hydroxymethylbutenyl diphosphate reductase in controlling the supply of plastidial isoprenoid precursors. Plant Journal **40:** 188-199

Buttery RG, Teranishi R, Ling LC, Flath RA, Stern DJ (1988) Quantitative studies on origins of fresh tomato aroma volatiles. Journal of Agricultural and Food Chemistry **36:** 1247-1250

Cane DE, Kang I (2000) Aristolochene synthase: Purification, molecular cloning, high-level expression in *Escherichia coli*, and characterization of the *Aspergillus terreus* cyclase. Archives of Biochemistry and Biophysics **376:** 354-364

Carretero-Paulet L, Cairó A, Botella-Pavía P, Besumbes O, Campos N, Boronat A, Rodríguez-Concepción M (2006) Enhanced flux through the methylerythritol 4-phosphate pathway in Arabidopsis plants overexpressing deoxyxylulose 5-phosphate reductoisomerase. Plant Molecular Biology **62:** 683-695

Chang KN, Zhong S, Weirauch MT, Hon G, Pelizzola M, Li H, Huang SS, Schmitz RJ, Urich MA, Kuo D, Nery JR, Qiao H, Yang A, Jamali A, Chen H, Ideker T, Ren B, Bar-Joseph Z, Hughes TR, Ecker JR (2013) Temporal transcriptional response to ethylene gas drives growth hormone cross-regulation in Arabidopsis. Elife **2:** e00675

Chen F, Tholl D, Bohlmann J, Pichersky E (2011) The family of terpene synthases in plants: a mid-size family of genes for specialized metabolism that is highly diversified throughout the kingdom. Plant Journal **66:** 212-229

Chung MY, Vrebalov J, Alba R, Lee J, McQuinn R, Chung JD, Klein P, Giovannoni J (2010) A tomato (*Solanum lycopersicum*) APETALA2/ERF gene, SlAP2a, is a negative regulator of fruit ripening. Plant Journal **64:** 936-947

Cordoba E, Salmi M, Leon P (2009) Unravelling the regulatory mechanisms that modulate the MEP pathway in higher plants. Journal of Experimental Botany **60:** 2933-2943

Crowhurst RN, Gleave AP, MacRae EA, Ampomah-Dwamena C, Atkinson RG, Beuning LL, Bulley SM, Chagne D, Marsh KB, Matich AJ, Montefiori M, Newcomb RD, Schaffer RJ, Usadel B, Allan AC, Boldingh HL, Bowen JH, Davy MW, Eckloff R, Ferguson AR, Fraser LG, Gera E, Hellens RP, Janssen BJ, Klages K, Lo KR, MacDiarmid RM, Nain B, McNeilage MA, Rassam M, Richardson AC, Rikkerink EH, Ross GS, Schröder RA, Snowden KC, Souleyre EJ, Templeton MD, Walton EF, Wang D, Wang MY, Wang YY, Wood M, Wu R, Yauk Y-K, Laing WA (2008) Analysis of expressed sequence tags from *Actinidia*: applications of a cross species EST database for gene discovery in the areas of flavor, health, color and ripening. BMC Genomics **9:** 351

Dong L, Miettinen K, Goedbloed M, Verstappen FWA, Voster A, Jongsma MA, Memelink J, Krol Svd, Bouwmeester HJ (2013) Characterization of two geraniol synthases from *Valeriana officinalis* and *Lippia dulcis*: Similar activity but difference in subcellular localization. Metabolic Engineering **20:** 198-211

Duchêne E, Butterlin G, Claudel P, Dumas V, Jaegli N, Merdinoglu D (2009) A grapevine (*Vitis vinifera L.*) deoxy-D-xylulose synthase gene colocates with a major quantitative trait loci for terpenol content. Theoretical and Applied Genetics **118:** 541–552

Dudareva N, Cseke L, Blanc VM, Pichersky E (1996) Evolution of floral scent in *Clarkia*: Novel patterns of S-linalool synthase gene expression in the *C. breweri* flower. Plant Cell **8:** 1137-1148

Emanuelsson O, Nielsen H, von Heijne G (1999) ChloroP, a neural network-based method for predicting chloroplast transit peptides and their cleavage sites. Protein Science **8:** 978-984

Enfissi EM, Fraser PD, Lois LM, Boronat A, Schuch W, Bramley PM (2005) Metabolic engineering of the mevalonate and non-mevalonate isopentenyl diphosphate-forming pathways for the production of health-promoting isoprenoids in tomato. Plant Biotechnology Journal **3:** 17-27

Espley RV, Brendolise C, Chagne D, Kutty-Amma S, Green S, Volz R, Putterill J, Schouten HJ, Gardiner SE, Hellens RP, Allan AC (2009) Multiple Repeats of a Promoter Segment Causes Transcription Factor Autoregulation in Red Apples. Plant Cell **21:** 168-183

Estévez JM, Cantero A, Reindl A, Reichler S, León P (2001) 1-Deoxy-D-xylulose-5-phosphate synthase, a limiting enzyme for plastidic isoprenoid biosynthesis in plants. Journal of Biological Chemistry **276:** 22901-22909

Green SA, Chen X, Matich AJ (2012) *In planta* transient expression analysis of monoterpene synthases. Methods in Enzymology **515:** 43-61

Green SA, Chen X, Nieuwenhuizen NJ, Matich AJ, Wang MY, Bunn BJ, Yauk YK, Atkinson RG (2012) Identification, functional characterization, and regulation of the enzyme responsible for floral (*E*)-nerolidol biosynthesis in kiwifruit (*Actinidia chinensis*). Journal of Experimental Botany **63:** 1951-1967

Guo H, Ecker JR (2003) Plant responses to ethylene gas are mediated by SCF(EBF1/EBF2)-dependent proteolysis of EIN3 transcription factor. Cell **115:** 667-677

Hall DE, Robert JA, Keeling CI, Domanski D, Quesada AL, Jancsik S, Kuzyk MA, Hamberger B, Borchers CH, Bohlmann J (2011) An integrated genomic, proteomic and biochemical analysis of (+)-3-carene biosynthesis in Sitka spruce (*Picea sitchensis*) genotypes that are resistant or susceptible to white pine weevil. Plant Journal **65:** 936-948

Hao YJ, Song QX, Chen HW, Zou HF, Wei W, Kang XS, Ma B, Zhang WK, Zhang JS, Chen SY (2010) Plant NAC-type transcription factor proteins contain a NARD domain for repression of transcriptional activation. Planta **232:** 1033-1043

Hegedus D, Yu M, Baldwin D, Gruber M, Sharpe A, Parkin I, Whitwill S, Lydiate D (2003) Molecular characterization of *Brassica napus* NAC domain transcriptional activators induced in response to biotic and abiotic stress. Plant Molecular Biology **53:** 383-397

Hellens RP, Allan AC, Friel EN, Bolitho K, Grafton K, Templeton MD, Karunairetnam S, Gleave AP, Laing WA (2005) Transient expression vectors for functional genomics, quantification of promoter activity and RNA silencing in plants. Plant Methods **1:** 1-14

Hong GJ, Xue XY, Mao YB, Wang LJ, Chen XY (2012) Arabidopsis MYC2 interacts with DELLA proteins in regulating sesquiterpene synthase gene expression. Plant Cell **24:** 2635-2648

Huang S, Ding J, Deng D, Tang W, Sun H, Liu D, Zhang L, Niu X, Zhang X, Meng M, Yu J, Liu J, Han Y, Shi W, Zhang D, Cao S, Wei Z, Cui Y, Xia Y, Zeng H, Bao K, Lin L, Min Y, Zhang H, Miao M, Tang X, Zhu Y, Sui Y, Li G, Sun H, Yue J, Sun J, Liu F, Zhou L, Lei L, Zheng X, Liu M, Huang L, Song J, Xu C, Li J, Ye K, Zhong S, Lu B-R, He G, Xiao F, Wang H-L, Zheng H, Fei Z, Liu Y (2013) Draft genome of the kiwifruit *Actinidia chinensis*. Nat Commun **4**

Itkin M, Seybold H, Breitel D, Rogachev I, Meir S, Aharoni A (2009) TOMATO AGAMOUS-LIKE 1 is a component of the fruit ripening regulatory network. Plant Journal **60:** 1081-1095

Jensen MK, Kjaersgaard T, Nielsen MM, Galberg P, Petersen K, O'Shea C, Skriver K (2010) The *Arabidopsis thaliana* NAC transcription factor family: structure-function relationships and determinants of ANAC019 stress signalling. Biochemical Journal **426:** 183-196

Jeong J, Park Y, Jung H, Park S-H, Kim J-K (2009) Rice NAC proteins act as homodimers and heterodimers. Plant Biotechnology Reports **3:** 127-134

Karlova R, Rosin FM, Busscher-Lange J, Parapunova V, Do PT, Fernie AR, Fraser PD, Baxter C, Angenent GC, de Maagd RA (2011) Transcriptome and metabolite profiling show that APETALA2a is a major regulator of tomato fruit ripening. Plant Cell **23:** 923-941

Keeling CI, Weisshaar S, Lin RPC, Bohlmann J (2008) Functional plasticity of paralogous diterpene synthases involved in conifer defense. Proceedings of the National Academy of Sciences USA **105:** 1085-1090

Keller RK, Thompson R (1993) Rapid synthesis of isoprenoid diphosphates and their isolation in one-step using either thin-layer or flash chromatography. Journal of Chromatography **645:** 161-167

Kollner TG, Held M, Lenk C, Hiltpold I, Turlings TC, Gershenzon J, Degenhardt J (2008) A maize (E)-beta-caryophyllene synthase implicated in indirect defense responses against herbivores is not expressed in most American maize varieties. Plant Cell **20:** 482-494

Kou XH, Watkins CB, Gan SS (2012) Arabidopsis AtNAP regulates fruit senescence. Journal of Experimental Botany **63:** 6139-6147

Li Y, Zhu B, Xu W, Zhu H, Chen A, Xie Y, Shao Y, Luo Y (2007) LeERF1 positively modulated ethylene triple response on etiolated seedling, plant development and fruit ripening and softening in tomato. Plant Cell Reports **26:** 1999-2008

Lin ZF, Hong YG, Yin MG, Li CY, Zhang K, Grierson D (2008) A tomato HD-Zip homeobox protein, LeHB-1, plays an important role in floral organogenesis and ripening. Plant Journal **55:** 301-310

Lois LM, Rodriguez-Concepcion M, Gallego F, Campos N, Boronat A (2000) Carotenoid biosynthesis during tomato fruit development: regulatory role of 1-deoxy-D-xylulose 5-phosphate synthase. Plant Journal **22:** 503-513

MacLeod AJ, Pieris NM (1984) Comparison of the volatile components of some mango cultivars. Phytochemistry **23:** 361-366

Mahmoud SS, Croteau RB (2001) Metabolic engineering of essential oil yield and composition in mint by altering expression of deoxyxylulose phosphate reductoisomerase and menthofuran synthase. Proceedings of the National Academy of Sciences USA **98:** 8915-8920

Manning K, Tor M, Poole M, Hong Y, Thompson AJ, King GJ, Giovannoni JJ, Seymour GB (2006) A naturally occurring epigenetic mutation in a gene encoding an SBP-box transcription factor inhibits tomato fruit ripening. Nature Genetics **38:** 948-952

Mansfield MA (1995) Rapid immunodetection on polyvinylidene fluoride membrane blots without blocking. Analytical Biochemistry **229:** 140-143

Martel C, Vrebalov J, Tafelmeyer P, Giovannoni JJ (2011) The tomato MADS-Box transcription factor RIPENING INHIBITOR interacts with promoters involved in numerous ripening processes in a COLORLESS NONRIPENING-dependent manner. Plant Physiology **157:** 1568-1579

Matich AJ, Young H, Allen JM, Wang MY, Fielder S, McNeilage MA, MacRae EA (2003) *Actinidia arguta*: volatile compounds in fruit and flowers. Phytochemistry **63:** 285-301

Matthews PD, Wurtzel ET (2000) Metabolic engineering of carotenoid accumulation in *Escherichia coli* by modulation of the isoprenoid precursor pool with expression of deoxyxylulose phosphate synthase. Applied Microbiology and Biotechnology **53:** 396-400

Montefiori M, Espley RV, Stevenson D, Cooney J, Datson PM, Saiz A, Atkinson RG, Hellens RP, Allan AC (2011) Identification and characterisation of F3GT1 and F3GGT1, two glycosyltransferases responsible for anthocyanin biosynthesis in red-fleshed kiwifruit (*Actinidia chinensis*). Plant Journal **65:** 106-118

Moufida S, Marzouk B (2003) Biochemical characterization of blood orange, sweet orange, lemon, bergamot and bitter orange. Phytochemistry **62:** 1283-1289

Munoz-Bertomeu J, Arrillaga I, Ros R, Segura J (2006) Up-regulation of 1-deoxy-D-xylulose-5-phosphate synthase enhances production of essential oils in transgenic spike lavender. Plant Physiology **142:** 890-900

Nieuwenhuizen NJ, Beuning LL, Sutherland PW, Sharma NN, Cooney JM, Bieleski LRF, Schröder R, MacRae EA, Atkinson RG (2007) Identification and characterisation of acidic and novel basic forms of actinidin, the highly abundant cysteine protease from kiwifruit. Functional Plant Biology **34:** 946-961

Nieuwenhuizen NJ, Green SA, Chen X, Bailleul EJD, Matich AJ, Wang MY, Atkinson RG (2013) Functional genomics reveals that a compact terpene synthase gene family can account for terpene volatile production in apple. Plant Physiology **161:** 787-804

O'Maille PE, Malone A, Dellas N, Hess BA, Smentek L, Sheehan I, Greenhagen BT, Chappell J, Manning G, Noel JP (2008) Quantitative exploration of the catalytic landscape separating divergent plant sesquiterpene synthases. Nature Chemical Biology **4:** 617-623

Ooka H, Satoh K, Doi K, Nagata T, Otomo Y, Murakami K, Matsubara K, Osato N, Kawai J, Carninci P, Hayashizaki Y, Suzuki K, Kojima K, Takahara Y, Yamamoto K, Kikuchi S (2003) Comprehensive analysis of NAC family genes in *Oryza sativa* and *Arabidopsis thaliana*. DNA Research **10:** 239-247

Orlova I, Nagegowda DA, Kish CM, Gutensohn M, Maeda H, Varbanova M, Fridman E, Yamaguchi S, Hanada A, Kamiya Y, Krichevsky A, Citovsky V, Pichersky E, Dudareva N (2009) The small subunit of snapdragon geranyl diphosphate synthase modifies the chain length specificity of tobacco geranylgeranyl diphosphate synthase *in planta*. Plant Cell **21:** 4002-4017

Phillips MA, Leon P, Boronat A, Rodriguez-Concepcion M (2008) The plastidial MEP pathway: unified nomenclature and resources. Trends in plant science **13:** 619-623

Potuschak T, Lechner E, Parmentier Y, Yanagisawa S, Grava S, Koncz C, Genschik P (2003) EIN3-dependent regulation of plant ethylene hormone signaling by two Arabidopsis F box proteins: EBF1 and EBF2. Cell **115:** 679-689

Rodriguez-Concepcion M, Boronat A (2002) Elucidation of the methylerythritol phosphate pathway for isoprenoid biosynthesis in bacteria and plastids. A metabolic milestone achieved through genomics. Plant Physiology **130:** 1079-1089

Rodriguez A, Alquezar B, Pena L (2013) Fruit aromas in mature fleshy fruits as signals of readiness for predation and seed dispersal. New Phytologist **197:** 36-48

Rushton PJ, Bokowiec MT, Han S, Zhang H, Brannock JF, Chen X, Laudeman TW, Timko MP (2008) Tobacco transcription factors: novel insights into transcriptional regulation in the *Solanaceae*. Plant Physiology **147:** 280-295

Rynkiewicz MJ, Cane DE, Christianson DW (2001) Structure of trichodiene synthase from *Fusarium sporotrichioides* provides mechanistic inferences on the terpene cyclization cascade. Proceedings of the National Academy of Sciences USA **98:** 13543-13548

Schägger H, von Jagow G (1987) Tricine-sodium dodecyl sulfatepolyacrylamide gel electrophoresis for the separation of proteins in the range from 1 to 100 kDa. Analytical Biochemistry **166:** 368–379

Shan W, Kuang J-f, Chen L, Xie H, Peng H-h, Xiao Y-y, Li X-p, Chen W-x, He Q-g, Chen J-y, Lu W-j (2012) Molecular characterization of banana NAC transcription factors and their interactions with ethylene signalling component EIL during fruit ripening. Journal of Experimental Botany **63:** 5171-5187

Solano R, Stepanova A, Chao Q, Ecker JR (1998) Nuclear events in ethylene signaling: a transcriptional cascade mediated by ETHYLENE-INSENSITIVE3 and ETHYLENE-RESPONSE-FACTOR1. Genes & Development **12:** 3703-3714

Tran LS, Nakashima K, Sakuma Y, Simpson SD, Fujita Y, Maruyama K, Fujita M, Seki M, Shinozaki K, Yamaguchi-Shinozaki K (2004) Isolation and functional analysis of Arabidopsis stress-inducible NAC transcription factors that bind to a drought-responsive cis-element in the early responsive to dehydration stress 1 promoter. Plant Cell **16:** 2481-2498

Triglia T (2000) Inverse PCR (IPCR) for obtaining promoter sequence. Methods in Molecular Biology **130:** 79-83

Verdonk JC, Haring MA, van Tunen AJ, Schuurink RC (2005) ODORANT1 regulates fragrance biosynthesis in petunia flowers. Plant Cell **17:** 1612-1624

Vrebalov J, Pan IL, Arroyo AJ, McQuinn R, Chung M, Poole M, Rose J, Seymour G, Grandillo S, Giovannoni J, Irish VF (2009) Fleshy fruit expansion and ripening are regulated by the Tomato SHATTERPROOF gene TAGL1. Plant Cell **21:** 3041-3062

Vrebalov J, Ruezinsky D, Padmanabhan V, White R, Medrano D, Drake R, Schuch W, Giovannoni J (2002) A MADS-box gene necessary for fruit ripening at the tomato ripening-inhibitor (Rin) locus. Science **296:** 343-346

Wang MY, Wohlers M, Chen X, Marsh KB (2011) Changes in volatile production and sensory quality of Actinidia arguta fruit during fruit maturation. Acta Horticulturae **913:** 677-684

Williams DC, McGarvey DJ, Katahira EJ, Croteau R (1998) Truncation of limonene synthase preprotein provides a fully active 'Pseudomature' form of this monoterpene cyclase and reveals the function of the amino-terminal arginine pair. Biochemistry **37:** 12213-12220

Xiao Y-Y, Chen J-Y, Kuang J-F, Shan W, Xie H, Jiang Y-M, Lu W-J (2013) Banana ethylene response factors are involved in fruit ripening through their interactions with ethylene biosynthesis genes. Journal of Experimental Botany **64:** 2499-2510

Xie Q, Frugis G, Colgan D, Chua NH (2000) Arabidopsis NAC1 transduces auxin signal downstream of TIR1 to promote lateral root development. Genes & Development **14:** 3024-3036

Xu YH, Wang JW, Wang S, Wang JY, Chen XY (2004) Characterization of GaWRKY1, a cotton transcription factor that regulates the sesquiterpene synthase gene (+)-delta-cadinene synthase-A. Plant Physiology **135:** 507-515

Xue GP (2005) A CELD-fusion method for rapid determination of the DNA-binding sequence specificity of novel plant DNA-binding proteins. Plant Journal **41:** 638-649

Yamasaki K, Kigawa T, Inoue M, Yamasaki T, Yabuki T, Aoki M, Seki E, Matsuda T, Tomo Y, Terada T, Shirouzu M, Tanaka A, Seki M, Shinozaki K, Yokoyama S (2005) Solution structure of the major DNA-binding domain of *Arabidopsis thaliana* ethylene-insensitive3-like3. Journal of Molecular Biology **348:** 253-264

Yanagisawa S, Yoo SD, Sheen J (2003) Differential regulation of EIN3 stability by glucose and ethylene signalling in plants. Nature **425:** 521-525

Yin XR, Allan AC, Chen KS, Ferguson IB (2010) Kiwifruit EIL and ERF genes involved in regulating fruit ripening. Plant Physiology **153:** 1280-1292

Yoshikuni Y, Ferrin TE, Keasling JD (2006) Designed divergent evolution of enzyme function. Nature **440:** 1078-1082

Zhang K, Gan SS (2012) An abscisic acid-AtNAP transcription factor-SAG113 protein phosphatase 2C regulatory chain for controlling dehydration in senescing Arabidopsis leaves. Plant Physiology **158:** 961-969

Zhang Z, Zhang H, Quan R, Wang XC, Huang R (2009) Transcriptional regulation of the ethylene response factor LeERF2 in the expression of ethylene biosynthesis genes controls ethylene production in tomato and tobacco. Plant Physiology **150:** 365-377

Zhu MK, Chen GP, Zhou S, Tu Y, Wang Y, Dong TT, Hu ZL (2014) A new tomato NAC (NAM/ATAF1/2/CUC2) transcription factor, SlNAC4, functions as a positive regulator of fruit ripening and carotenoid accumulation. Plant and Cell Physiology **55:** 119-135

Zvi MM, Shklarman E, Masci T, Kalev H, Debener T, Shafir S, Ovadis M, Vainstein A (2012) PAP1 transcription factor enhances production of phenylpropanoid and terpenoid scent compounds in rose flowers. New Phytologist **195:** 335-345

Figure legends:

Figure 1 Total headspace terpene volatiles released from the ripe fruit of fourteen *Actinidia* species obtained by purge and trap followed by thermal desorption and semi-quantification by GC-MS. Average terpene concentrations are shown +/- S.E. The number of accessions tested for each species is shown in brackets.

Figure 2 Rates of volatile terpene release by *Actinidia arguta* 'Hortgem Tahi' (A) and *A. chinensis* 'Hort16A' (B) during fruit development (d; days after pollination) and ripening (stages a0-a5 for 'Hortgem Tahi' and c0-c4 for 'Hort16A' fruit, ranging from harvest to over-ripe - see text). Measurements were made in triplicate ± S.E using a purge and trap method followed by thermal desorption and semi-quantification by GC-MS against authentic standards. Only terpenes representing >1% of total terpene content are shown. Real-time qPCR analysis of *AaTPS1* (C, upper panel) and *AcTPS1* (D, upper panel) gene expression levels were performed on pooled fruit samples using gene specific primers given in Table S2. Error bars are based on four technical replicates and data were normalized against the housekeeping gene EF1α. Western analysis of AaTPS1 (C, lower panel) and AcTPS1 (D, lower panel) protein concentrations at equivalent time points using a polyclonal antibody raised against AcTPS1. Change in firmness (squares/left scale) and ethylene (circles/right scale) production in 'Hortgem Tahi' (E) and 'Hort16A' (F) during fruit ripening.

Figure 3 Phylogenetic analysis of the AaTPS1 and AcTPS1 homologous in *A. chinensis* 'HongYang'. Protein sequences extracted from the kiwifruit genome were aligned using ClustalW and manually curated (Fig S2A and B).The evolutionary history was inferred using the Neighbor Joining method with the Jukes-Cantor genetic distance model. The consensus tree is shown based on 80 percent support threshold. The percentage of trees in which the associated taxa clustered together is shown next to the branches based on a 1000 bootstrap replicates. The tree is drawn to scale, with branch lengths measured in the number of substitutions per site. The analysis involved 11 amino acid sequences and no outgroups. Evolutionary analyses were conducted in Geneious 6.1.6.

Figure 4 Percentage terpene volatiles produced by recombinant AaTPS1 and AcTPS1 enzymes *in vitro* and by ripe (stage a3/a4 - see text) *Actinidia arguta* 'Hortgem Tahi' fruit. The recombinant enzymes expressed in *E. coli* were purified by Ni^{2+} affinity and gel filtration chromatography and incubated with GDP as substrate. After solvent extraction, volatile terpenes were analyzed by enantioselective GC-MS. Extractions were performed in triplicate.

Figure 5 Expression of MEP pathway genes during fruit ripening in *Actinidia arguta* (black bars, ripening stages a0, a3, a5 - see text) and *A. chinensis* (grey bars, ripening stages c0, c2, c4 - see text). Real time qPCR analyses were performed on pooled fruit samples using gene-specific primer given in Table S2. Error bars are based on four technical replicates and data were normalized against the housekeeping gene EF1α. Error bars +/- SE. MEP pathway intermediate abbreviations: CDP-ME, 4-diphosphocytidyl-methylerythritol; CDP-MEP, CDP-ME 2-phosphate; DMADP, dimethylallyl diphosphate; DXP, deoxyxylulose 5-phosphate; GAP, glyceraldehyde 3-phosphate; GDP, geranyl diphosphate; HBMPP, hydroxymethylbutenyl 4-diphosphate; IDP, isopentenyl diphosphate; ME-cPP, methylerythritol 2,4-cyclodiphosphate; MEP, methylerythritol 4-phosphate. Enzyme abbreviations in bold: CMK, CDP-ME kinase (EC 2.7.1.148); CMS, CDP-ME synthase (EC 2.7.7.60); DXR, DXP reductoisomerase (EC 1.1.1.267); DXS, DXP synthase (EC 2.2.1.7); HDR, HMBPP reductase (EC 1.17.1.2); HDS, HMBPP synthase (EC 1.17.4.3); IDI, IDP isomerase (EC 5.3.3.2); MCS, ME-cPP synthase (EC 4.6.1.12); ssGDPS: Geranyl diphosphate synthase small subunit (EC 2.5.1.1). Enzymes considered to be rate determining according to literature are boxed. *TPS data are shown in Fig 2C and 2D.

Figure 6 Monoterpene volatiles produced by transient over-expression of *Actinidia* DXS, DXR, HDR and IDI in combination with *AaTPS1* and *AcTPS1* in *Nicotiana benthamiana* leaves. Volatiles were sampled 7 d post infiltration and analyzed by headspace sampling/GC-MS. Analyses were performed on six infiltrated leaves (~3-4 g) in three biological replicates. Error bars represent +/- SE.

Figure 7 (A) Schematic showing the location of potential NAC and EIL TF binding sites and Ethylene Response Elements (EREs) in the Aa *TPS*1_{pro}-911 and Ac *TPS*1_{pro}-3000 promoter fragments. (B) Schematic of the Ac *TPS*1_{pro}-600, Ac *TPS*1_{pro}-229 and Aa *TPS*1_{pro}-238 promoter truncation constructs cloned with the luciferase reporter gene of pGreenII 0800-

LUC. (C) Potential NAC TF binding sites in the *AcTPS1* and *AaTPS1* promoters aligned with NAC TF binding sites from *Arabidopsis thaliana* AtNAP (Zhang and Gan, 2012), ANAC055 (Tran et al., 2004), NAC1 (Xie et al., 2000) and *Triticum aestivum* TaNAC69 (Xue, 2005). Numbers for *AaTPS1* and *AcTPS1* indicate bp upstream of the ATG.

Figure 8 Expression of NAC and EIL TFs during fruit ripening in *Actinidia arguta* (black bars, ripening stages a0-a5 - see text) and *A. chinensis* (grey bars, ripening stages c0-c4 - see text). Real time qPCR analyses were performed on pooled fruit samples using gene-specific primers given in Table S2. Error bars are based on four technical replicates and data were normalized against the housekeeping gene EF1α. Error bars = +/- SE.

Figure 9 (A) Promoter activation assay of Aa *TPS*1_{pro}-911 by *Actinidia arguta* fruit NAC TF combinations. *NAC1*, *2*, *3*, *4*: single TF, *NAC1/2*, *1/3* etc.: mix of two NAC TFs, *NAC1-4*: mix of four TFs. *Agrobacterium* harboring *35S-NAC1-4* cloned from ripe *A. arguta* fruit cDNA were co-infiltrated into *Nicotiana benthamiana* leaves with Aa *TPS*1_{pro}-911 fused to the firefly luciferase gene. Activation is given by the ratio of firefly:renilla luminescence (LUC/REN). The same vector containing a CaMV *35S* promoter driven GUS reporter gene was used as a baseline activation control. (B) Promoter activation of Ac *TPS*1_{pro}-3000, -600, and -229 by a mix of EIL (n=5) or a mix of NAC (n=4) fruit TFs. (C) Promoter activation assay of Aa *TPS*1_{pro}-911 by *A. arguta* (Aa) and *A. chinensis* (Ac) fruit EIL and NAC combinations. *EIL1*, *2*, *3*, *4* single TF, *EIL1-5*: Mix of five EILs, *NAC1-4*: mix of four *NACs*, *EIL/NAC*: Mix of five EIL and four NAC TFs. (D) Promoter activation of a minimal Aa *TPS*1_{pro}-238, $_{pro}$-238Mut and Ac *TPS*1_{pro}-229 promoter with mixtures of *EIL* and *NAC* TFs. Nucleotide substitutions in Aa *TPS*1_{pro}-238Mut (underlined) and the proximal NAC core binding motif (boxed) are shown in Fig S9. (E) Promoter activation assay by NAC TFs of Ac *TPS*1_{pro}-208 (Fig S9) containing one (I), three (II) and five (III) tandem copies of the *AaTPS1* NAC binding region (..GTTTACGTATTC..) as shown in (F). Experiments are based on eight biological replicates except C and D (n=4). All data were log10 transformed prior to statistical analysis to stabilize the residual variation. Pair-wise comparisons were performed by Tukey's HSD test at $\alpha = 0.01$. Means with the same letter are not significantly different at the 0.01 level.

Figure 10 Electrophoretic mobility shift assays (EMSAs) show that AaNAC2-4 (N2-N4) bind to a 28 base pair double strand DNA fragment of the *AaTPS1* promoter (Aa) but not to the *AcTPS1* promoter (Ac). (A) Sequences alignment of the DNA probes used for the EMSA with the NAC core underlined. (B) EMSAs of 3'-biotin labeled double strand DNA probes with the AaNAC1-4 DNA binding domain proteins. Lane 1: Aa DNA probe only, no protein; lane 2, Ac DNA probe only, no protein. Lane 3-10: Aa or Ac DNA probe incubated with AaNAC1-4 protein combinations.

Table 1 Enzyme kinetic properties of recombinant AaTPS1 and AcTPS1. Purified recombinant enzymes were obtained by Ni^{2+} affinity and gel filtration chromatography. Kinetic parameters were determined for GDP (1-50 µM) in the presence of 20 mM $MgCl_2$ and for Mg^{2+} (0.2-25 mM) and Mn^{2+} (0-500 µM) in the presence of 25 µM GDP. All values represent mean ± SE, n=3. K_m: Michaelis constant; V_{max}: maximum velocity; k_{cat}: turnover.

Table 1 Enzyme kinetic properties of recombinant AaTPS1 and AcTPS1. Purified recombinant enzymes were obtained by Ni^{2+} affinity and gel filtration chromatography. Kinetic parameters were determined for GDP (1-50 µM) in the presence of 20 mM $MgCl_2$ and for Mg^{2+} (0.2-25 mM) and Mn^{2+} (0-500 µM) in the presence of 25 µM GDP. All values represent mean ± SE, n=3. K_m: Michaelis constant; V_{max}: maximum velocity; k_{cat}: turnover.

	K_m (µM)	V_{max}	k_{cat} (s^{-1})	k_{cat}/K_m (s^{-1} mM^{-1})
AcTPS1				
GDP (Mg^{2+})	6.1 ± 0.2		0.0076 ± 0.0004	1.3 ± 0.08
Mg^{2+} (GDP)	1478± 103	100%		
Mn^{2+} (GDP)	20.2 ± 2.0	~200%		
AaTPS1				
GDP (Mg^{2+})	13.1 ± 1.0		0.0195 ± 0.0020	1.5 ± 0.10
Mg^{2+} (GDP)	1503± 208	100%		
Mn^{2+} (GDP)	28.6 ± 1.1	~80%		

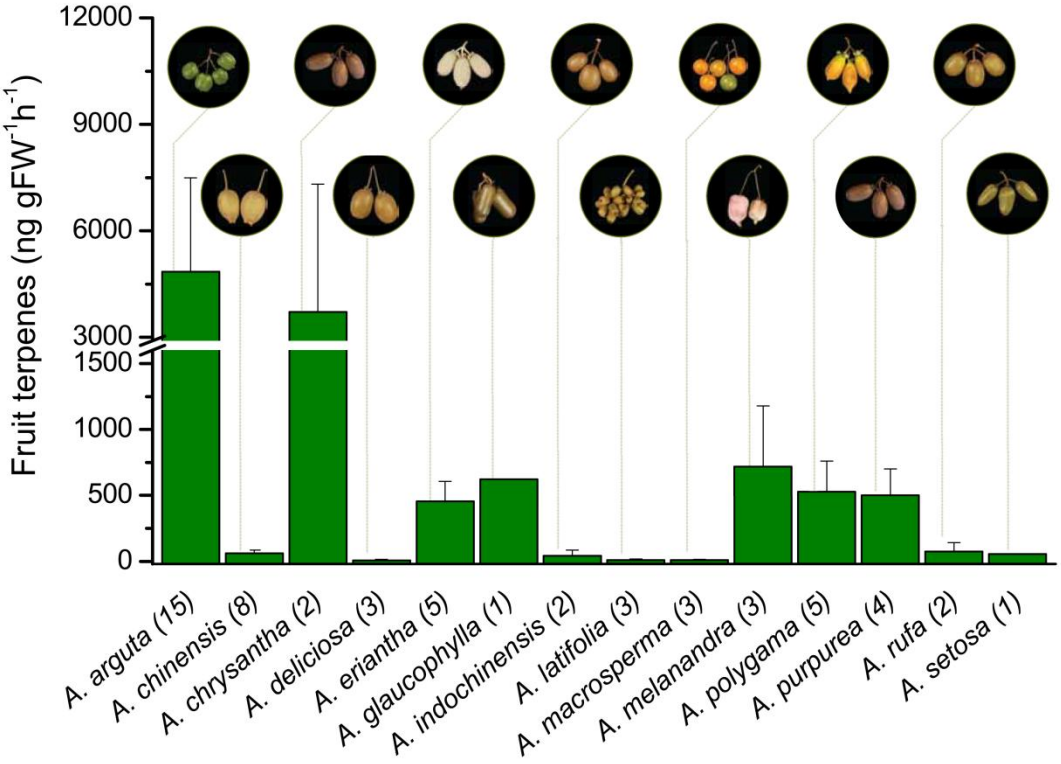

Figure 1 Total headspace terpene volatiles released from the ripe fruit of fourteen *Actinidia* species obtained by purge and trap followed by thermal desorption and semi-quantification by GC-MS. Average terpene concentrations are shown +/- S.E. The number of accessions tested for each species is shown in brackets.

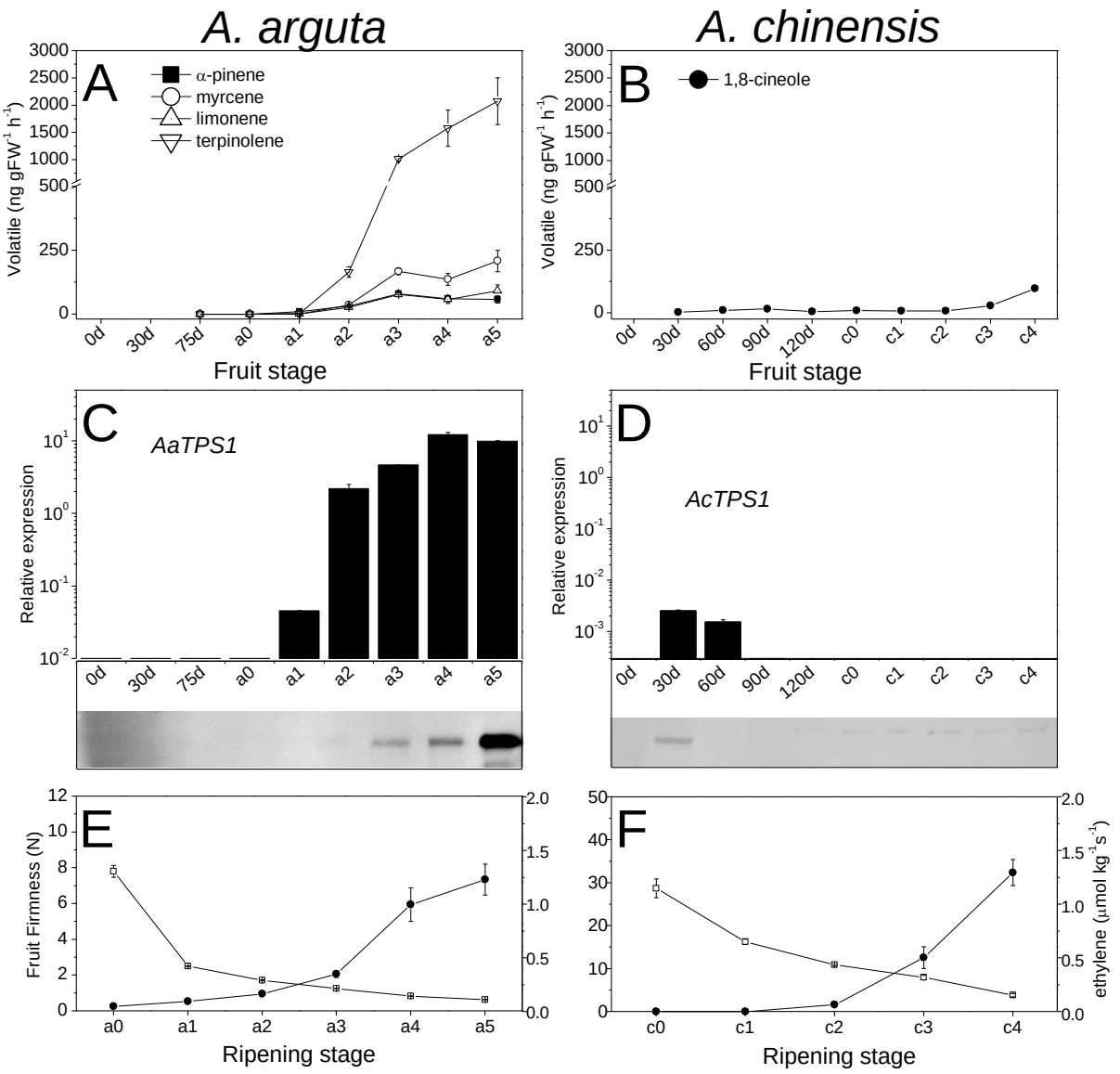

Figure 2 Rates of volatile terpene release by *Actinidia arguta* 'Hortgem Tahi' (A) and *A. chinensis* 'Hort16A' (B) during fruit development (d; days after pollination) and ripening (stages a0-a5 for 'Hortgem Tahi' and c0-c4 for 'Hort16A' fruit, ranging from harvest to over-ripe - see text). Measurements were made in triplicate ± S.E using a purge and trap method followed by thermal desorption and semi-quantification by GC-MS against authentic standards. Only terpenes representing >1% of total terpene content are shown. Real-time qPCR analysis of *AaTPS1* (C, upper panel) and *AcTPS1* (D, upper panel) gene expression levels were performed on pooled fruit samples using gene specific primers given in Table S2. Error bars are based on four technical replicates and data were normalized against the housekeeping gene EF1α. Western analysis of AaTPS1 (C, lower panel) and AcTPS1 (D, lower panel) protein concentrations at equivalent time points using a polyclonal antibody

raised against AcTPS1. Change in firmness (squares/left scale) and ethylene (circles/right scale) production in ‘Hortgem Tahi’ (E) and ‘Hort16A’ (F) during fruit ripening.

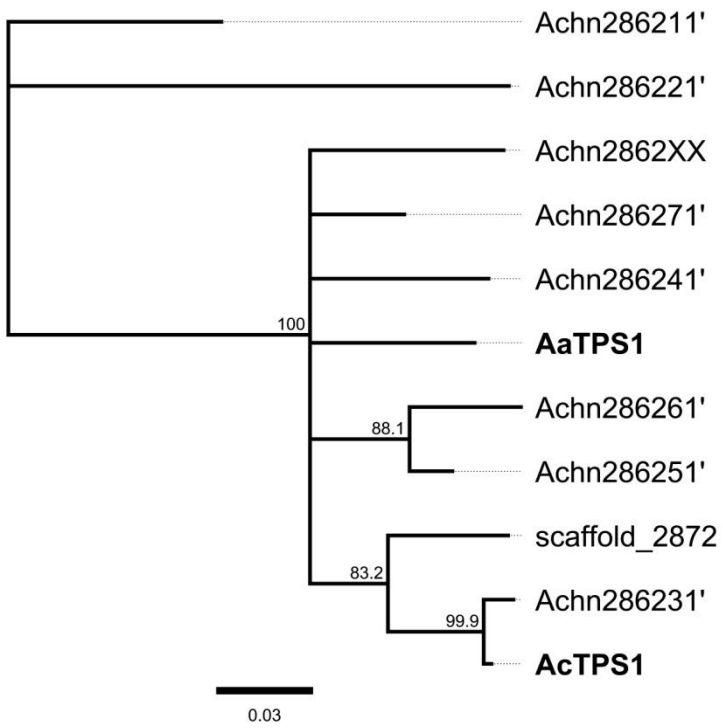

Figure 3 Phylogenetic analysis of the AaTPS1 and AcTPS1 homologous in *A. chinensis* 'HongYang'. Protein sequences extracted from the kiwifruit genome were aligned using ClustalW and manually curated (Fig S2A and B). The evolutionary history was inferred using the Neighbor Joining method with the Jukes-Cantor genetic distance model. The consensus tree is shown based on 80 percent support threshold. The percentage of trees in which the associated taxa clustered together is shown next to the branches based on a 1000 bootstrap replicates. The tree is drawn to scale, with branch lengths measured in the number of substitutions per site. The analysis involved 11 amino acid sequences and no outgroups. Evolutionary analyses were conducted in Geneious 6.1.6.

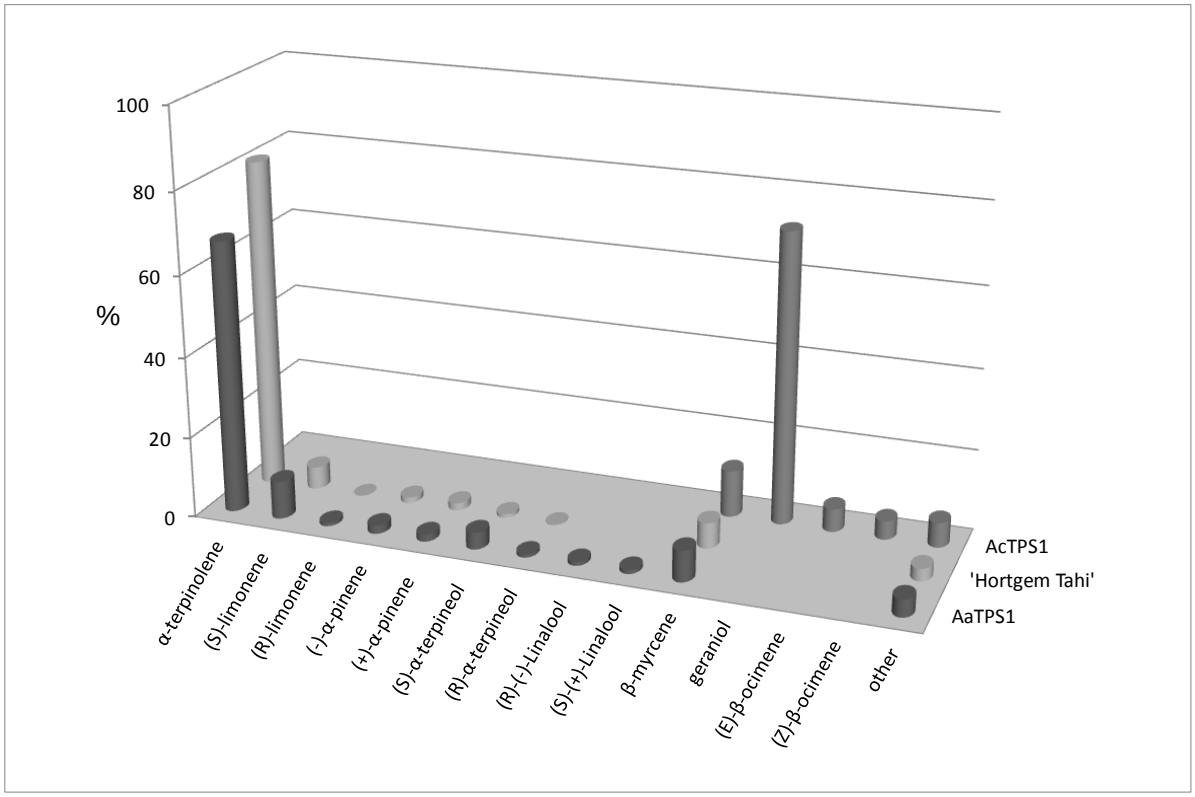

Figure 4 Percentage terpene volatiles produced by recombinant AaTPS1 and AcTPS1 enzymes *in vitro* and by ripe (stage a3/a4 - see text) *Actinidia arguta* 'Hortgem Tahi' fruit. The recombinant enzymes expressed in *E. coli* were purified by Ni^{2+} affinity and gel filtration chromatography and incubated with GDP as substrate. After solvent extraction, volatile terpenes were analyzed by enantioselective GC-MS. Extractions were performed in triplicate.

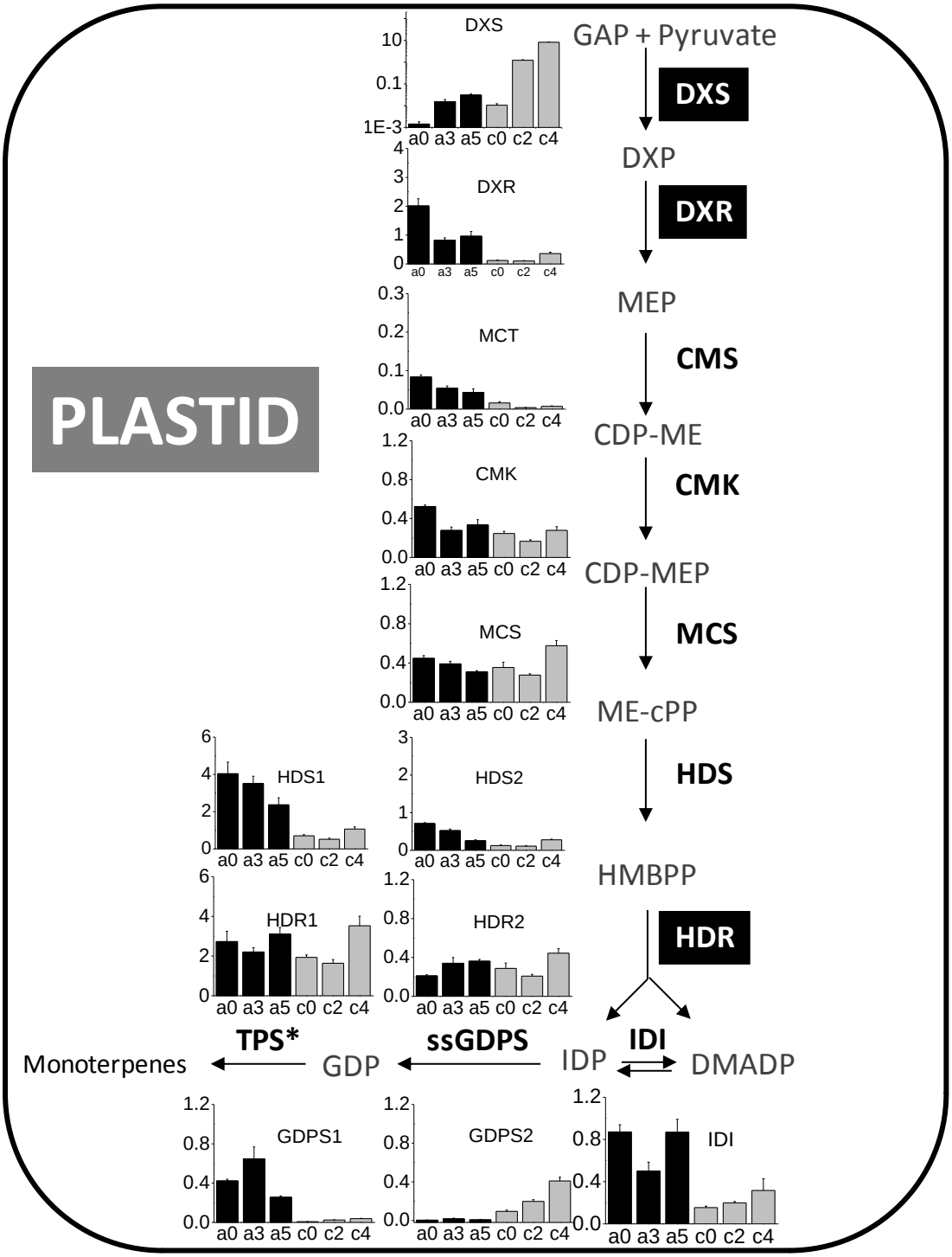

Figure 5 Expression of MEP pathway genes during fruit ripening in *Actinidia arguta* (black bars, ripening stages a0, a3, a5 - see text) and *A. chinensis* (grey bars, ripening stages c0, c2, c4 - see text). Real time qPCR analyses were performed on pooled fruit samples using gene-specific primer given in Table S2. Error bars are based on four technical replicates and data were normalized against the housekeeping gene EF1α. Error bars +/- SE. MEP pathway intermediate abbreviations: CDP-ME, 4-diphosphocytidyl-methylerythritol; CDP-MEP, CDP-ME 2-phosphate; DMADP, dimethylallyl diphosphate; DXP, deoxyxylulose 5-

phosphate; GAP, glyceraldehyde 3-phosphate; GDP, geranyl diphosphate; HBMPP, hydroxymethylbutenyl 4-diphosphate; IDP, isopentenyl diphosphate; ME-cPP, methylerythritol 2,4-cyclodiphosphate; MEP, methylerythritol 4-phosphate. Enzyme abbreviations in bold: CMK, CDP-ME kinase (EC 2.7.1.148); CMS, CDP-ME synthase (EC 2.7.7.60); DXR, DXP reductoisomerase (EC 1.1.1.267); DXS, DXP synthase (EC 2.2.1.7); HDR, HMBPP reductase (EC 1.17.1.2); HDS, HMBPP synthase (EC 1.17.4.3); IDI, IDP isomerase (EC 5.3.3.2); MCS, ME-cPP synthase (EC 4.6.1.12); ssGDPS: Geranyl diphosphate synthase small subunit (EC 2.5.1.1). Enzymes considered to be rate determining according to literature are boxed. *TPS data are shown in Fig 2C and 2D.

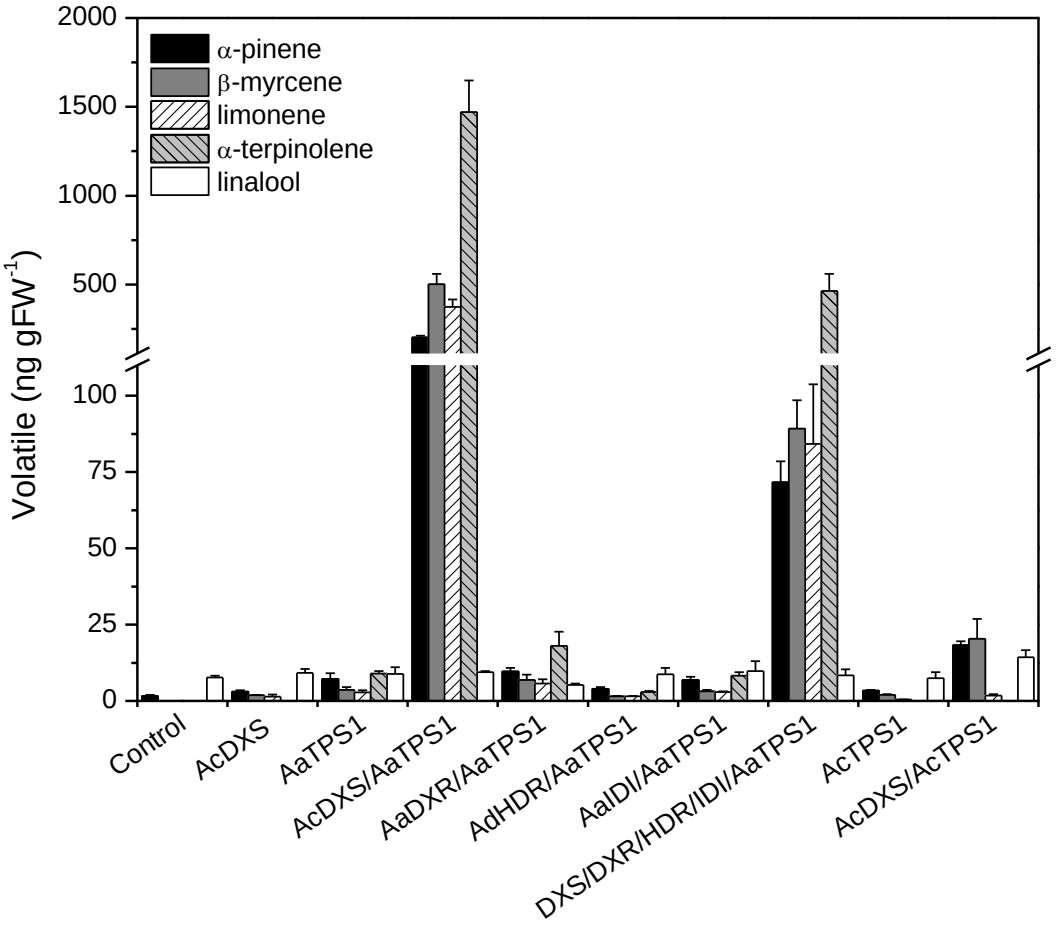

Figure 6 Monoterpene volatiles produced by transient over-expression of *Actinidia* DXS, DXR, HDR and IDI in combination with *AaTPS1* and *AcTPS1* in *Nicotiana benthamiana* leaves. Volatiles were sampled 7 d post infiltration and analyzed by headspace sampling/GC-MS. Analyses were performed on six infiltrated leaves (~3-4 g) in three biological replicates. Error bars represent +/- SE.

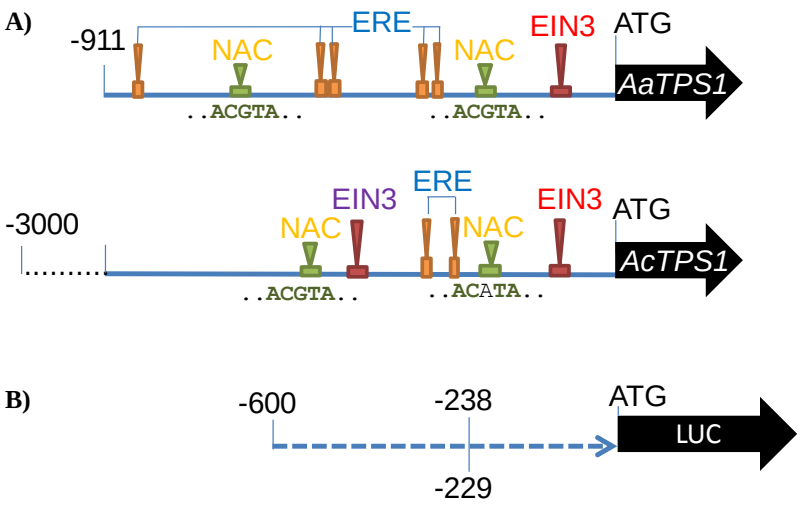

C)

AtNAP:	C**ACGTAAGT**	
NAC1:	TG**ACGTAAG**G	
ANAC055:	AC**ACGCA**TGT	
TaNAC69:	**YACGNNWCY**	
TaNAC69:	**YACGTMAYY**	
AaTPS1:	CA**ACGTA**A**GC**	(position -657 to -648)
AcTPS1:	T**CACGTA**A**TC**	(position -511 to -520)
AaTPS1:	T**TACGTA**T**TC**	(position -227 to -218)
AcTPS1:	C**CAC**A**TA**T**CC**	(position -218 to -209)
Consensus:	**YACGTAABY**	

Figure 7 (A) Schematic showing the location of potential NAC and EIL TF binding sites and Ethylene Response Elements (EREs) in the Aa *TPS*1$_{pro}$-911 and Ac *TPS*1$_{pro}$-3000 promoter fragments. (B) Schematic of the Ac *TPS*1$_{pro}$-600, Ac *TPS*1$_{pro}$-229 and Aa *TPS*1$_{pro}$-238 promoter truncation constructs cloned with the luciferase reporter gene of pGreenII 0800-LUC. (C) Potential NAC TF binding sites in the *AcTPS1* and *AaTPS1* promoters aligned with NAC TF binding sites from *Arabidopsis thaliana* AtNAP (Zhang and Gan, 2012), ANAC055 (Tran et al., 2004), NAC1 (Xie et al., 2000) and *Triticum aestivum* TaNAC69 (Xue, 2005). Numbers for *AaTPS1* and *AcTPS1* indicate bp upstream of the ATG.

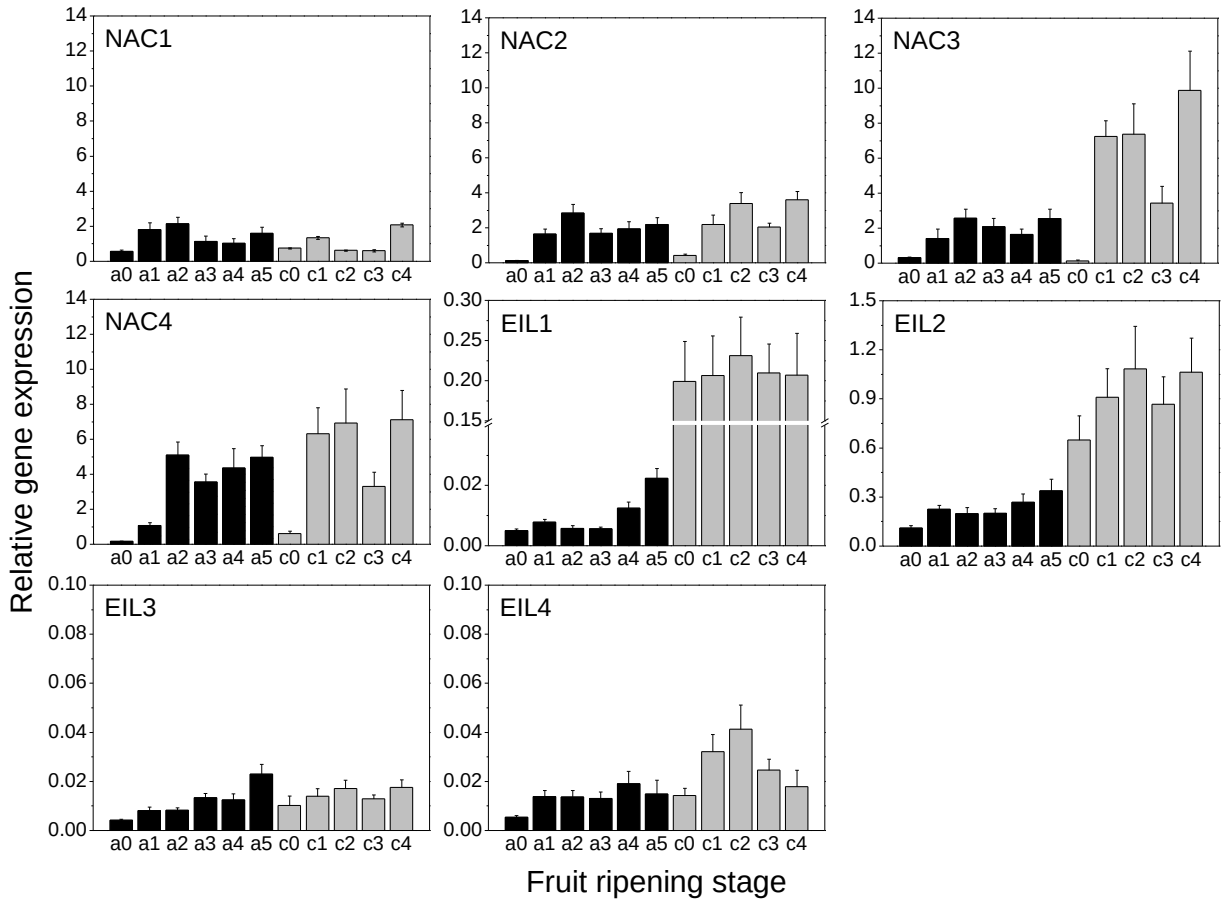

Figure 8 Expression of NAC and EIL TFs during fruit ripening in *Actinidia arguta* (black bars, ripening stages a0-a5 - see text) and *A. chinensis* (grey bars, ripening stages c0-c4 - see text). Real time qPCR analyses were performed on pooled fruit samples using gene-specific primers given in Table S2. Error bars are based on four technical replicates and data were normalized against the housekeeping gene EF1α. Error bars = +/- SE.

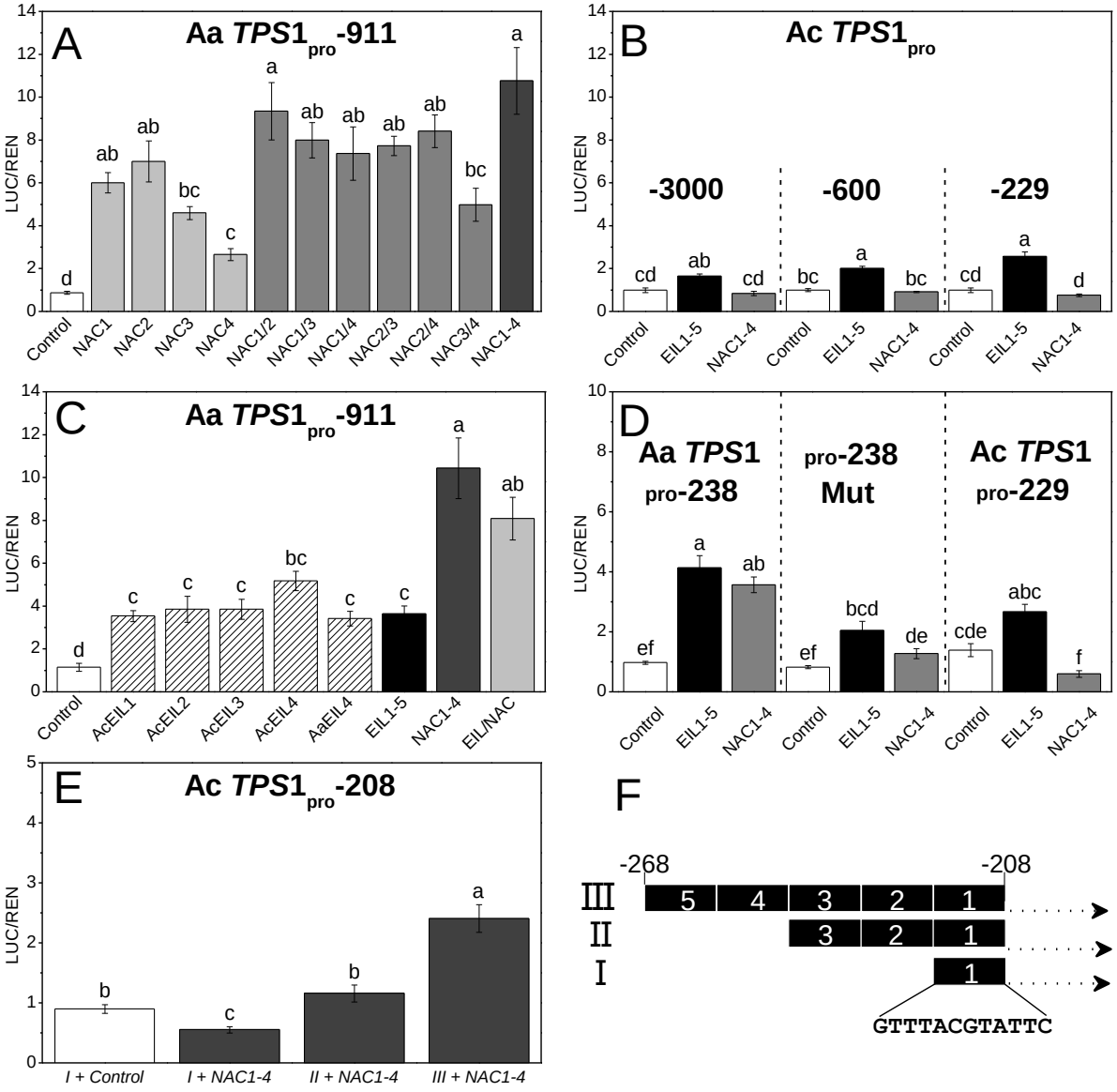

Figure 9 (A) Promoter activation assay of Aa *TPS*1$_{pro}$-911 by *Actinidia arguta* fruit *NAC* TF combinations. *NAC1*, *2*, *3*, *4*: single TF, *NAC1/2*, *1/3* etc.: mix of two *NAC* TFs, *NAC1-4*: mix of four TFs. *Agrobacterium* harboring *35S-NAC1-4* cloned from ripe *A. arguta* fruit cDNA were co-infiltrated into *Nicotiana benthamiana* leaves with Aa *TPS*1$_{pro}$-911 fused to the firefly luciferase gene. Activation is given by the ratio of firefly:renilla luminescence (LUC/REN). The same vector containing a CaMV *35S* promoter driven *GUS* reporter gene was used as a baseline activation control. (B) Promoter activation of Ac *TPS*1$_{pro}$-3000, -600, and -229 by a mix of *EIL* (n=5) or a mix of *NAC* (n=4) fruit TFs. (C) Promoter activation assay of Aa *TPS*1$_{pro}$-911 by *A. arguta* (Aa) and *A. chinensis* (Ac) fruit *EIL* and *NAC* combinations. *EIL1*, *2*, *3*, *4* single TF, *EIL1-5*: Mix of five EILs, *NAC1-4*: mix of four *NACs*, *EIL/NAC*: Mix of five *EIL* and four *NAC* TFs. (D) Promoter activation of a minimal Aa *TPS*1$_{pro}$-238, $_{pro}$-238Mut and Ac *TPS*1$_{pro}$-229 promoter with mixtures of *EIL* and *NAC* TFs.

Nucleotide substitutions in Aa *TPS*1$_{pro}$-238Mut (underlined) and the proximal NAC core binding motif (boxed) are shown in Fig S9. (E) Promoter activation assay by *NAC* TFs of Ac *TPS*1$_{pro}$-208 (Fig S9) containing one (I), three (II) and five (III) tandem copies of the *AaTPS1* NAC binding region (..GTTTACGTATTC..) as shown in (F). Experiments are based on eight biological replicates except C and D (n=4). All data were log10 transformed prior to statistical analysis to stabilize the residual variation. Pair-wise comparisons were performed by Tukey's HSD test at $\alpha = 0.01$. Means with the same letter are not significantly different at the 0.01 level.

A

```
     1                            28
Aa:  GAGAGAAGAGTTTACGTATTCAAACAGA
     ||||.||||.|..||.|||.||||||.||
Ac:  GAGACAAGAATCCACATATCCAAACGGA
```

B

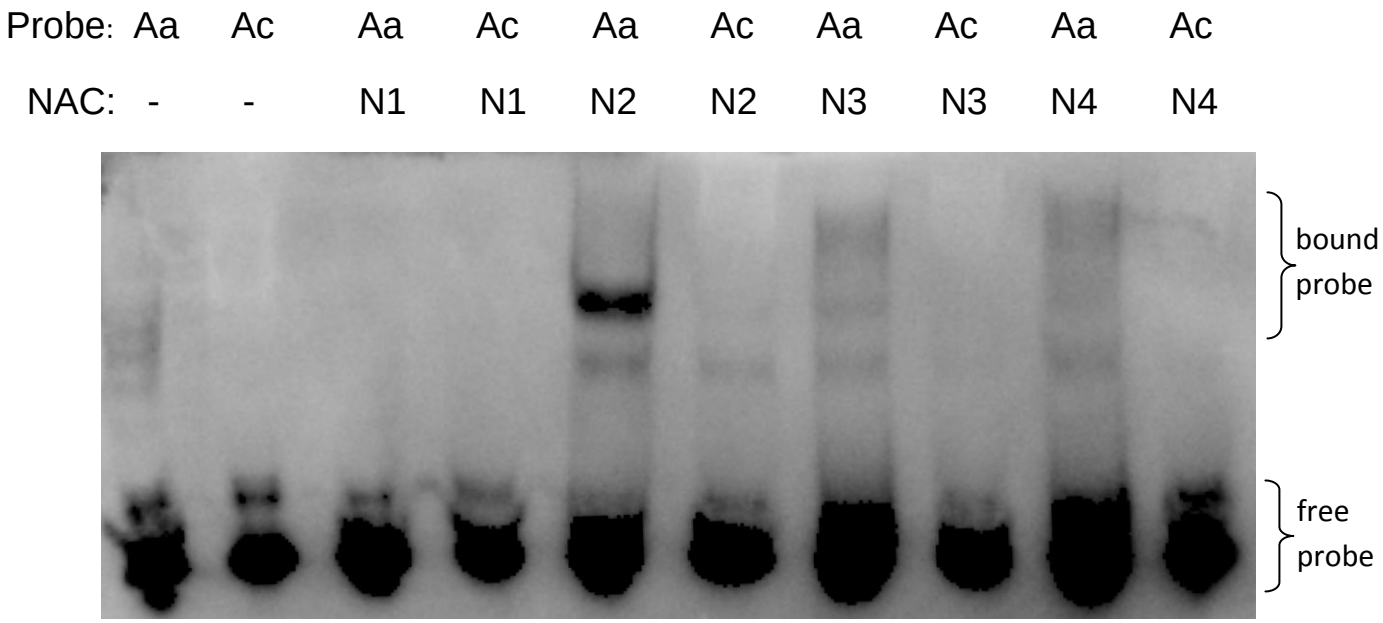

Figure 10. Electrophoretic mobility shift assays (EMSAs) show that AaNAC2-4 (N2-N4) bind to a 28 base pair double strand DNA fragment of the *AaTPS1* promoter (Aa) but not to the *AcTPS1* promoter (Ac). (A) Sequences alignment of the DNA probes used for the EMSA with the NAC core underlined. (B) EMSAs of 3'-biotin labeled double strand DNA probes with the AaNAC1-4 DNA binding domain proteins. Lane 1: Aa DNA probe only, no protein; lane 2, Ac DNA probe only, no protein. Lane 3-10: Aa or Ac DNA probe incubated with AaNAC1-4 protein combinations.

A)

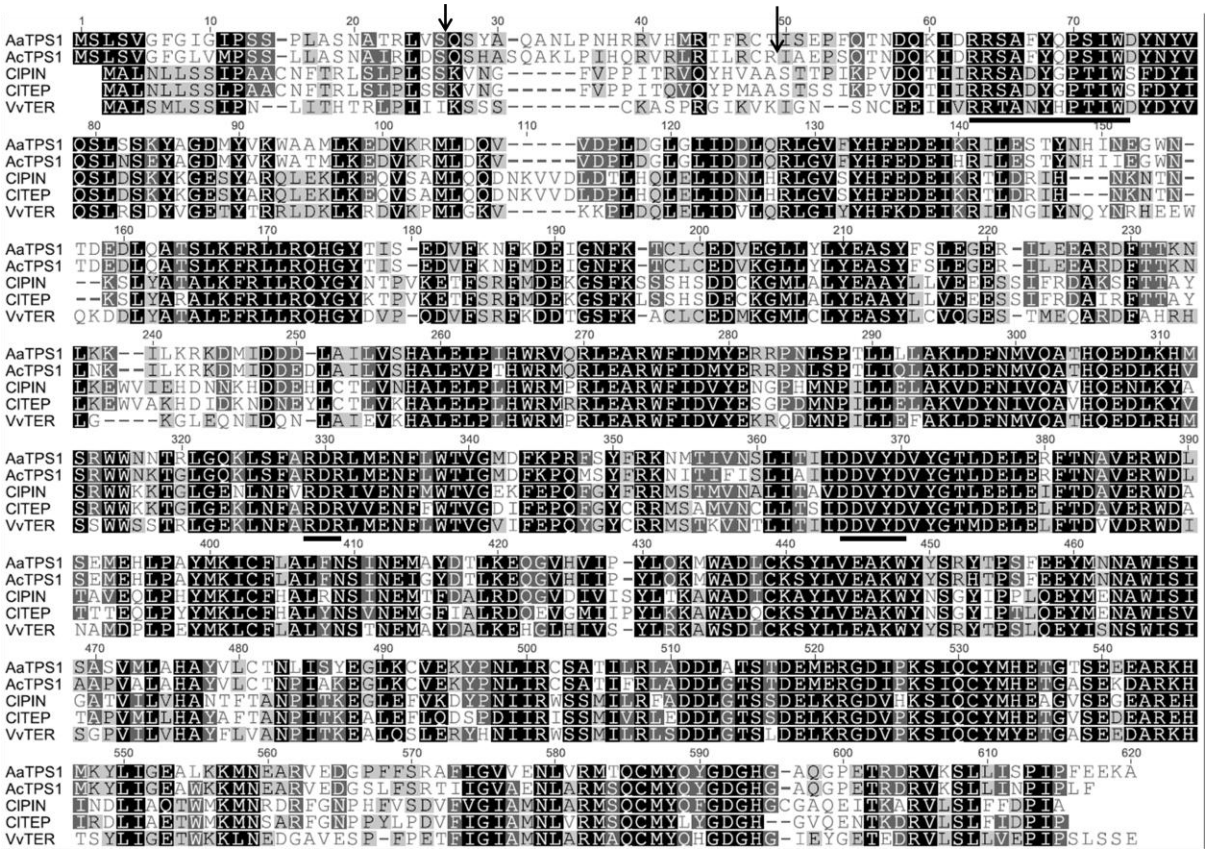

B)

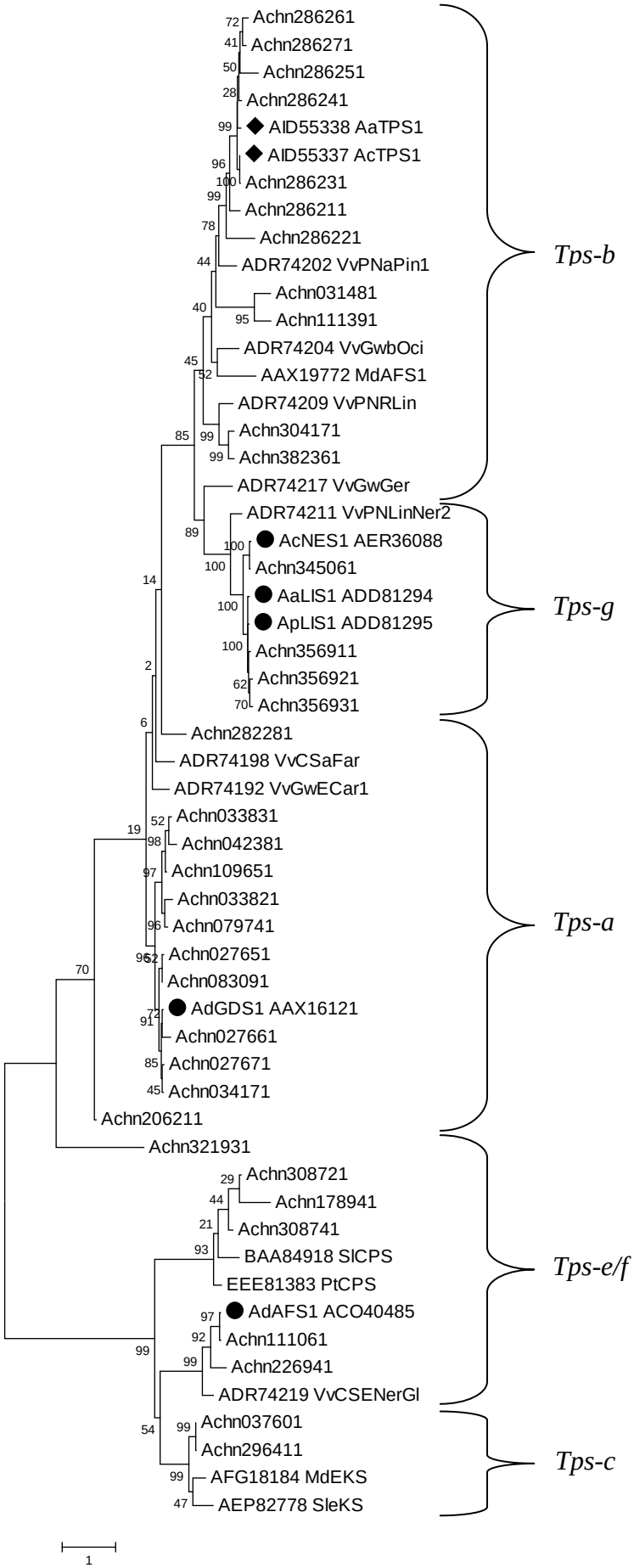
Achn286261
Achn286271
Achn286251
Achn286241
AID55338 AaTPS1
AID55337 AcTPS1
Achn286231
Achn286211
Achn286221
ADR74202 VvPNaPin1
Achn031481
Achn111391
ADR74204 VvGwbOci
AAX19772 MdAFS1
ADR74209 VvPNRLin
Achn304171
Achn382361
ADR74217 VvGwGer
ADR74211 VvPNLinNer2
AcNES1 AER36088
Achn345061
AaLIS1 ADD81294
ApLIS1 ADD81295
Achn356911
Achn356921
Achn356931
Achn282281
ADR74198 VvCSaFar
ADR74192 VvGwECar1
Achn033831
Achn042381
Achn109651
Achn033821
Achn079741
Achn027651
Achn083091
AdGDS1 AAX16121
Achn027661
Achn027671
Achn034171
Achn206211
Achn321931
Achn308721
Achn178941
Achn308741
BAA84918 SlCPS
EEE81383 PtCPS
AdAFS1 ACO40485
Achn111061
Achn226941
ADR74219 VvCSENerGl
Achn037601
Achn296411
AFG18184 MdEKS
AEP82778 SleKS
Tps-b
Tps-g
Tps-a
Tps-e/f
Tps-c
1

Figure S1.
(A) Alignment of the deduced amino acid sequences of *AaTPS1* and *AcTPS1* and other *Tps-b* subfamily terpene synthases. Abbreviations with GenBank accessions in brackets: AaTPS1 (*Actinidia arguta* terpene synthase 1 - AID55338), AcTPS1 (*A. chinensis* terpene synthase 1 - AID55337), ClPIN (*Citrus limon* (-)-β-pinene synthase - AAM53945), ClTEP (*Citrus limon* γ-terpinene synthase - AAM53943) and VvTER (*Vitis vinifera* (-)-α-terpineol synthase - AAS79351). The highly conserved metal cofactor binding region (DDXXD) as well as the conserved RXR and RRX_8W motifs are underlined. The cleavage sites of the predicted chloroplast targeting peptides (ChloroP predictions) are marked with arrowheads. Sequence alignments were constructed using ClustalX (Thompson, 1997) and visualized using MEGA5 (Tamura et al., 2011).

(B) Unrooted Maximum Likelihood tree of *AcTPS1* and *AaTPS1* with other terpene synthases from kiwifruit, grape, apple, tomato and poplar. *AcTPS1* and *AaTPS1* from this work are indicated by black diamonds. Previously published functionally characterized kiwifruit TPS sequences are indicated by black circles. Thirty-five TPS gene models (Achn numbers) were identified in the kiwifruit 'Hongyang' genome (Huang et al., 2013) using BLASTP searches (cut-off < $1e^{-2}$) using full length TPS protein sequences from grape, tomato, apple, poplar as query sequences. The evolutionary history was inferred by using the Maximum Likelihood method based on the Dayhoff matrix based model (Schwarz and Dayhoff, 1979). The percentage of trees in which the associated taxa clustered together is shown next to the branches. Initial tree(s) for the heuristic search were obtained automatically by applying Neighbor-Join and BioNJ algorithms to a matrix of pairwise distances estimated using a JTT model, and then selecting the topology with superior log likelihood value. The tree is drawn to scale, with branch lengths measured in the number of substitutions per site. The analysis involved 55 amino acid sequences. There were a total of 2260 positions in the final dataset. Evolutionary analyses were conducted in MEGA6 (Tamura et al., 2013). Multiple amino acid sequence alignments of the TPS genes were first performed with ClustalW using the using Geneious® v6.1.6 (www.geneious.com), the alignment was then exported in Phylip format and imported in MEGA6 for the analysis. Bootstrap values are shown as a percentage based on 1000 replicates. The scale bar represents expected changes per site. TPS families are bases on (Bohlmann et al., 1998; Dudareva et al., 2003).

Abbreviations with GenBank accessions in brackets are as follows: AaTPS1 = *Actinidia arguta* terpene synthase 1 (AID55338); AcTPS1 = *A. chinensis* terpene synthase 1 (AID55337); AdAFS1 = *A. deliciosa* (E,E)-α-farnesene synthase (ACO40485); AdGDS1 = *A. deliciosa* (+)-germacreneD synthase (AAX16121); AaLIS1 = *A. arguta* linalool synthase (ADD81294); ApLIS1 = *A. polygama* linalool synthase (ADD81295); AcNES1 = *A. chinensis* nerolidol syntase (AER36088); VvGwECar1 = *Vitis vinifera* (E)-β-caryophyllene synthase (ADR74192), VvCSaFar = (E,E)-α-farnesene synthase (ADR74198), VvPNRLin = (3R)-linalool synthase (ADR74209), VvPNaPin1 = pinene synthase (ADR74202), VvGwbOci = (E)-β-ocimene synthase (ADR74204), VvGwGer = geraniol synthase (ADR74217), VvPNLinNer2 = (3S)-linalool/(E)-nerolidol synthase (ADR74211), VvCSENerGl = P(E)-nerolidol/(E,E)-geranyl linalool synthase (ADR74219); MdAFS1 = *Malus domestica* (E,E)-α-farnesene synthase (AAX19772), MdEKS = ent-kaurene synthase (AFG18184); SleKS = *Solanum lycopersicum* ent-kaurene synthase (AEP82778), SlCPS = copalyl diphosphate synthase (BAA84918); PtCPS = *Populus trichocarpa* copalyl diphosphate synthase (EEE81383).

A

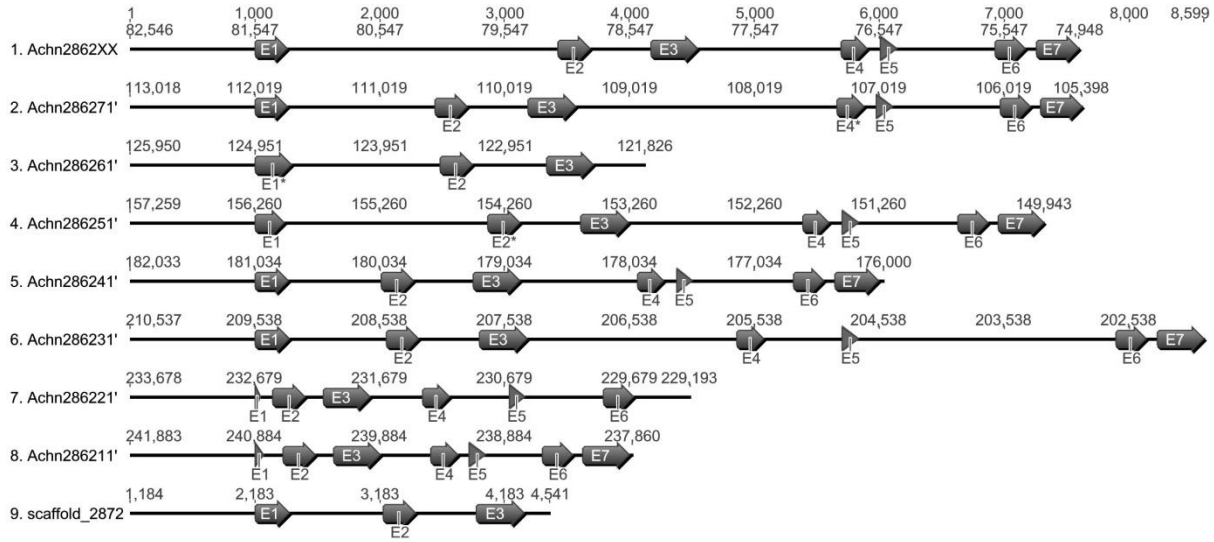
1 1,000 2,000 3,000 4,000 5,000 6,000 7,000 8,000 8,599
1. Achn2862XX
82,546 81,547 80,547 79,547 78,547 77,547 76,547 75,547 74,948
E1 E2 E3 E4 E5 E6 E7
2. Achn286271'
113,018 112,019 111,019 110,019 109,019 108,019 107,019 106,019 105,398
E1 E2 E3 E4* E5 E6 E7
3. Achn286261'
125,950 124,951 123,951 122,951 121,826
E1* E2 E3
4. Achn286251'
157,259 156,260 155,260 154,260 153,260 152,260 151,260 149,943
E1 E2* E3 E4 E5 E6 E7
5. Achn286241'
182,033 181,034 180,034 179,034 178,034 177,034 176,000
E1 E2 E3 E4 E5 E6 E7
6. Achn286231'
210,537 209,538 208,538 207,538 206,538 205,538 204,538 203,538 202,538
E1 E2 E3 E4 E5 E6 E7
7. Achn286221'
233,678 232,679 231,679 230,679 229,679 229,193
E1 E2 E3 E4 E5 E6
8. Achn286211'
241,883 240,884 239,884 238,884 237,860
E1 E2 E3 E4 E5 E6 E7
9. scaffold_2872
1,184 2,183 3,183 4,183 4,541
E1 E2 E3

B


Achn286211'
Achn286221'
Achn2862XX
Achn286271'
Achn286241'
AaTPS1
Achn286261'
Achn286251'
scaffold_2872
Achn286231'
AcTPS1

C

	Achn286261'	scaffold_2872	Achn286231'	AcTPS1	Achn2862XX	Achn286271'	Achn286241'	Achn286251'	AaTPS1	Achn286211'	Achn286221'
Achn286261'		80.1%	80.1%	80.4%	80.9%	86.6%	82.0%	95.4%	80.3%	71.7%	68.5%
scaffold_2872	80.1%		93.0%	93.4%	88.0%	87.7%	86.4%	93.7%	87.4%	74.2%	69.5%
Achn286231'	80.1%	93.0%		98.8%	87.9%	88.6%	87.1%	87.0%	87.6%	80.3%	72.1%
AcTPS1	80.4%	93.4%	98.8%		88.4%	89.2%	87.7%	87.8%	88.2%	80.6%	73.1%
Achn2862XX	80.9%	88.0%	87.9%	88.4%		89.6%	86.0%	86.7%	86.5%	79.5%	72.6%
Achn286271'	86.6%	87.7%	88.6%	89.2%	89.6%		89.4%	91.3%	89.3%	81.2%	74.3%
Achn286241'	82.0%	86.4%	87.1%	87.7%	86.0%	89.4%		90.4%	88.4%	78.8%	73.6%
Achn286251'	95.4%	93.7%	87.0%	87.8%	86.7%	91.3%	90.4%		87.9%	77.1%	72.2%
AaTPS1	80.3%	87.4%	87.6%	88.2%	86.5%	89.3%	88.4%	87.9%		81.1%	73.7%
Achn286211'	71.7%	74.2%	80.3%	80.6%	79.5%	81.2%	78.8%	77.1%	81.1%		79.8%
Achn286221'	68.5%	69.5%	72.1%	73.1%	72.6%	74.3%	73.6%	72.2%	73.7%	79.8%	

Figure S2.
(A) Mapping of *AcTPS1* exons 1-7 onto scaffolds in the kiwifruit genome. To improve the TPS gene models identified in the kiwifruit genome, exons 1-7 of *AcTPS1* were used as BLASTn query sequences against the kiwifruit genome scaffold database (http://bioinfo.bti.cornell.edu/cgi-bin/kiwi/home.cgi). A schematic showing the structure of eight tandemly repeated, full-length and partial TPS1-like gene models (Achn286211'-XX) identified on scaffold_575 (length 316,842 bp) is shown. Scaffold_2872 (length 5307 bp) also contained a portion homologous to *AcTPS1* exons 1-3.

(B) Amino acid alignment of manually curated kiwifruit TPS1-like gene models. Exons 1-7 for each TPS1-like gene model were extracted from the kiwifruit scaffold database, joined together, translated into protein and aligned using Geneious® v6.1.6/ClustalW/default settings (www.geneious.com). Sequences were manually curated to maximise alignment and the designated with a prime (') symbol. Only three genes (Achn286231', Achn286241' and Achn2862XX) showed an intact structure of seven complete exons and no in-frame stop codons (asterisks). The conserved RRX8W and DDXXD domains are boxed.

C) Sequence identity table of aligned kiwifruit TPS1-like amino acid sequences.

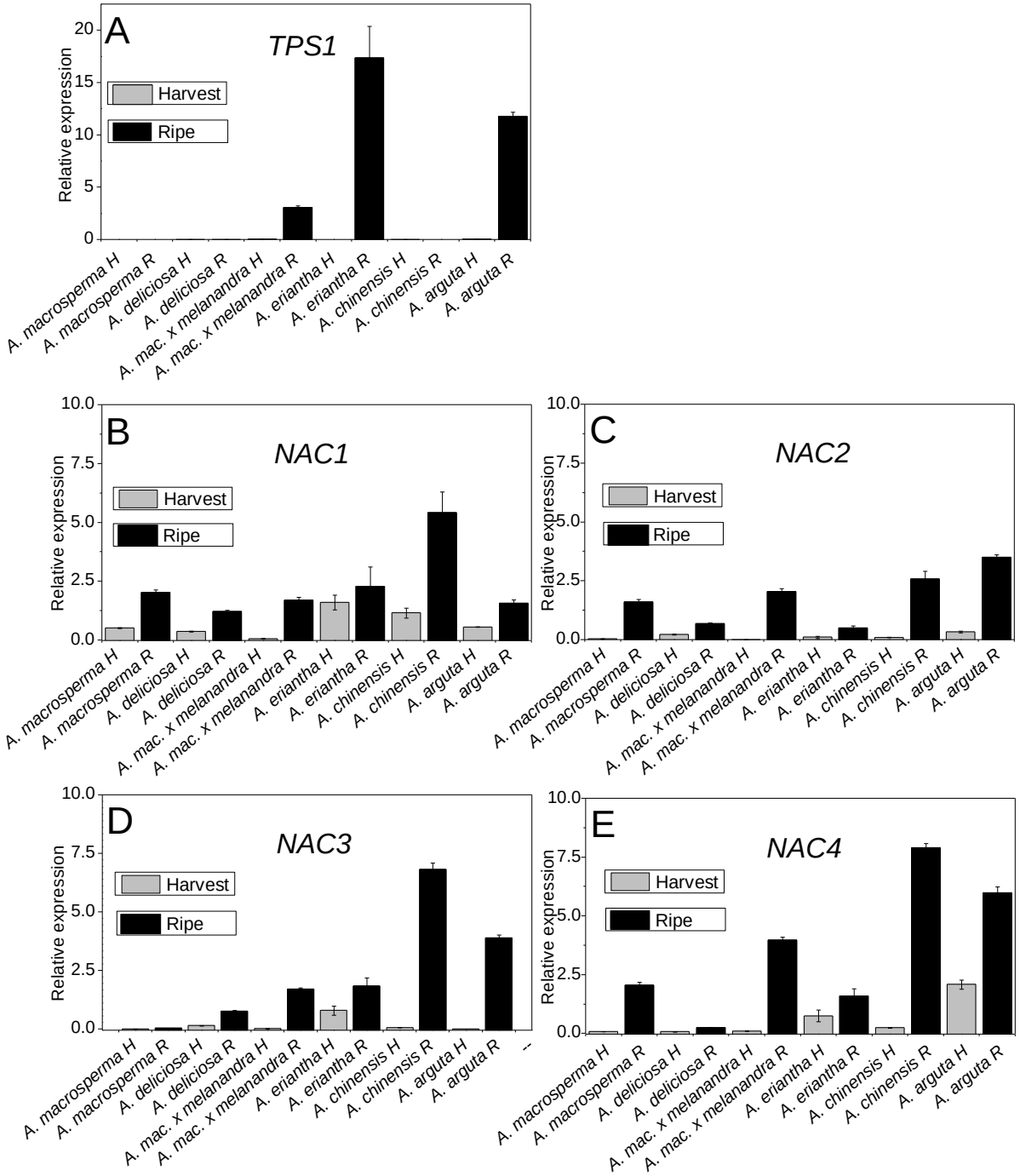

Figure S3.

Real-time qPCR analysis of *TPS1* (A) and *NAC1-4* (B-E) gene expression levels in harvest (H) and ripe (R) fruit for six *Actinidia* species. Analyses were performed on pooled fruit samples using gene specific primers given in Table S2. The *TPS1* primers were designed to amplify both *AaTPS1* and *AcTPS1*. Achn286241 and Achn2862XX expression was also tested using gene specific primers but both were not expressed in harvest or ripe fruit. Error bars are based on four technical replicates and data were normalized against the housekeeping gene EF1α. The *A. mac.* x *melanandra* sample represent fruit from an interspecific cross between *A. macrosperma* and *A. melanandra*.

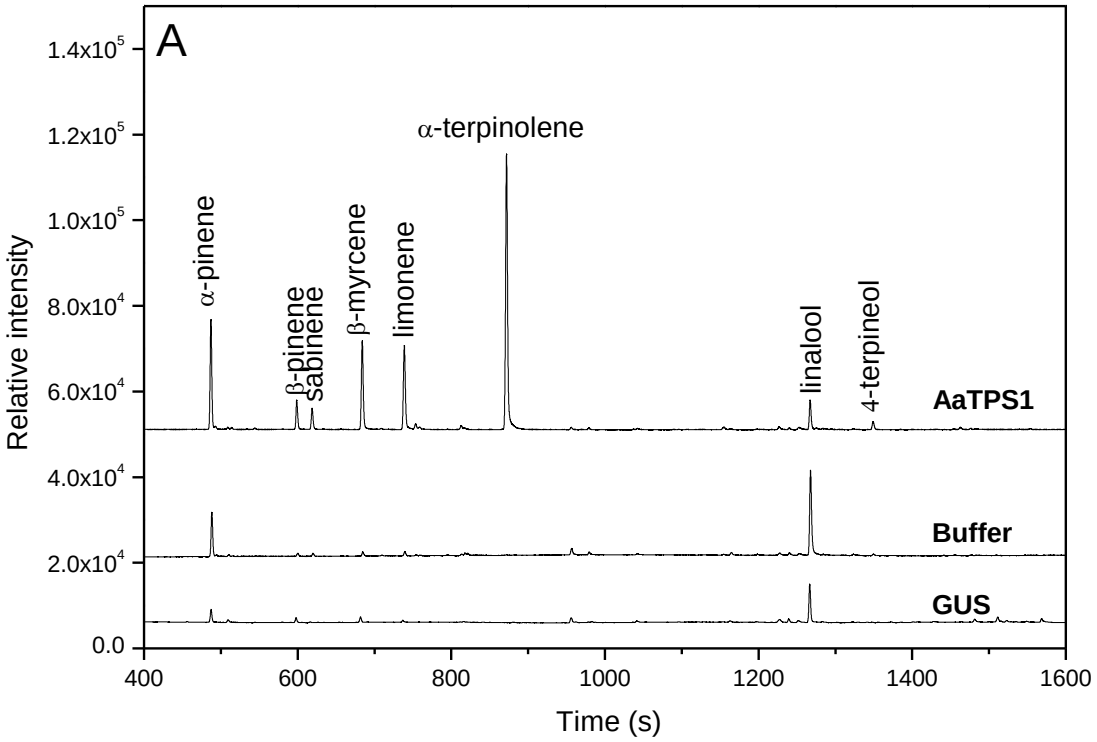
A
Relative intensity
Time (s)
α-pinene
β-pinene
sabinene
β-myrcene
limonene
α-terpinolene
linalool
4-terpineol
AaTPS1
Buffer
GUS

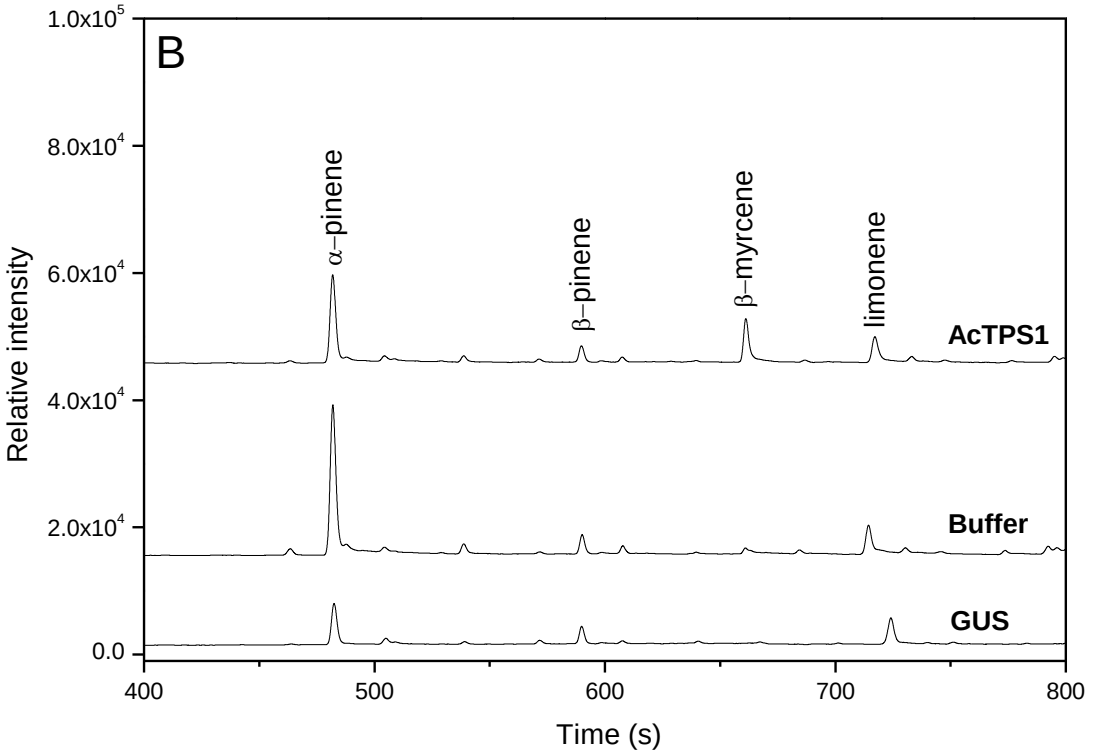
B
Relative intensity
Time (s)
α–pinene
β–pinene
β–myrcene
limonene
AcTPS1
Buffer
GUS

Figure S4. GC-MS analysis of the monoterpenes produced by transient expression of *AaTPS1* and *AcTPS1 in planta.* The complete open reading frames of *AaTPS1* and *AcTPS1* were cloned into the binary vector pHEX2 and transformed into *Agrobacterium tumefaciens*. Bacterial cell suspensions were injected into the abaxial side of three young *Nicotiana benthamiana* leaves and volatiles were assayed 2 weeks after injection by dynamic headspace sampling of detached leaves. Leaves were infiltrated with buffer-only and with a vector expressing the *GUS* reporter gene (pHEX2-GUS) as controls. (A) *AaTPS1* - upper trace; buffer-only (mock infiltrated) - middle trace; *GUS* - lower trace. (B) *AcTPS1* - upper trace; buffer-only - middle trace; *GUS* - lower trace. Analyses were made in triplicate with only a single representative trace shown for each treatment.

A

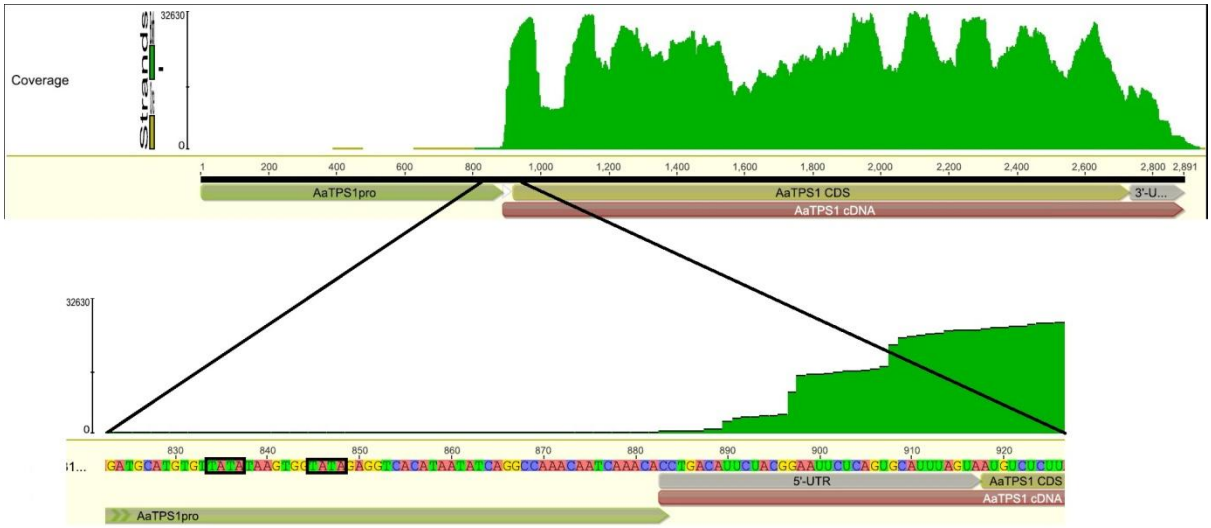
Coverage
Strands
32630
0
1
200
400
600
800
1,000
1,200
1,400
1,600
1,800
2,000
2,200
2,400
2,600
2,800
2,891
AaTPS1pro
AaTPS1 CDS
3'-U...
AaTPS1 cDNA
32630
0
830
840
850
860
870
880
890
900
910
920
5'-UTR
AaTPS1 CDS
AaTPS1 cDNA
AaTPS1pro

B

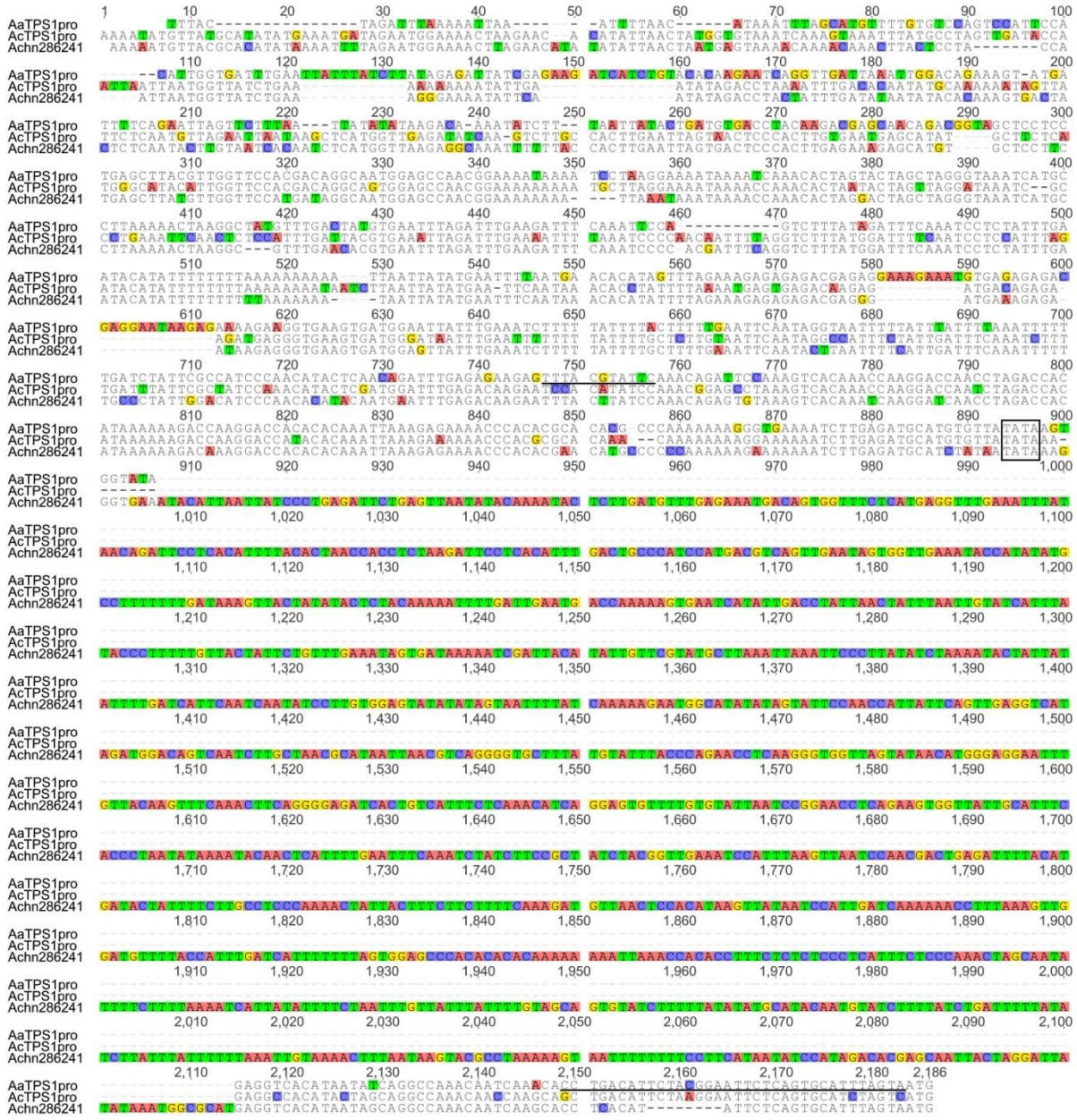

Figure S5.
(A) Identifying the transcriptional start site in the 5'-UTR of *AaTPS1*. Illumina sequencing data derived from *Actinidia arguta* fruit mRNA (ripening stage C3, Fig 2) was read mapped against the *AaTPS1* gene (*AaTPS1* promoter fused to the *AaTPS1* cDNA). Boxed sequences = putative TATA boxes. The 5'-UTR (in grey) is estimated to be 35 bp from the ATG (start of translation). Read mapping was performed using Geneious® v6.1.6/Align/Assemble/Map to reference. Parameters: Custom, Word length 30, Index word length 15, ignore words repeated more than 12 times, Max mismatch per read 10%, Maximum ambiguity 4, No gaps allowed. Library size: 37,154,393 reads (41-88 bp post trimming).

(B) Sequence alignment of *AaTPS1*, *AcTPS1* and *Achn286241* promoter regions. The kiwifruit genome scaffold database (http://bioinfo.bti.cornell.edu/cgi-bin/kiwi/home.cgi) was searched using BLASTn to identify regions of homology to the *AaTPS1* promoter. The *AaTPS1* promoter sequence (~0.9 kb) was then aligned with the *AcTPS1* (~0.9 kb) and *Achn286241* (~2.2 kb) upstream regions using Geneious® v6.1.6/Muscle align/default settings (www.geneious.com). The *AaTPS1* promoter shares significant sequence identity to the *AcTPS1* (68%) and *Achn286241* promoter (71%, excluding insertion) but not to other TPS1-like genes on scaffold_575. *Achn286241* shows an insertion of ~1.2 kb around the predicted TATA region (boxed), while *AcTPS1* shows significant divergence in the predicted NAC binding site (underlined at bp 750). The 5'-UTR in *AaTPS1* is underlined upstream of the ATG start codon (as determined above). The *AcTPS1* promoter sequence used in this work is 99% identical to the 3 kb Achn286231 upstream region.

```
AaTPS1pro-668   1 GCTCCTCCTGAGCTTACGTTGGTTCCACGACAGGCAATGGAGCCAACGGAAAATAAAATC 60
                  GCT CTC TG GC TAC TTGGTTCCACGACAGGCA TGGAGCCAACGGAAAA AAAAT
AcTPS1pro-648   1 GCTTCTCATGGGCATACATTGGTTCCACGACAGGCAGTGGAGCCAACGGAAAAAAAAATG 60

AaTPS1pro-668  61 CTAAGGAAAATAAAATCAAACACTAGTACTAGCTAGGGTAAATCATGCCTTAAAAACTAA 120
                  CT AGGAAAATAAAA CAAACACTA TACTAG TAGG TAAATC  GCC T AAA   AA
AcTPS1pro-648  61 CTTAGGAAAATAAAACCAAACACTAATACTAGTTAGGATAAATC--GCCCTGAAATTCAA 118

AaTPS1pro-668 121 GGCTATGTTTGACTATGTGAATTTAGATTTGAAGATTTCAAATTCC-----------AGT 169
                  CT     TTTGA TA GTGAA TTAGATTTGAA ATTT AAAT CC            GT
AcTPS1pro-648 119 CTCTCCATTTGATTACGTGAAATTAGATTTGAAAATTTTAAATCCCCAACAATTTTAGGT 178

AaTPS1pro-668 170 CTTTATAGATTTCAAATCCTCTATTTGAATACATATTTTTTTTAAAAAAAAAA---TTAA 226
                  CTTTAT GATTT  AATCCTC ATTT  ATACATATTTTTTTTAAAAAAAA A   TTAA
AcTPS1pro-648 179 CTTTATGGATTTTCAATCCTCCATTTAGATACATATTTTTTTTAAAAAAAATAATCTTAA 238

AaTPS1pro-668 227 TTATATGAATTTTAATGAACACATAGTTTAGAAAGAGAGAGACGAGAGGAAAGAAATGTG 286
                  TTATATGAA TT AAT AACAC TA TTTA AA GAG GAGAC AGAG          TG
AcTPS1pro-648 239 TTATATGAA-TTCAATAAACACCTATTTTAAAATGAGTGAGACAAGAG---------ATG 288

AaTPS1pro-668 287 AGAGAGACGAGGAATAAGAGAAAAGAAGGTGAAGTGATGGAATTATTTGAAATCTTTTTA 346
                  A AGAGA             A A GA GGTGAAGTGATGG AT ATTTGAA T TTTTA
AcTPS1pro-648 289 ACAGAGA-------------AGATGAGGGTGAAGTGATGGGATAATTTGAATTTTTTTTA 335

AaTPS1pro-668 347 TTTTACTTTTTGAATTCAATAGGTAATTTTTATTTATTTTAAATTTTTTGATCTATTCGC 406
                  TTTT CT TT  AATTCAATAGG  ATTT TATT ATTT AAAT TTTTGAT TATTCGC
AcTPS1pro-648 336 TTTTGCTCTTGTAATTCAATAGGCCATTTCTATTGATTTCAAATCTTTTGATTTATTCGC 395

AaTPS1pro-668 407 CATCCCAACATACTCAACAGATTTGAGAGAAGAGTTTACGTATTCAAACAGATTCCAAAG 466
                   ATCC AACATACTC A  GATTTGAGA AAGA T  AC TAT CAAAC GA  C AAAG
AcTPS1pro-648 396 TATCCAAACATACTCGATGGATTTGAGACAAGAATCCACATATCCAAACGGAGCCTAAAG 455

AaTPS1pro-668 467 TCACAAACCAAGGACCAACCTAGACCACATAAAAAAGACCAAGGACCACACACAAATTAA 526
                  TCACAAACCAAGGACCAA CTAGACCACATAAAAAAGACCAAGGACCA ACACAAATTAA
AcTPS1pro-648 456 TCACAAACCAAGGACCAATCTAGACCACATAAAAAAGACCAAGGACCATACACAAATTAA 515

AaTPS1pro-668 527 AGAGAAAACCCACACGCACACGCCCAAAAAAAGGGTGAAAATCTTGAGATGCATGTGTTA 586
                  AGA AAAACCCAC CGCACA    CAAAAAAA GG  AAAATCTTGAGATGCATGTGTTA
AcTPS1pro-648 516 AGAAAAAACCCACGCGCACAAA--CAAAAAAAAGGAAAAAATCTTGAGATGCATGTGTTA 573

AaTPS1pro-668 587 TATAAGTGGTATAGAGGTCACATAATATCAGGCCAAACAATCAAACACCTGACATTCTAC 646
                  TATAA       AGAGG CACATA TA CAGGCCAAACAA CAA CA CTGACATTCTA
AcTPS1pro-648 574 TATAA-------AGAGGCCACATACTAGCAGGCCAAACAACCAAGCAGCTGACATTCTAA 626

AaTPS1pro-668 647 GGAATTCTCAGTGCATTTAGCCATG 671
                  GGAATTCTCAGTGCAT TAGCCATG
AcTPS1pro-648 627 GGAATTCTCAGTGCATCTAGCCATG 651
```

Figure S6. Binding sites in the *AaTPS1* and *AcTPS1* promoter regions. The translational start codon is indicated in bold. Highlighted promoter elements are: EIN3 binding site AYGWAYCT (Kosugi and Ohashi, 2000); EIN3 binding site ATGCATCT (Boutrot et al., 2010); NAC binding site YACGTAABY (Fig 6); Ethylene Response Elements (EREs) AWTTCAAA (Montgomery et al., 1993; Itzhaki et al., 1994; Tapia et al., 2005). Underlined: 5'-untranslated region (5'-UTR) based on Fig. S5A (*AaTPS1*) or available EST information (*AcTPS1*).

A)

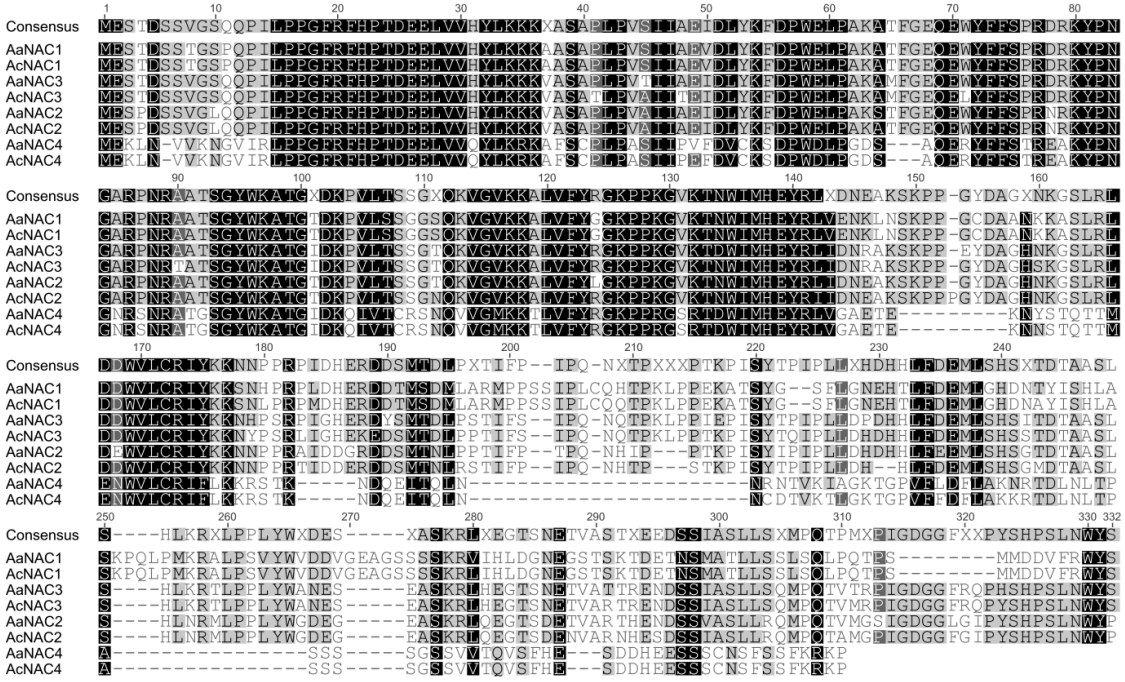
Consensus
AaNAC1
AcNAC1
AaNAC3
AcNAC3
AaNAC2
AcNAC2
AaNAC4
AcNAC4

B)

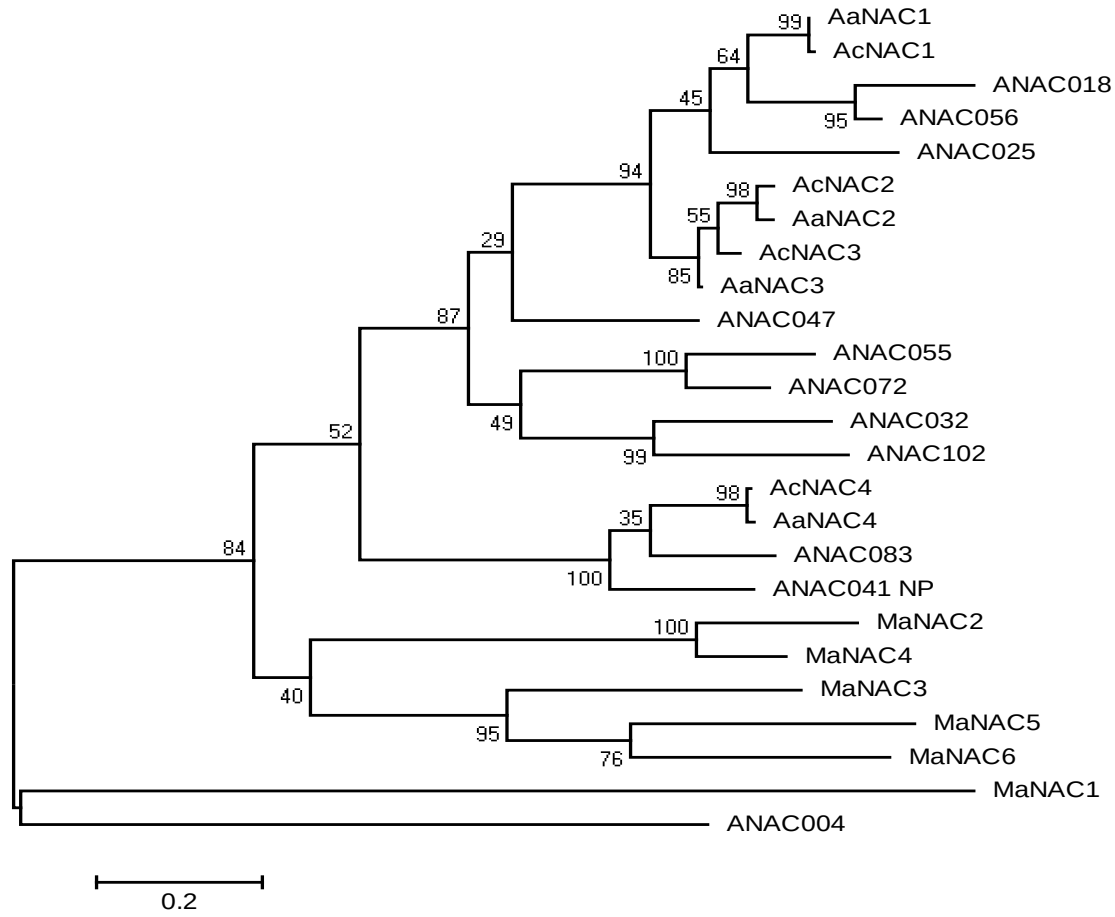

Figure S7.
(A) ClustalW alignment of the *Actinidia chinensis* (Ac) and *A. arguta* (Aa) *NAC1-4* proteins.

(B) Unrooted Maximum Likelihood tree of selected *Arabidopsis thaliana* (Ooka et al., 2003), *A. arguta* (Aa) and *A. chinensis* (Ac) NACs. *A. arguta*: AaNAC1 (KF319046), AaNAC2 (KF319047), AaNAC3 (KF319048), AaNAC4 (KF319049), *A. chinensis*: AcNAC1 (KF319050), AcNAC2 (KF319051), AcNAC3 (KF319052), AcNAC4 (KF319053). The evolutionary history was based on the JTT matrix-based model (Jones et al., 1992). The percentage of trees in which the associated taxa clustered together is shown next to the branches. Initial tree(s) for the heuristic search were obtained automatically by applying Neighbor-Join and BioNJ algorithms to a matrix of pairwise distances estimated using a JTT model, and then selecting the topology with superior log likelihood value. The tree is drawn to scale, with branch lengths measured in the number of substitutions per site. All positions containing gaps and missing data were eliminated. There were a total of 158 positions in the final dataset. Evolutionary analyses were conducted in MEGA5 (Tamura et al., 2011).

A)

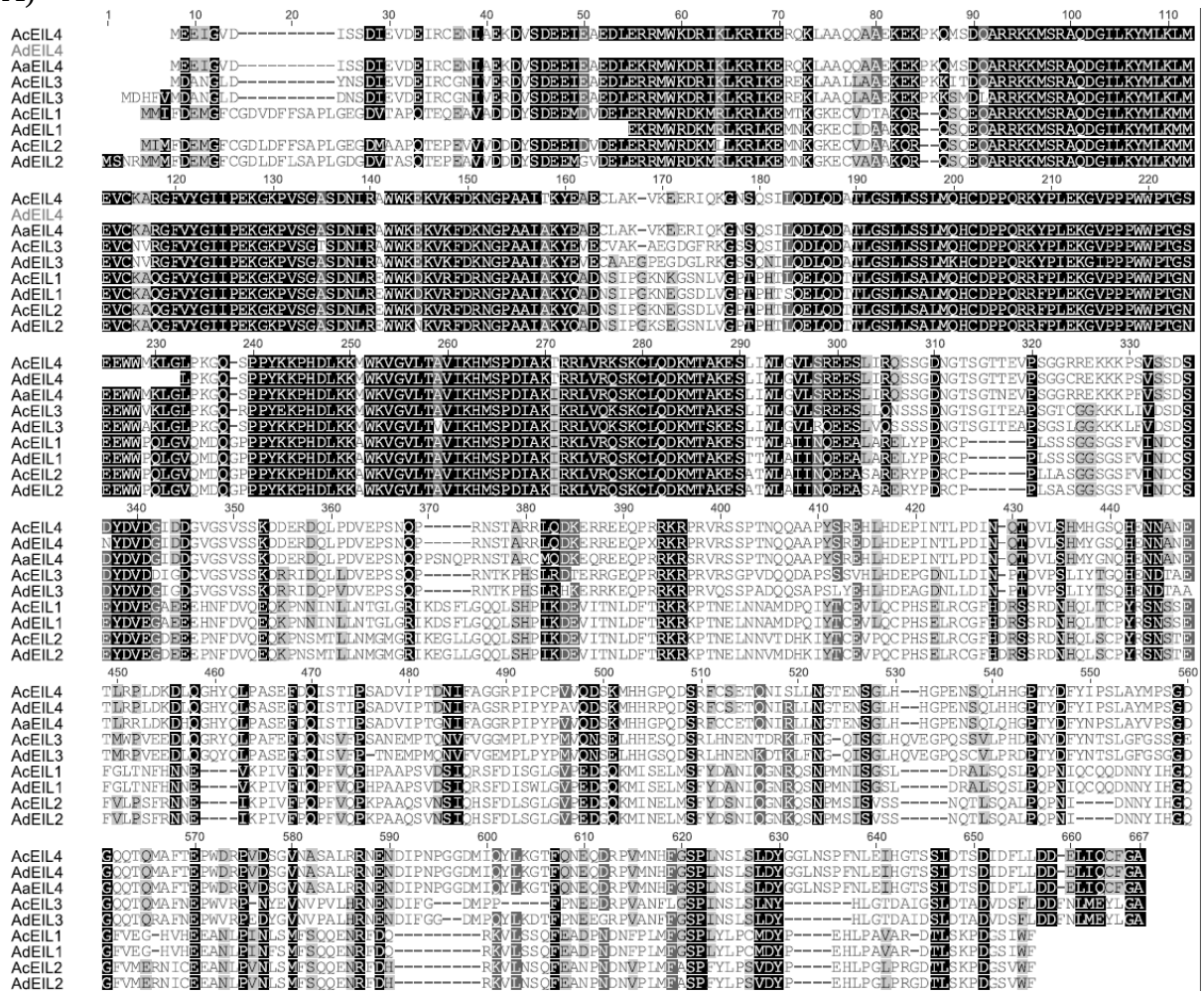
AcEIL4
AdEIL4
AaEIL4
AcEIL3
AdEIL3
AcEIL1
AdEIL1
AcEIL2
AdEIL2

B)

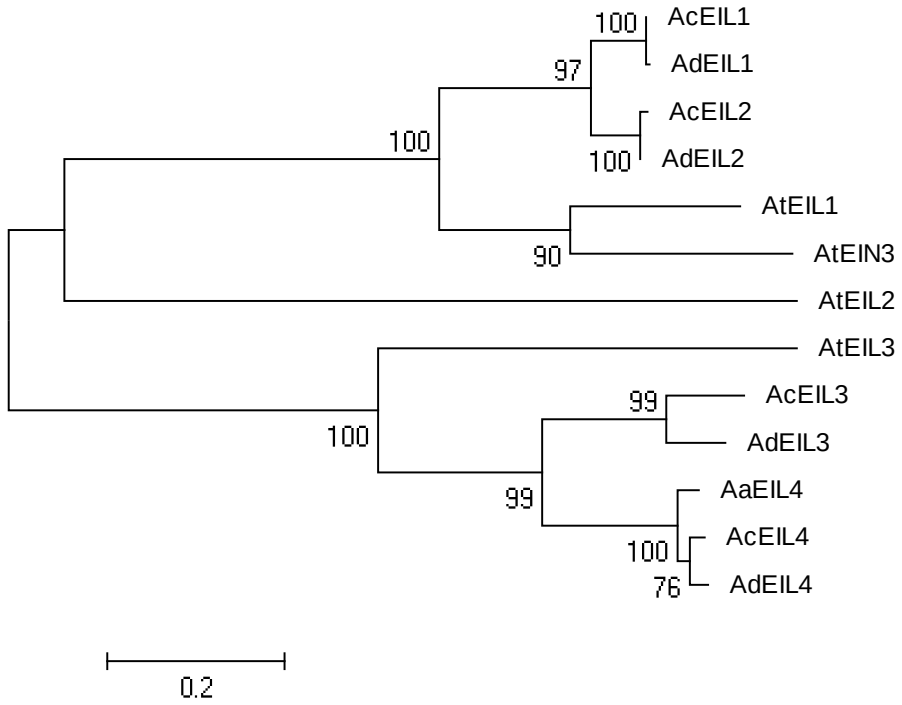

Figure S8.
(A) ClustalW alignment of the *Actinidia deliciosa* (Ad), *A. chinensis* (Ac) and *A. arguta* (Aa) *EIL1-4* proteins.

(B) Unrooted Maximum Likelihood tree of *A. deliciosa* (Ad), *A. arguta* (Aa) and *A. chinensis* (Ac) EIN3-like (EIL) transcription factors compared to *Arabidopsis thaliana*. Arabidopsis (At) EIN3 (GenBank AAC49749), EIL1 (AAC49746), EIL2 (AAC49747) and EIL3 (AAC49748), *A. deliciosa* (Yin et al., 2010): AdEIL1 (EU170633), AdEIL2 (EU887511), AdEIL3 (EU887512), AdEIL4 (EU887513), *A. chinensis*: AcEIL1 (KF319041), AcEIL2 (KF319042), AcEIL3 (KF319043), AcEIL4 (KF319044), *A. arguta*: AaEIL4 (KF319045). The tree was generated as described in Fig S7. There were a total of 239 positions in the final dataset.

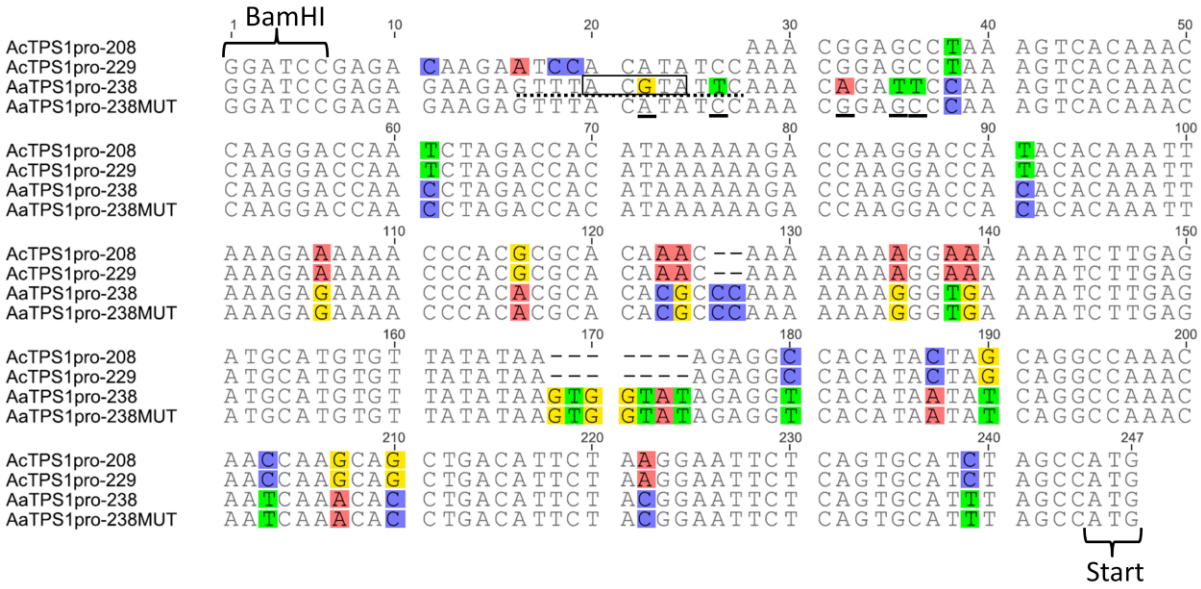

Figure S9. Sequence alignment of minimal Aa *TPS*1$_{pro}$ and Ac *TPS*1$_{pro}$ promoter fragments. The conserved NAC binding core ACGTA is boxed in Aa *TPS*1$_{pro}$-238 and substitutions in $_{pro}$-238Mut are underlined. The NAC 12 bp (GTTTACGTATTC) sequence fused to Ac *TPS*1$_{pro}$-208 (see Fig 8E) is highlighted with a dotted line. The translational ATG start codon and *Bam*HI cloning site are highlighted.

Table S1. Characteristics of *Actinidia arguta* 'Hortgem Tahi' and *A. chinensis* 'Hort16A' ripening fruit. SSC: soluble solids content. nd: not determined

Species	**ripening stage**	**firmness (N)**	**fruit weight (g)**	**SSC (**°Brix**)**
A. arguta	a0	7.80 ± 0.33	13.46 ± 0.57	nd
A. arguta	a1	2.50 ± 0.02	14.74 ± 0.44	11.74 ± 0.19
A. arguta	a2	1.72 ± 0.02	15.50 ± 0.46	12.13 ± 0.30
A. arguta	a3	1.26 ± 0.01	14.10 ± 0.41	12.42 ± 0.22
A. arguta	a4	0.83 ± 0.02	13.53 ± 0.54	13.76 ± 0.81
A. arguta	a5	0.63 ± 0.01	13.29 ± 0.44	13.20 ± 0.67
A. chinensis	c0	31.1 ± 3.0		16.66 ± 0.42
A. chinensis	c1	8.4 ± 0.5		19.11 ± 0.22
A. chinensis	c2	6.5 ± 0.3	nd	18.83 ± 0.26
A. chinensis	c3	3.1 ± 0.2		19.33 ± 0.34
A. chinensis	c4	2.6 ± 0.1		18.89 ± 0.34

Table S2. Cloning and PCR primers

Primer	Sequence
***A) Transient terpene synthase and MEP pathway gene over-expression of pHEX2 vector in* Nicotiana benthamiana**	
AacTPS1_F1	CACCATGTCTCTTAGTGTTGGTTTTGG
AaTPS1_R1	CTAAGCTTTCTCCTCAAAGGGAATGGGACTGATTAGTAG
AcTPS1_R1	TTAAAAAAGGGGAATGGGATTGATTAGTAGTGACTTGACTCG
AdHDRF1	GGGGACAAGTTTGTACAAAAAAGCAGGCTATGATGATTTCTCTGCAATTCTG
AdHDRR1	GGGGACCACTTTGTACAAGAAAGCTGGGTCTAAGCCAATTGCAGGGC
AcDXSF	CACCATGGCTGCTAGTGTTGTTCTC
AcDXSR	CAAGGATTATTCTTAGTTGAAAGGA
AaDXRF1	GGGGACAAGTTTGTACAAAAAAGCAGGCTATGGCTCTAAATTTGCTATCCC
AaDXRR1	GGGGACCACTTTGTACAAGAAAGCTGGGTTCATACAGGAACAGGACTC
AaIDIF1	GGGGACAAGTTTGTACAAAAAAGCAGGCTATGTCCCTCTCTCTCTCC
AaIDIR1	GGGGACCACTTTGTACAAGAAAGCTGGGTTTAAGTCAATTTGTGAATGGTTTTCAT
B) NAC and EIL plant over-expression in pHEX2	
pH_AacNAC1F	AAAAAGCAGGCTCCATGGAGAGCACGGATTCG
pH_AacNAC1R	AGAAAGCTGGGTCTAGGAGTACCATCGAAAG
pH_AacNAC2F	AAAAAGCAGGCTCCATGGAGAGCCCGGATTCG
pH_AacNAC2R	AGAAAGCTGGGTTAGGGTACCAATTCAAGCTAG
pH_AacNAC3F	AAAAAGCAGGCTCCATGGAGAGCACGGATTCA
pH_AacNAC3R	AGAAAGCTGGGTCTAAGAGTACCAATTCAAGCTAG
pH_AacNAC4F	AAAAAGCAGGCTCCATGGAGAAGCTCAACGTTG
pH_AacNAC4R	AGAAAGCTGGGTCTAAGGTTTTCTTTTAAAGGATGAG
pH_AcEIL1F	AAAAAGCAGGCTGGATGATGATATTTGATGAAATGGGG
pH_AcEIL1R	AGAAAGCTGGGTCTAGAACCAAATCGAGCC
pH_AcEIL2F	AAAAAGCAGGCTGGATGATAATGTTTGACGAGATGGG
pH_AcEIL2R	AGAAAGCTGGGTCTAGAACCATACTGAGCC
pH_AcEIL3F	AAAAAGCAGGCTGGATGGATGCCAATGGGTTG
pH_AcEIL3R	AGAAAGCTGGGTCTATGCCCCAAGGTATTC
pH_AacEIL4F	AAAAAGCAGGCTGGATGGAAGAGATTGGAGTTGATAT
pH_AacEIL4R	AGAAAGCTGGGTTTATGCACCAAAGCATTGGATC
C) Real time PCR analysis	
TPS genes	
TPSRTF1 (Fig. 2)	CGTTGAGAGGTGGGATCTGAGTGAA
TPSRTR1 (Fig. 2)	GACACCTTGCTCCTTTAGGGTGTCA
TPSUF (Fig. S9)	TTGCCATATTGGTGAGTCATGCCTT
TPSUR ((Fig. S9)	TGTGGGACTCAAATTAGGTCTTCTCTCA
MEP genes	
DXS_F1	GCCTCCCTGTTTGAAGAACTTGGAT
DXS_R1	CAGGCATGGCCTTGACCTTCTT
DXR_F1	TGCAAGCTTGGGTCACTGACATTT
DXR_R1	CGGCTTTCTCATTTGCAGCACTAA
MCT_F1	CACTCGCATCTGCAGCTAACCAGTT
MCT_R1	TCCACAGCCTTGGCAGAGCAA
CMK_F1	TATTGTCCACGGCTTGCAGCAA
CMK_R1	CAATGATTTGGAACCTCCTGCATTT
MDS_F1	TCGAGCCAGGTTACCCTCTCATCAT

MDS_R1	GGCGCCCAAAATTGCATCAA
HDS_F1	TGGAGCACCACCAACATACCCAA
HDS_R1	TGCCCGGTGTTTCTATTGCCAT
HDS_F2	CCGTCTTTGTATTCCTCATCCTGCA
HDS_R2	TAGATGGTCTTGGAGATGGCATTCT
HDR_F1	CACAATAGGGGTAACATCTGGTGCC
HDR_R1	CAATTGCAGGGCTTCTTCTCGTTTA
HDR_F2	ATGATGTTGTGGTTTTGCCTGCAT
HDR_R2	CCAAACCTTAGAAACCCATGGACAA
IDI_F1	CGAACCCTGATGAAGTTGCTGACAT
IDI_R1	TGAACCATGGGGACAGCTTCAAA
ssuGDPSII_F1	CTTCGAGCCCATGCACCACCTA
ssuGDPSII_R1	CTCACACGCGGCGACGCATA
ssuGDPSII_F2	CCCGTCTCTTCCATGGCCGTAT
ssuGDPSII_R2	CGGAACTAGCCTTGTGGACCATGTA

NAC genes

AcNAC1F	AAGAGCAACCTCCCAAGACCAA
AaNAC1F	AAGAGCAACCACCCACGACCAT
NAC1R	GAAGGTGGCATTCTTGCAAGCAT
NAC2F	CCGGTGGCGATCATAGCTGAAAT
NAC2R	CCGGTTCCTCGGACTGAAAAAAT
NAC3F	CAAACCCCAAAACTCCCACCAA
NAC3R	GCTGTGACTGAGCATTTCGTCGAA
NAC4F	TAGGACTGATTGGATCATGCACGAA
NAC4R	CGGCAAAGAACCCAATTCTCCATA

EIL genes

AcEIL1F	GAGAATCGGTTTGATCAGCGCAA
AcEIL1R	CCGAACATCAAGGGGAAGTTATCATT
AcEIL2F	GGGCAAAAAATGATCAACGAGCTT
AcEIL2R	GAAGAAACTGAGATGCTCATGGGATTT
AcEIL3F	ACACAGAACGTATTTGTTGGTGGCAT
AcEIL3R	TGAGATTCATGATGCAACTCGGAGTT
AcEIL4F	ACCGGATGTGGAACCATCTAATCAA
AcEIL4R	CTCTCGTCGCTCTTTGTCTTGCAA
AaEIL4F	AATCAACCACCATCTAATCAACCTCGA
AaEIL4R	AGGGCTTGATCTTACTCGTGATCTTTTT

Reference

AdEF1F	GCACTGTCATTGATGCTCCT
AdEF1R	CCAGCTTCAAAACCACCAGT

D) Bacterial protein expression of Ac- and AaTPS1 in the pET200 vector

p200_AcTPS1F	CACCGAAAACCTGTATTTTCAGGGAATTGCGGAGCCTAGCCAAACC
p200_AcTPS1R	TTAAAAAAGGGGAATGGGATTGATTAGTAGTGACTTGACTCG
p200_AaTPS1F	CACCAGGCGATCCGCGTTCTACCAACCTTC
p200_AaTPS1R	CTAAGCTTTCTCCTCAAAGGGAATGGGACTGATTAGTAG

E) Promoter constructs of pGreenII 0800-LUC

F1_717	AAACATAGTGCATATTGTGCGTCCTGA
F2_757	AATCGATCGTAACATTCACACAACCG
R1_131	GGTTCCGAAATCGTGCATCGAA

R2_101	CGCATATGTACCCTTCGATGATTGG
AaproF	TTAAGGATCCTTTACTAGATTTAAAAATTAAATTTTAACATA
AaproR	TTAACCATGGCTAAATGCACTGAGAATTC
AcproF	TTAAGGATCCCTCCTAAAATAGAGTTACAAAAAA
AcproR	TTAACCATGGCTAGATGCACTGAG
F-238	TTAAGGATCCGAGAGAAGAGTTTACGTATTCAA
F-229	TTAAGGATCCGAGACAAGAATCCACATATCC
F-238mut	TTAAGGATCCGAGAGAAGAGTTTACATATCCAAACGGAGCCCAAAGTCACAAACCAA
F-600	AAAAGGATCCTAAGGAAAATAAAAYCAAACACTA
208 (I)F	TTAAGGATCCGTTTACGTATTCAAACGGAGCCTAAAGTCACA
208 (II)F	TTAAGGATCCGTTTACGTATTCGTTTACGTATTCGTTTACGTATTCAAACGGAGCCTAAAGTCACA
208 (III)F	TTAAGGATCCGTTTACGTATTCGTTTACGTATTCGTTTACGTATTCGTTTACGTATTCAAACGGAGCCTA AAGTCACA

F) Bacterial protein expression of the NAC DNA binding domains in pET300

AaNAC1DBF	AAAAAGCAGGCTCCATGGAGAGCACGGATTCG
AaNAC1DBR	AGAAAGCTGGGTTCATGGTCGTGGGTGGTT
AaNAC2DBF	AAAAAGCAGGCTCCATGGAGAGCCCGGATTCG
AaNAC2DBR	AGAAAGCTGGGTTCAGGCTCTTGGTGGGTT
AaNAC3DBF	AAAAAGCAGGCTCCATGGAGAGCACGGATTCA
AaNAC3DBR	AGAAAGCTGGGTTCAGGGTCTTGATGGGTG
AaNAC4DBF	AAAAAGCAGGCTCCATGGAGAAGCTCAACGTTG
AaNAC4DBR	AGAAAGCTGGGTTCAATTTTTAGTACTTCTTTTCTTCAAAAATA

Table S3. Ripe fruit headspace terpene compounds in fourteen kiwifruit species. Headspace volatile levels were determined by dynamic headspace sampling of pulped fruit for 20 minutes and compounds were identified by GC-MS.

		Species (# accessions)																											
		A. arguta (n=15)		*A. chinensis* (n=8)		*A. chrysantha* (n=2)		*A. deliciosa* (n=3)		*A. eriantha* (n=5)		*A. glaucophylla* (n=1)		*A. indochinensis* (n=2)		*A. kolomikta* (n=3)		*A. macrosperma* (n=3)		*A. melanandra* (n=3)		*A. polygama* (n=5)		*A. purpurea* (n=4)		*A. rufa* (n=2)		*A. setosa* n=1	
Compound (ng . g^{-1}·h^{-1})	**DB WAX Retention index (s)**	AVERAGE	MAX	AVERAGE	MAX	AVERAGE	MAX	AVERAGE	MAX	AVERAGE	MAX	AVERAGE	MAX	AVERAGE	MAX	AVERAGE	MAX	AVERAGE	MAX	AVERAGE	MAX	AVERAGE	MAX	AVERAGE	MAX	AVERAGE	MAX	AVERAGE	MAX
unknown 1	1021	0.0	0.0	0.0	0.0	0.0	0.0	0.0	0.0	0.0	0.0	0.0	0.0	0.0	0.0	0.0	0.0	0.0	0.0	2.0	6.1	0.0	0.0	0.0	0.0	0.0	0.0	0.0	0.0
pinene, alpha-	1026	245.7	3248.5	0.6	7.2	68.2	157.4	0.0	0.0	33.9	63.8	144.4	159.5	2.2	6.5	0.0	0.0	0.0	0.0	24.1	46.5	38.6	87.6	13.9	55.4	27.7	55.4	0.0	0.0
thujene, alpha-	1033	5.2	42.9	0.0	0.0	0.0	0.0	0.0	0.0	0.0	0.0	0.0	0.0	0.0	0.0	0.0	0.0	0.0	0.0	2.1	4.5	30.4	191.8	55.3	213.3	110.6	213.3	0.0	0.0
fenchene, alpha-	1051	0.0	0.6	0.0	0.0	0.0	0.0	0.0	0.0	0.0	0.0	0.0	0.0	0.0	0.0	0.0	0.0	0.0	0.0	0.0	0.0	0.0	0.0	0.0	0.0	0.0	0.0	0.0	0.0
camphene	1063	2.4	26.3	0.0	0.0	0.0	0.0	0.0	0.0	0.0	0.0	0.0	0.0	0.0	0.0	0.0	0.0	0.0	0.0	0.6	1.7	0.6	2.5	1.4	5.4	2.7	5.4	0.0	0.0
pinene, beta-	1107	137.7	1654.2	2.4	83.3	11.9	29.2	0.0	0.0	27.1	84.2	11.1	16.5	0.0	0.0	0.0	0.0	0.0	0.0	9.0	20.1	20.0	48.1	14.4	28.9	24.9	28.9	3.9	7.8
terpinene, beta or sabinene	1121	151.3	2022.5	0.4	5.1	0.0	0.0	0.0	0.0	2.3	13.9	156.0	168.8	0.0	0.0	0.0	0.0	0.0	0.0	2.1	5.0	66.8	200.0	1.0	4.0	2.0	4.0	0.0	0.0
menthene, p-	1132	0.0	0.0	5.3	82.7	2.9	7.2	2.6	15.5	2.0	11.9	0.0	0.0	6.8	20.3	0.0	0.0	0.0	0.0	0.0	0.0	0.0	0.0	0.0	0.0	0.0	0.0	0.0	0.0
terpinene, alpha-	1172	63.8	1084.6	0.2	5.3	5.7	22.7	0.0	0.0	0.0	0.0	0.0	0.0	0.0	0.0	0.0	0.0	0.0	0.0	0.7	2.1	0.4	1.6	0.0	0.0	0.0	0.0	0.0	0.0
myrcene, beta-	1169	879.8	7596.4	0.0	0.0	16.7	34.7	0.0	0.0	6.9	41.1	22.3	35.3	0.0	0.0	0.0	0.0	0.0	0.0	97.4	187.6	155.7	535.2	37.4	95.4	27.2	51.5	47.7	95.4
limonene	1198	289.8	3331.0	1.0	18.7	223.6	558.9	0.0	0.0	18.8	64.2	72.6	93.8	3.3	9.8	0.0	0.0	0.0	0.0	80.4	144.0	58.5	168.6	17.7	67.7	33.9	67.7	1.6	3.2
phellandrene, beta-	1215	26.6	455.7	0.0	0.0	2.4	9.5	0.0	0.0	0.0	0.0	2.0	2.1	0.0	0.0	0.0	0.0	0.0	0.0	0.0	0.0	8.1	44.9	0.0	0.0	0.0	0.0	0.0	0.0
eucalyptol	1216	427.9	7529.0	66.7	333.2	6.4	25.6	0.0	0.0	0.0	0.0	0.0	0.0	19.1	57.2	0.0	0.0	0.0	0.0	0.0	0.0	63.2	144.1	0.0	0.0	0.0	0.0	0.0	0.0
unknown 2	1217	0.0	0.0	0.0	0.0	0.0	0.0	0.0	0.0	0.0	0.0	0.0	0.0	0.0	0.0	0.0	0.0	0.0	0.0	0.0	0.0	0.0	0.0	68.5	271.3	135.7	271.3	1.4	2.7
ocimene, (*Z*)-beta-	1230	9.1	107.2	0.0	0.0	1.7	6.7	0.0	0.0	0.0	0.0	0.0	0.0	0.0	0.0	0.0	0.0	0.0	0.0	0.0	0.0	1.2	8.4	36.7	146.7	0.0	0.0	73.4	146.7
terpinene, gamma-	1250	146.8	2455.1	0.6	12.0	2.7	9.2	0.0	0.0	0.0	0.0	15.5	19.2	0.0	0.0	0.0	0.0	0.0	0.0	0.2	0.5	10.5	25.4	0.4	1.5	0.8	1.5	0.0	0.0
ocimene, (*E*)-beta-	1230	9.1	107.2	0.0	0.0	1.7	6.7	0.0	0.0	0.0	0.0	0.0	0.0	0.0	0.0	0.0	0.0	0.0	0.0	0.0	0.0	1.2	8.4	36.7	146.7	0.0	0.0	73.4	146.7
unknown 3	1267	0.0	0.0	0.0	0.0	0.0	0.0	0.0	0.0	0.0	0.0	0.0	0.0	0.0	0.0	0.0	0.0	0.0	0.0	0.0	0.0	0.0	0.0	0.7	2.6	0.0	0.0	1.3	2.6
cymene, p-	1268	163.9	2729.0	17.4	260.0	10.5	26.2	1.0	6.0	0.2	0.9	73.7	101.0	0.0	0.0	0.0	0.0	0.0	0.0	4.3	13.0	9.5	25.9	1.9	7.5	3.8	7.5	0.0	0.0
dimethylstyrene	1278	161.9	1755.7	0.2	9.1	253.2	571.7	0.0	0.0	24.3	120.8	20.6	29.8	0.0	0.0	9.6	23.4	4.0	16.0	0.0	0.0	4.8	21.0	0.0	0.0	0.0	0.0	0.0	0.0
terpinolene	1285	1132.8	7546.9	0.7	13.0	160.7	537.5	29.4	176.2	253.4	869.5	0.0	0.0	0.0	0.0	0.0	0.0	0.2	0.9	489.1	1193.2	0.0	0.0	174.5	697.8	348.9	697.8	0.0	0.0
terpinolene, iso-	1286	45.7	391.5	0.2	3.2	2300.1	5208.5	0.0	0.0	38.3	134.8	12.9	16.2	0.0	0.0	0.0	0.0	0.0	0.0	0.0	0.0	0.9	3.3	2.5	9.8	4.9	9.8	0.0	0.0
unknown 4	1408	0.0	0.0	0.0	0.0	0.0	0.0	0.0	0.0	0.0	0.0	0.0	0.0	0.0	0.0	0.0	0.0	0.0	0.0	0.0	0.0	6.7	37.1	0.0	0.0	0.0	0.0	0.0	0.0
perillen	1409	1.4	25.3	0.0	0.0	0.0	0.0	0.0	0.0	0.0	0.0	0.0	0.0	0.0	0.0	2.9	8.6	0.0	0.0	0.0	0.0	0.0	0.0	0.0	0.0	0.0	0.0	0.0	0.0
unknown 5	1414	0.0	0.0	0.0	0.0	0.0	0.0	0.0	0.0	0.0	0.0	0.0	0.0	0.0	0.0	0.0	0.0	0.0	0.0	0.8	2.5	0.0	0.0	0.0	0.0	0.0	0.0	0.0	0.0
mentha-1,3,8-triene, p	1399	12.1	128.5	0.0	0.0	1.9	7.5	0.0	0.0	0.0	0.0	0.0	0.0	0.0	0.0	0.0	0.0	0.0	0.0	0.5	1.5	0.0	0.0	0.3	1.0	0.5	1.0	0.0	0.0
unknown 6	1461	0.6	11.0	0.0	0.0	0.0	0.0	0.0	0.0	0.0	0.0	0.0	0.0	0.0	0.0	0.0	0.0	0.0	0.0	0.0	0.0	0.0	0.0	0.0	0.0	0.0	0.0	0.0	0.0
linalool	1538	0.4	5.7	0.0	0.0	12.9	35.6	0.0	0.0	0.0	0.0	0.0	0.0	0.0	0.0	0.0	0.0	2.6	10.3	0.0	0.0	16.0	51.1	0.0	0.0	0.0	0.0	0.0	0.0
linalool acetate	1538	0.0	0.0	0.0	0.0	0.0	0.0	0.0	0.0	0.0	0.0	0.0	0.0	0.0	0.0	0.0	0.0	0.4	1.5	0.0	0.0	1.4	9.8	0.0	0.0	0.0	0.0	0.0	0.0
unknown 8	1560	0.0	0.0	0.0	0.0	55.8	193.4	0.0	0.0	0.0	0.0	0.0	0.0	0.0	0.0	3.7	11.0	0.0	0.0	0.0	0.0	0.0	0.0	0.0	0.0	0.0	0.0	0.0	0.0
unknown 9	1582	1.4	24.3	0.0	0.0	0.0	0.0	0.0	0.0	0.0	0.0	0.0	0.0	0.0	0.0	0.0	0.0	0.0	0.0	1.5	4.4	0.0	0.0	0.0	0.0	0.0	0.0	0.0	0.0
terpine-4-ol	1600	74.5	1341.9	0.0	0.0	0.0	0.0	0.0	0.0	0.0	0.0	0.0	0.0	0.0	0.0	0.0	0.0	0.0	0.0	0.0	0.0	0.0	0.0	0.0	0.0	0.0	0.0	0.0	0.0
Unknown 10	1620	1.3	23.0	0.0	0.0	0.0	0.0	0.0	0.0	0.0	0.0	0.0	0.0	0.0	0.0	0.0	0.0	0.0	0.0	0.0	0.0	2.3	6.8	0.0	0.0	0.0	0.0	0.0	0.0
terpineol, alpha-	1695	124.0	1988.3	0.0	0.0	5.4	17.9	0.0	0.0	0.0	0.0	0.0	0.0	0.0	0.0	0.0	0.0	0.0	0.0	0.0	0.0	31.4	118.9	0.0	0.0	0.0	0.0	0.0	0.0
citral	1704	1.2	15.3	0.0	0.0	19.6	52.9	0.0	0.0	0.0	0.0	10.8	16.3	0.0	0.0	0.0	0.0	0.0	0.0	3.3	8.7	0.1	1.0	1.1	4.4	2.2	4.4	0.0	0.0
geranylacetone	1835	0.0	0.0	16.3	192.4	0.0	0.0	8.0	21.5	0.0	0.0	0.0	0.0	1.7	5.1	2.8	8.5	0.0	0.0	0.0	0.0	0.0	0.0	0.0	0.0	0.0	0.0	0.0	0.0
cymen-8-ol, p-	1851	1.6	24.1	0.0	0.0	42.1	103.5	0.0	0.0	0.0	0.0	1.9	3.8	0.0	0.0	0.0	0.0	0.0	0.0	3.3	9.1	0.5	3.2	1.9	7.4	3.7	7.4	0.0	0.0
geranylacetone	1855	3.0	15.7	3.3	125.0	3.5	9.0	0.0	0.0	2.5	13.9	0.0	0.0	11.5	29.8	2.9	5.7	2.7	8.9	0.0	0.0	5.8	18.1	0.0	0.0	0.0	0.0	0.0	0.0

Key:

>10	ng . g^{-1}· h^{-1}
>100	ng . g^{-1}· h^{-1}

Supplemental References:

Bohlmann, J., Meyer-Gauen, G., and Croteau, R. (1998). Plant terpenoid synthases: Molecular biology and phylogenetic analysis. Proc. Natl. Acad. Sci. USA **95,** 4126-4133.

Boutrot, F., Segonzac, C., Chang, K.N., Qiao, H., Ecker, J.R., Zipfel, C., and Rathjen, J.P. (2010). Direct transcriptional control of the Arabidopsis immune receptor FLS2 by the ethylene-dependent transcription factors EIN3 and EIL1. Proc. Natl. Acad. Sci. USA **107,** 14502-14507.

Dudareva, N., Martin, D., Kish, C.M., Kolosova, N., Gorenstein, N., Faldt, J., Miller, B., and Bohlmann, J. (2003). (*E*)-β-ocimene and myrcene synthase genes of floral scent biosynthesis in snapdragon: Function and expression of three terpene synthase genes of a new terpene synthase subfamily. Plant Cell **15,** 1227-1241.

Huang, S.X., Ding, J., Deng, D.J., Tang, W., Sun, H.H., Liu, D.Y., Zhang, L., Niu, X.L., Zhang, X., Meng, M., Yu, J.D., Liu, J., Han, Y., Shi, W., Zhang, D.F., Cao, S.Q., Wei, Z.J., Cui, Y.L., Xia, Y.H., Zeng, H.P., Bao, K., Lin, L., Min, Y., Zhang, H., Miao, M., Tang, X.F., Zhu, Y.Y., Sui, Y., Li, G.W., Sun, H.J., Yue, J.Y., Sun, J.Q., Liu, F.F., Zhou, L.Q., Lei, L., Zheng, X.Q., Liu, M., Huang, L., Song, J., Xu, C.H., Li, J.W., Ye, K.Y., Zhong, S.L., Lu, B.R., He, G.H., Xiao, F.M., Wang, H.L., Zheng, H.K., Fei, Z.J., and Liu, Y.S. (2013). Draft genome of the kiwifruit Actinidia chinensis. Nature Communications **4**.

Itzhaki, H., Maxson, J.M., and Woodson, W.R. (1994). An ethylene-responsive enhancer element is involved in the senescence-related expression of the carnation glutathione-S-transferase (GST1) gene. Proc. Natl. Acad. Sci. USA **91,** 8925-8929.

Jones, D.T., Taylor, W.R., and Thornton, J.M. (1992). The rapid generation of mutation data matrices from protein sequences. Comput. Appl. Biosci. **8,** 275-282.

Kosugi, S., and Ohashi, Y. (2000). Cloning and DNA-binding properties of a tobacco Ethylene-Insensitive3 (EIN3) homolog. Nucleic Acids Res. **28,** 960-967.

Montgomery, J., Goldman, S., Deikman, J., Margossian, L., and Fischer, R.L. (1993). Identification of an ethylene-responsive region in the promoter of a fruit ripening gene. Proc. Natl. Acad. Sci. USA **90,** 5939-5943.

Ooka, H., Satoh, K., Doi, K., Nagata, T., Otomo, Y., Murakami, K., Matsubara, K., Osato, N., Kawai, J., Carninci, P., Hayashizaki, Y., Suzuki, K., Kojima, K., Takahara, Y., Yamamoto, K., and Kikuchi, S. (2003). Comprehensive analysis of NAC family genes in *Oryza sativa* and *Arabidopsis thaliana*. DNA Res. **10,** 239-247.

Schwarz, R., and Dayhoff, M. (1979). Matrices for detecting distant relationships. In Atlas of protein sequences, M. Dayhoff, ed, pp. 353-358.

Tamura, K., Stecher, G., Peterson, D., Filipski, A., and Kumar, S. (2013). MEGA6: Molecular Evolutionary Genetics Analysis Version 6.0. Mol. Biol. Evol. **30,** 2725-2729.

Tamura, K., Peterson, D., Peterson, N., Stecher, G., Nei, M., and Kumar, S. (2011). MEGA5: molecular evolutionary genetics analysis using maximum likelihood, evolutionary distance, and maximum parsimony methods. Mol. Biol. Evol. **28,** 2731-2739.

Tapia, G., Verdugo, I., Yañez, M., Ahumada, I., Theoduloz, C., Cordero, C., Poblete, F., González, E., and Ruiz-Lara, S. (2005). Involvement of ethylene in stress-induced expression of the TLC1.1 retrotransposon from *Lycopersicon chilense* Dun. Plant Physiol. **138,** 2075-2086.

Thompson, J.D., Gibson,T.J., Plewniak,F., Jeanmougin,F. and Higgins,D.G. (1997). The ClustalX windows interface: flexible strategies for multiple sequence alignment aided by quality analysis tools. Nucleic Acids Res. **24,** 4876-4882.

Yin, X.R., Allan, A.C., Chen, K.S., and Ferguson, I.B. (2010). Kiwifruit EIL and ERF genes involved in regulating fruit ripening. Plant Physiol. **153,** 1280-1292.